Technology Collaboration Programme
by iea

Evaluating technology options to mitigate greenhouse gas emissions

# IEAGHG Technical Report 2023-03

# Techno-Economic Assessment of Electrochemical $CO_2$ Conversion Technologies

October 2023

IEA GREENHOUSE GAS R&D PROGRAMME

## Acknowledgements & Citations

This report describes work undertaken by TNO on behalf of IEAGHG. The principal researchers were: R.J. Detz, C.J. Ferchaud, A.J. Kalkman, C. Sánchez Martínez, M. Saric, M.V. Shinde.

To ensure the quality and technical integrity of the research undertaken by IEAGHG each study is managed by an appointed IEAGHG manager. The report is also reviewed by a panel of independent technical experts before its release. The expert reviewers for this report were: Sara Budinis, IEA and Tony Feric, US DOE. The IEAGHG manager for this report was: Jasmin Kemper.

The report should be cited in literature as follows: *'IEAGHG, "Techno-economic assessment of electro-chemical CO2 conversion technologies", 2023-03, October 2023.'*

Further information or copies of the report can be obtained by contacting IEAGHG at:

Email: mail@ieaghg.org
Phone: +44 (0)1242 802911
Address: IEAGHG, Pure Offices, Cheltenham Office Park Hatherley Lane, Cheltenham, Gloucestershire, GL51 6SH, UK

## About IEAGHG

**Blazing the way to net zero with leading CCS research.** *We advance technology to accelerate project development & deployment.*

We are at the forefront of cutting-edge carbon, capture and storage (CCS) research. We advance technology that reduces carbon emissions and accelerates the deployment of CCS projects by improving processes, reducing costs, and overcoming barriers. Our authoritative research is peer-reviewed and widely used by governments and industry worldwide. As CCS technology specialists, we regularly input to organisations such as the IPCC and UNFCCC, contributing to the global net-zero transition.

## About the IEA

The International Energy Agency (IEA), an autonomous agency, was established in November 1974. Its primary mandate is twofold: to promote energy security amongst its member countries through collective response to physical disruptions in oil supply, and provide authoritative research and analysis on ways to ensure reliable, affordable and clean energy. The IEA created Technology Collaboration Programmes (TCPs) to further facilitate international collaboration on energy related topics.

# TECHNO-ECONOMIC ASSESSMENT OF ELECTROCHEMICAL $CO_2$ CONVERSION TECHNOLOGIES

This study aims to assess the costs and greenhouse gas (GHG) emissions performance of selected electrochemical $CO_2$ conversion pathways. It applies a learning curve method to project costs up to 2050.

## Key Messages

- Of several pathways reported in the literature, this study identified six pathways that have reached sufficient technology readiness level (TRL > 4) and sufficient data to allow for a first techno-economic assessment (TEA).
- The pathways include processes that produce carbon monoxide (CO), syngas (CO + $H_2$), formic acid (HCOOH) and ethylene ($C_2H_4$), either by low-temperature (LT) electrolysis, high-temperature (HT) solid oxide electrolysis or a tandem LT/HT process.
- HT electrolysis to produce syngas is the closest to reach break-even levelised production costs compared to the fossil reference. The economic performance of all routes is mainly determined by the CAPEX component and thanks to steep learning of the HT pathways, these routes are likely first to reach break-even. LT electrolysis processes still need a substantial reduction in investment costs to reach break-even.
- The GHG performance of the pathways is highly dependent on the emission factor of the electricity used. Electrochemical production of formic acid, CO and syngas results or can soon result in substantial GHG savings compared to the fossil reference. $CO_2$ taxation between at least 60 and 636 €/t$CO_2$ is estimated to be required. Electrochemical production of ethylene would require a very low (< 50 g$CO_2$e/kWh) emission factor to be competitive with current production methods and $CO_2$ taxation of more than 2000 €/t$CO_2$ is estimated to be necessary.
- As the assessment in this study involves the assessment of relatively low TRL technologies, it is important to keep in mind that the related uncertainties can be high.
- The results of this study will be of interest to research organisations, industry, as well as financial RD&D sponsors.
- Recommendations:
  - This study identified several knowledge gaps and suggestions for future research direction, which can be picked up by research organisations. One overarching topic concerned information on the purity requirements of the $CO_2$ feed.
  - On a more general level, more development and investments are necessary to enhance TRL and decrease costs of the investigated $CO_2$ electroconversion routes. Especially pilot projects which demonstrate the entire process chain will be necessary to validate the projected economic and environmental performance.

## Background to the Study

Carbon capture and utilization (CCU) technologies show promise for providing valuable, cost-competitive products into the economy while simultaneously mitigating $CO_2$ emissions and climate change. Increased electrification and the rise of carbon-free, intermittent electrons has attracted global interest towards flexible CCU systems driven by electrical power. Electrochemical systems use electrons to reduce $CO_2$ into a multitude of products. The variety in products mirrors the diversity of electrochemical systems under development. For example, proton exchange membrane (PEM) electrolyzers function at (near) ambient conditions, while solid-oxide systems can operate at temperatures above 700°C. Unfortunately, existing $CO_2$ conversion processes are energy-intensive and expensive. R&D efforts typically focus on improving the energy efficiency and selectivity of laboratory-scale demonstrations. More information is needed to understand the technical and economic hurdles that unique reactor systems may face when scaling from lab and bench scale projects to demonstration and pilot scale applications.

This study seeks to evaluate the economics of electrochemical processes for producing three major product types: gaseous single carbon products (C1G), liquid single carbon products (C1L), and multi-carbon products (C2+). Gaseous single carbon products (C1G) include products such as syngas ($CO + H_2$) or synthetic natural gas, that can be processed further downstream to products like methanol. The other two classes, liquid single carbon products (C1L) and multi-carbon products (C2+), encompass products like formic acid or ethylene, respectively, that are market ready commodities.

To contextualize these evaluations, this study proposes to compare CCU electrochemical conversion economics and energy requirements with chloralkali production as an existing, industrial-scale electrochemical process. The industrial chloralkali process shows that it is possible to build and operate industrial scale electrochemical installations. Existing industry metrics can provide a qualitative comparison and potential price points to achieve commercial electrochemical production of CCU products.

## Scope of Work

IEAGHG commissioned TNO, The Netherlands, to:

1. Provide an overview of electrochemical $CO_2$ conversion technologies and track how the technology has developed and improved over the last several years.
    a. Use an established methodology to take developmental technology R&D data collected at the bench scale and project system-level performance and cost results at the industrial scale (e.g. filling data gaps, adding downstream processing performance/cost impacts) to map calculated cost at each historical development point. Project expected future technology development trends for the next decade (e.g. performance improvements, cost reductions) and include this cost result in the mapping.
    b. Conduct a similar analysis to map the development of the state-of-the-art technology for electrochemical chloralkali processes.
2. Evaluate the economics of electrochemical processes to establish stack-level performance metrics and identify R&D needs. Products should fall within the following three types:
    a. gaseous single carbon products ($C1_G$),
    b. liquid single carbon products ($C1_L$),
    c. and multi-carbon products (C2+).
3. Model the environmental greenhouse gas performance for each electrochemical process using various levels of a decarbonized electricity (DE) e.g. 100% decarbonized vs medium DE vs low DE grid (current electricity grid).
    a. What percentage of DE is needed in current electricity grids for specific electrochemical process to be competitive with existing alternatives in terms of carbon footprint?
4. Critically discuss the trade-offs between costs and other criteria, especially $CO_2$ emissions and identify relevant research questions and gaps.
    a. What are the economic trade-offs between energy efficiency and production?

b. What are the trade-offs between cost and environmental impacts (e.g. carbon footprint/$CO_2$ emissions)?

c.

## Findings of the Study

### Methods and approach

This study examines six $CO_2$ conversion routes that apply electricity as energy carrier to directly convert $CO_2$ into products by electrochemical means. The six routes were selected mainly based on technology readiness level (TRL > 4: route 1-5) and a tandem approach (TRL 3: route 6), for further techno-economic assessment (see Figure 1). The two key technologies for these routes, i.e. low temperature electrolysis and high temperature electrolysis are at a relatively low development level and thus the study includes the commercial chlor-alkali process as a reference and benchmark technology in the analysis. For each of the routes the study determines the technical status of the involved technology in terms of system size and configuration, TRL, energy and mass balances, current investment costs, and cumulative installed capacity. Chapter 3 of the report contains detailed descriptions of each route.

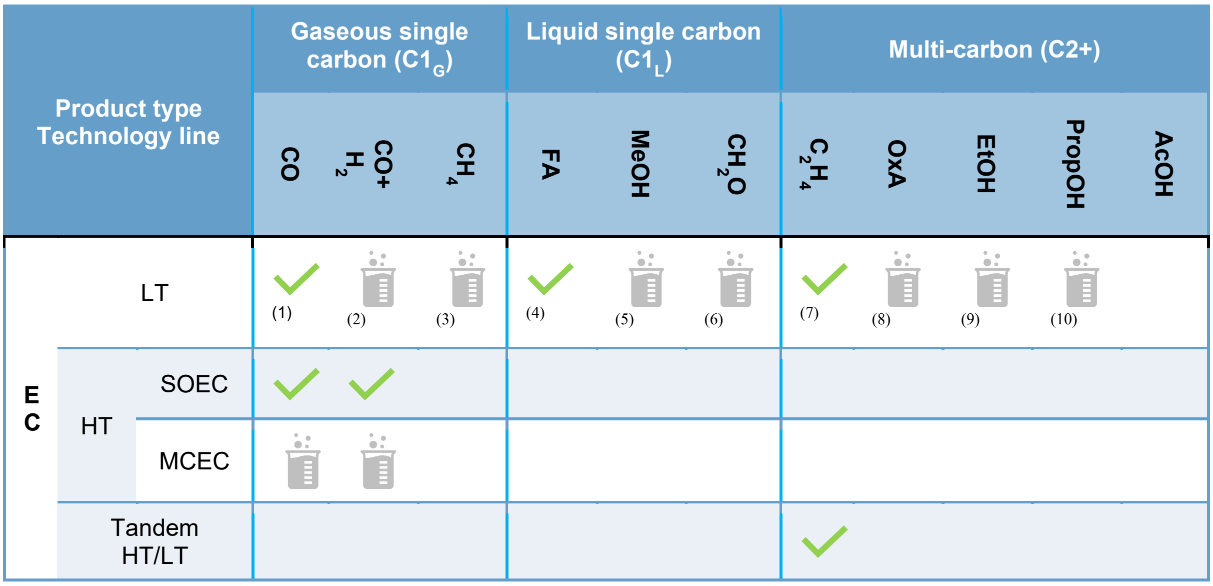

| Product type<br>Technology line | | | Gaseous single carbon ($C1_G$) | | | Liquid single carbon ($C1_L$) | | | Multi-carbon (C2+) | | | | |
|---|---|---|---|---|---|---|---|---|---|---|---|---|---|
| | | | CO | CO+$H_2$ | $CH_4$ | FA | MeOH | $CH_2O$ | $C_2H_4$ | OxA | EtOH | PropOH | AcOH |
| EC | LT | | ✓ (1) | 🧪 (2) | 🧪 (3) | ✓ (4) | 🧪 (5) | 🧪 (6) | ✓ (7) | 🧪 (8) | 🧪 (9) | 🧪 (10) | |
| | HT | SOEC | ✓ | ✓ | | | | | | | | | |
| | | MCEC | 🧪 | 🧪 | | | | | | | | | |
| | Tandem HT/LT | | | | | | | | ✓ | | | | |

**Figure 1 Scope overview with electrochemical $CO_2$ conversion technologies and products. Green ticks (✓) indicate routes that are in scope for this project and will be analysed in detail. Grey beaker symbols (🧪) indicate processes that are currently at a too low TRL (<4) to allow for science-based conclusions. EC=Electrochemical; SOEC=Solid Oxide Electrolysis Cell; MCEC=Molten Carbonates Electrolysis Cell; FA=Formic Acid; MeOH=Methanol; OxA=Oxalic Acid; EtOH=Ethanol; PropOH=n-propanol; AcOH=Acetic Acid.**

Today, no commercial $CO_2$ electroconversion routes are applied. The modelled base case has an input capacity of around 1.0 kt$CO_2$/year. This scale does approximately match the current development status of the key technology units but not the size of current plants that produce for instance syngas or ethylene based on fossil resources. To accommodate for this mismatch between the six routes and industrial facilities, it is assumed that scale-up occurs during the development towards TRL 9 and that cost reductions thanks to economies-of-scale are an intrinsic element of the technology learning curve. If heat or steam is required, it will be provided by an electric heating system, which operates at an efficiency of 95%. The energy source to drive the electrochemical $CO_2$ conversion process is electricity. The source of $CO_2$ substantially contributes to the sustainability of the approach and the production costs of the different compounds. $CO_2$ input is considered to be supplied from a circular source, such as from biogenic point sources, waste streams, or direct air capture. Table 1 summarises the main parameters for the TEA and the sensitivity analysis.

**Table 1 Main parameters for the TEA of $CO_2$ electroconversion**

| Parameter | Selected base value | Sensitivity range | Unit |
|---|---|---|---|
| **Production capacity** | 1 | 1 - 100 | kt$CO_2$ input/yr |
| **Plant lifetime** | 20 | 15 - 25 | years |
| **Annual operating time** | 4000 | 2000 - 8000 | h/yr |
| **Discount rate** | 10 | 5 - 15 | % |
| **Euro Reference year** | 2020 | | |
| **O&M cost factor** | 4 | 2 - 6 | % of initial CAPEX |
| **$H_2O$** | 1.0 | 0.5 – 2.0 | €/t$H_2O$ |
| **$CO_2$** | 50 | 20 - 150 | €/t$CO_2$ |
| **Electricity** | 40 | 20 - 60 | €/$MWh_e$ |

The study applies learning curve analysis to the direct investment costs of the technologies. Historical learning curves of these technologies are extrapolated or, if no data is available, of comparable technologies to project the cost curves up to at least 2030 for different compound annual growth rates (CAGRs) for the analyzed technologies. The CAGR values are based on various reported scenarios and existing plans and announcements for (comparable) technology deployment. No limitations regarding annual capacity additions due to restrictions in market size of a specific product category are considered. The CAPEX learning curves are employed to calculate the future total investment costs (including indirect costs) and levelized production costs and project costs are also projected up to 2050. Although less reliable due to the many uncertainties regarding the successful scale-up of the conversion routes, such projections illustrate the possible trajectories of technology deployment and related cost reductions.

The study also performs an analysis of the $CO_2$ emissions associated with each route to generate 1 GJ of product based on the emission factor of the electricity supply. The $CO_2$ feedstock is considered circular and does not contribute to emissions. Various levels of a decarbonized electricity are explored (e.g. based on solar PV, wind turbines, fossil-based generators, or the average grid) and compared with the fossil reference (including end-of-life emissions) in terms of carbon footprint.

## Costs

Figure 2 shows the cost breakdown of the total investment costs (CAPEX) for each of the routes for 1 MW scale plants. The LT conversion technology is currently significantly more expensive per kW of electricity input compared to the HT routes (routes 4 and 5). This is also observed for the tandem process (route 6) in which the contribution of the first HT step (HT CO production system, dark green area) is barely noticeable. The stack costs for LT systems are based on PEM technology for hydrogen production. For $CO_2$ reduction, the stack is operated at a lower power density, which results in significantly higher costs per kW electricity input. Next to relatively high specific stack costs, the presence of the $CO_2$ recovery loop, along with the purification unit for the end-product (pressure swing adsorption (PSA) for gaseous products, and distillation for formic acid) represent a large contribution to the high total investment costs**.** In comparison to specific investment costs of other chemical processes, such as water electrolysis or methanol synthesis, the costs correspondent to electrochemical $CO_2$ conversion processes are relatively high, especially the LT routes. This can be expected of technologies at a low TRL because these do find themselves still at the start of their learning curve and significant cost reductions can be expected as soon as these technologies are further developed and scaled up.

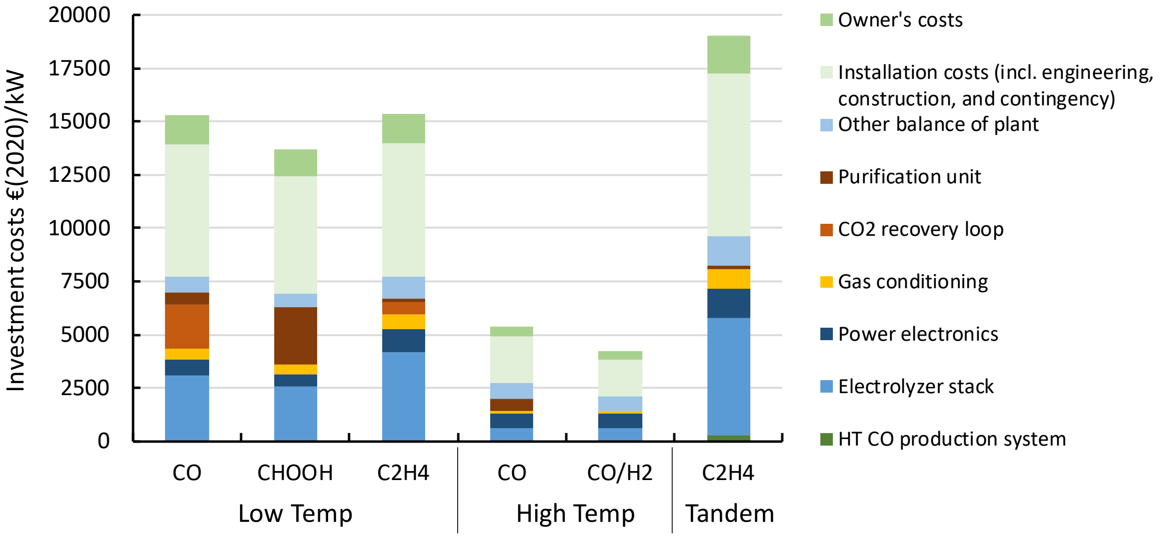

**Figure 2 Cost breakdown of the total investment costs for each route**

For LT electrochemical $CO_2$ conversion, the levelized costs to produce CO amount to approximately 500 €/GJ or 5.1 €/kg (Figure 3). Investment costs contribute more than 60%, O&M costs (incl. stack replacements) cover just above 30%, and the feedstocks, electricity and $CO_2$, together less than 10%. The investment costs dominate the LT CO production costs. This effect is typically exaggerated for low TRL technologies because several parameters (indirect investment costs and O&M cost components) are related to the main equipment costs. Formic acid can be produced for almost 700 €/GJ or 3.7 €/kg. The distribution of the costs over the different components is nearly identical to that of the LT CO production route. The costs per GJ of CHOOH are slightly higher compared to those of CO. This can be explained by the lower energy efficiency of the formic acid production process with respect to CO production (resp. 26% vs. 40%). This difference in cost per GJ product becomes more apparent for $C_2H_4$ production for which the energy efficiency is only 16%. The lower the efficiency, the more capacity in kW is required to produce a GJ of product, next to additional expenses for electricity. Together this results for the direct process (route 3) in levelized costs of nearly 1270 €/GJ or 60 €/kg ethylene of which the feedstock costs (electricity, $CO_2$, and $H_2O$) only represent 6% in total, while the rest is for CAPEX (60%), O&M (20%), and stack replacement costs (14%). The tandem process (route 6), which is slightly less efficient and has higher CAPEX, is even more expensive than route 3 and costs amount to more than 1600 €/GJ or 76 €/kg ethylene. The ethylene production costs are approximately two orders of magnitude higher as the fossil reference price. The HT processes benefit from relatively lower investment costs and higher energy efficiency. The levelized costs to produce CO are for route 4 slightly below 200 €/GJ or 1.9 €/kg. Nearly a quarter of these costs comes from the stack replacement costs, which are relatively high due to the low stack lifetime of only 8000 hours. Despite having an advantage in costs over the LT route (route 1), the fossil reference price is still at least ten times lower. Syngas production via HT route 5 results in levelized costs of around 80 €/GJ or 1.9 €/kg syngas. This route is currently the closest to its fossil reference of 7-18 €/GJ, and may under specific conditions already be competitive. Figure 4 shows exemplary the differences and similarities in sensitivity parameters for LT and HT systems for the production of CO (the report contains the corresponding diagrams for the other routes).

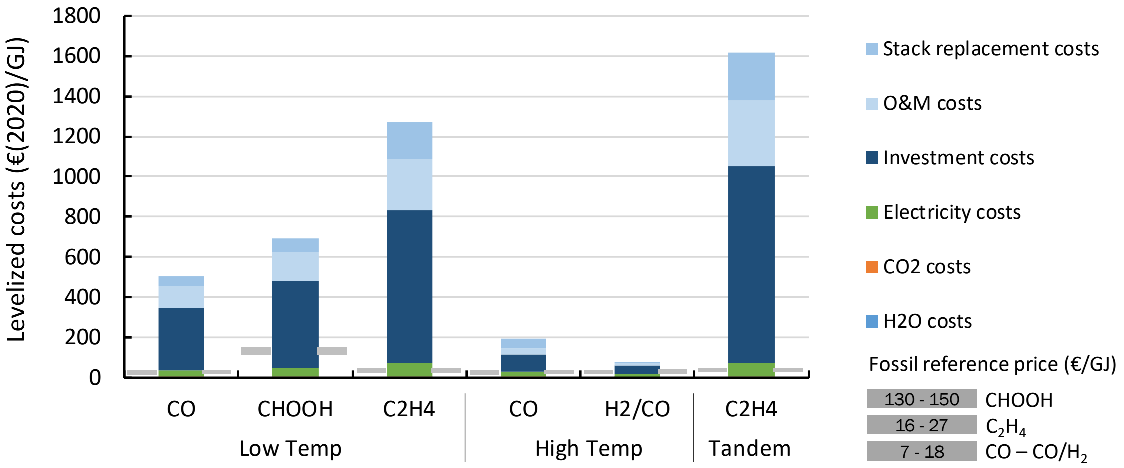

**Figure 3 Levelised production costs of the different routes**

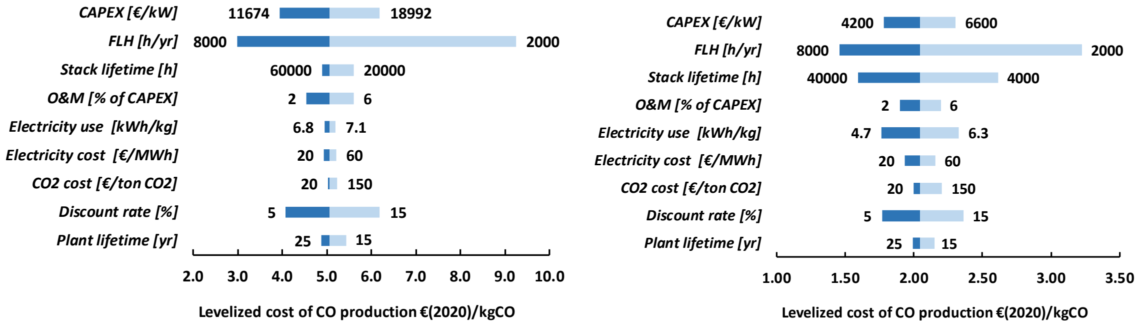

**Figure 4 Sensitivity analysis for LT (left) and HT (right) production of CO**

The study also applies a learning curve analysis on the CAPEX component of the six conversion routes to explore how several of these phenomena affect the future investment costs. The insights from these learning curves are used to project the production costs for 2030, 2040, and 2050, taking into account several performance improvements of the electrochemical conversion processes. LT systems to convert $CO_2$ into products are still at a pilot stage (kW scale systems) and current installed capacity is low (< MW). HT processes are slightly further in TRL but their cumulative installed capacity is also low (few MW) because the largest projects are currently developing MW systems. To project their learning curves, the initial cumulative experience and learning rate is based on that of comparable technology. For LT $CO_2$ conversion, the technology is fairly similar to the chlor-alkali and PEM fuel cell (PEMFC) processes. HT electroconversion systems differ substantially from their LT counterparts but show similarities with solid oxide fuel cell (SOFC) and solid oxide electrolysis cell (SOEC) technology. The projected learning curves for all routes are depicted in Figure 5.

## Table 2 Learning curve parameters (CIC = cumulative installed capacity, LR = learning rate)

| Study | Technology | CIC | LR (applied) | Year(s) |
|---|---|---|---|---|
| This study | LT $CO_2$ Electroconversion | 45 GW (2020) | 15 ± 5 | 2020 - 2050 |
| This study | HT $CO_2$ Electroconversion | 0.5 GW (2020) | 20 ± 5 | 2020 - 2050 |
| | | | | |
| Rubin *et al.* 2015 | Onshore wind | 837 GW (2021) [1] | 12 | 1979 - 2010 |
| ITRPV 2022 | Solar PV | 972 GW (2021) | 24 | 1976 - 2021 |
| Schoots *et al.* 2008 | LT Electrolysis | 15 GW (2006) | 18 ± 13 | 1956 - 2006 |
| Schmidt *et al.* 2017 | LT Electrolysis | 20 GW (2014) | 18 ± 6 | 1956 - 2014 |
| Krishnan *et al.* 2020 | LT Electrolysis | 20 GW (2016) | 16 ± 6 | 1956 - 2016 |
| Schoots *et al.* 2010 | PEMFC | 0.3 GW (2008) | 21 ± 4 | 1995 - 2006 |
| Rivera-Tinoco *et al.* 2012 | SOFC | 0.05 GW (2009) | 35 | 1986 - 2009 |
| Wei *et al.* 2017 | PEMFC | 0.8 GW (2015) | 18 | 2005 - 2015 |
| Wei *et al.* 2017 | SOFC | 0.1 GW (2015) | ~0 | 2001 - 2015 |
| Detz *et al.* 2018 | LT Electrolysis (AE) | 21 GW (2015) | 18 | 2015 - 2050 |
| Detz *et al.* 2018 | LT Electrolysis (PEM) | 0.8 GW (2015, PEMFC) | 21 (PEMFC) | 2015 - 2050 |
| Detz *et al.* 2018 | HT Electrolysis | 0.2 GW (2015, SOFC) | 27 (SOFC) | 2015 - 2050 |
| Bohm *et al.* 2019 | LT Electrolysis (AE) | 20 GW (2015) | 18 | |
| Bohm *et al.* 2019 | LT Electrolysis (PEM) | 1 GW (2015) | 18 | |
| Bohm *et al.* 2019 | HT Electrolysis | 0.1 GW (2015) | 18 | |
| Detz & Weeda 2022 | Electrolysis | 20 GW (2020) | 9 - 20 | 2020 - 2050 |
| IEA, 2021 | Electrolysis | 0.3 GW (2020) | 15 (stack) | 2020 - 2050 |
| | | | | |
| Calculated in this study | Chlor-alkali | 40 GW (2020) | | |
| Calculated in this study | LT Electrolysis | 3.3 GW (2020) | | |
| | | | | |

## Figure 5 Cost projections for the CAPEX (left) and levelised production costs (right) for all routes

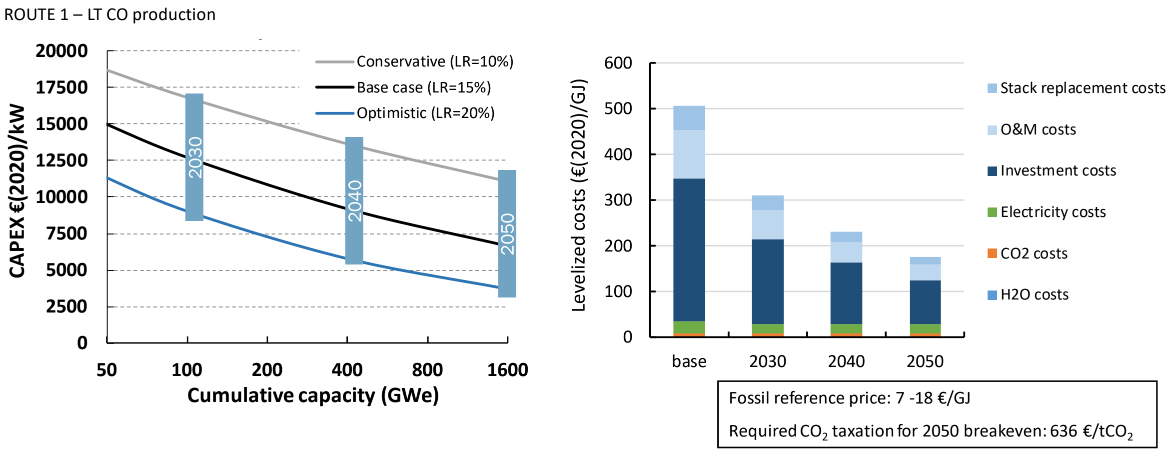

Fossil reference price: 7 -18 €/GJ

Required $CO_2$ taxation for 2050 breakeven: 636 €/$tCO_2$

---

[1] https://gwec.net/global-wind-report-2022/

ROUTE 2 – LT CHOOH production

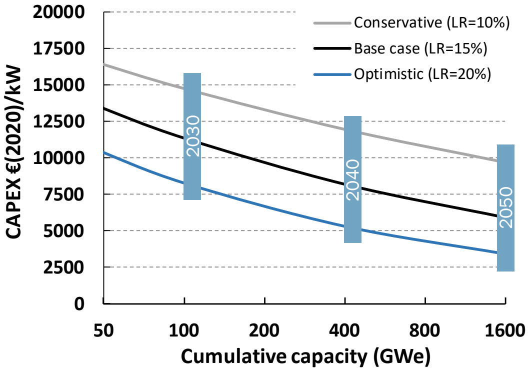

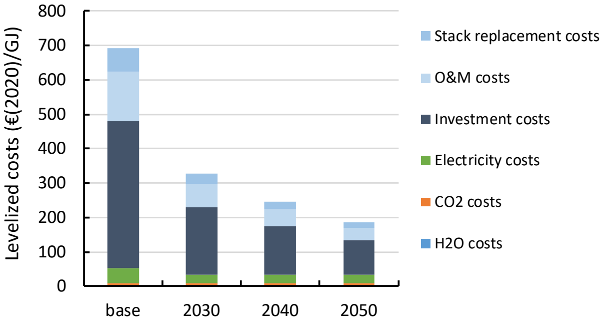

Fossil reference price: 130 - 150 €/GJ

Required $CO_2$ taxation for 2050 breakeven: 72 €/t$CO_2$

ROUTE 3 – LT $C_2H_4$ production

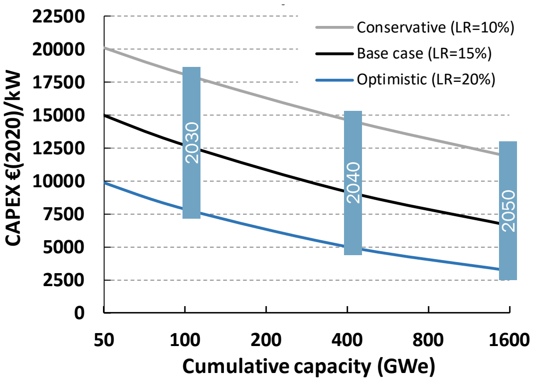

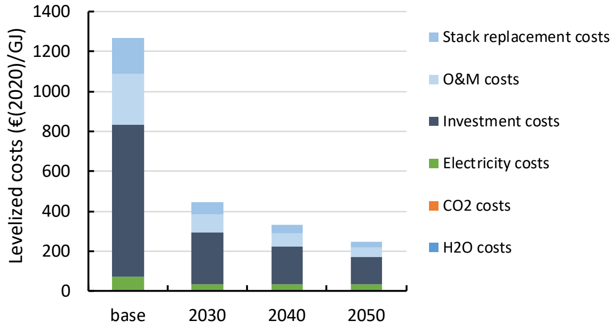

Fossil reference price: 16 - 27 €/GJ

Required $CO_2$ taxation for 2050 breakeven: 2330 €/t$CO_2$

ROUTE 4 – HT CO production

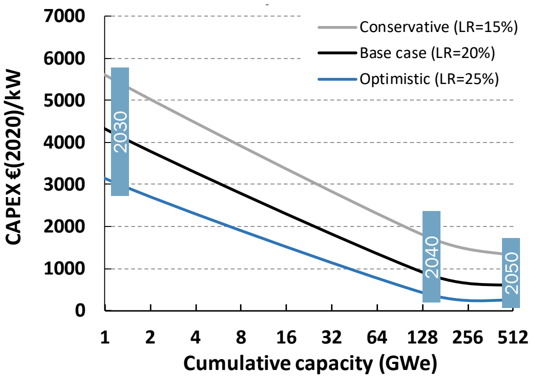

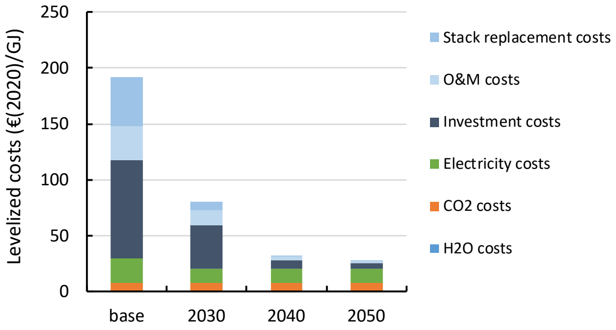

Fossil reference price: 7 - 18 €/GJ

Required $CO_2$ taxation for 2050 breakeven: 60 €/t$CO_2$

ROUTE 5 – HT CO/$H_2$ production

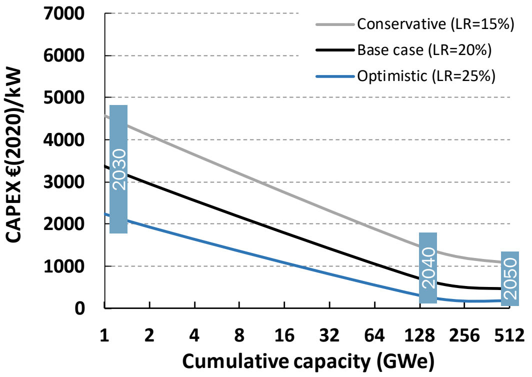

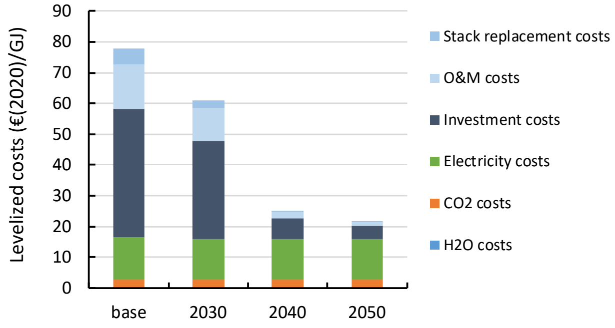

Fossil reference price: 7 - 18 €/GJ

Required $CO_2$ taxation for 2050 breakeven: 102 €/t$CO_2$

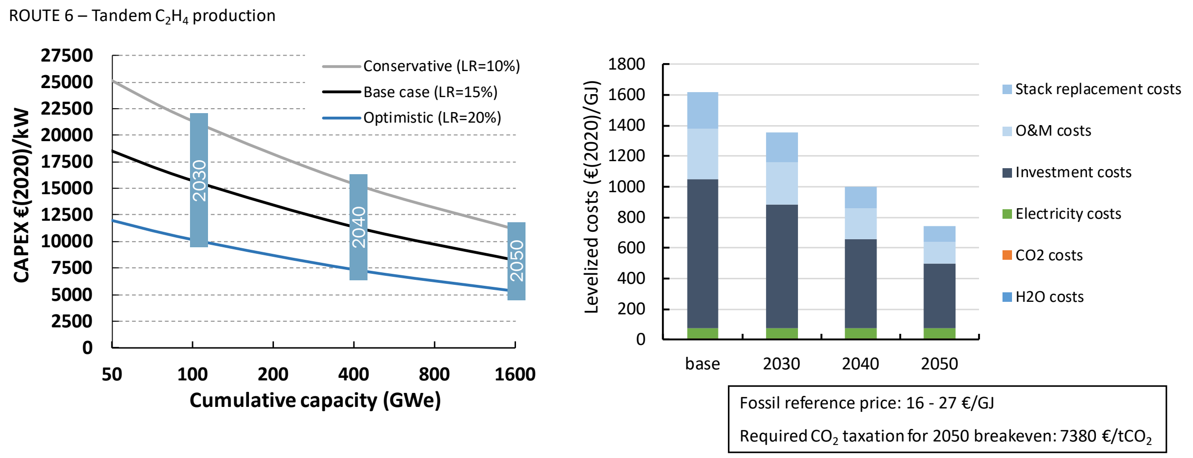
ROUTE 6 – Tandem $C_2H_4$ production

Fossil reference price: 16 - 27 €/GJ

Required $CO_2$ taxation for 2050 breakeven: 7380 €/t$CO_2$

## GHG performance

It will be important that the GHG emissions associated with the routes are significantly lower compared to their fossil reference. Figure 6 provides a first estimate of the $CO_2$ emissions for each of the six routes by comparing the indirect emissions from electricity use of the processes. The emission factor of the electricity supply clearly affects the total emissions of the route. To indicate the difference in energy related indirect emissions between point source capture and direct air capture (DAC), both scenarios are shown. The energy use of point source capture depends on the type of point source and gas stream and, thus, varies significantly. This study assumes a value (0.3 MWh/t$CO_2$) at the lower side of reported figures and that this energy can be supplied as electricity. For DAC, the energy use is determined to be at the high end of the reported range (2.0 MWh/t$CO_2$). By this, the analysis covers more or less the entire range of emissions related to the electricity use for the $CO_2$ supply. The results are compared with the emissions related to the fossil reference pathway, which is based on average 100 year global warming potential (GWP100) values from the SimaPro database.

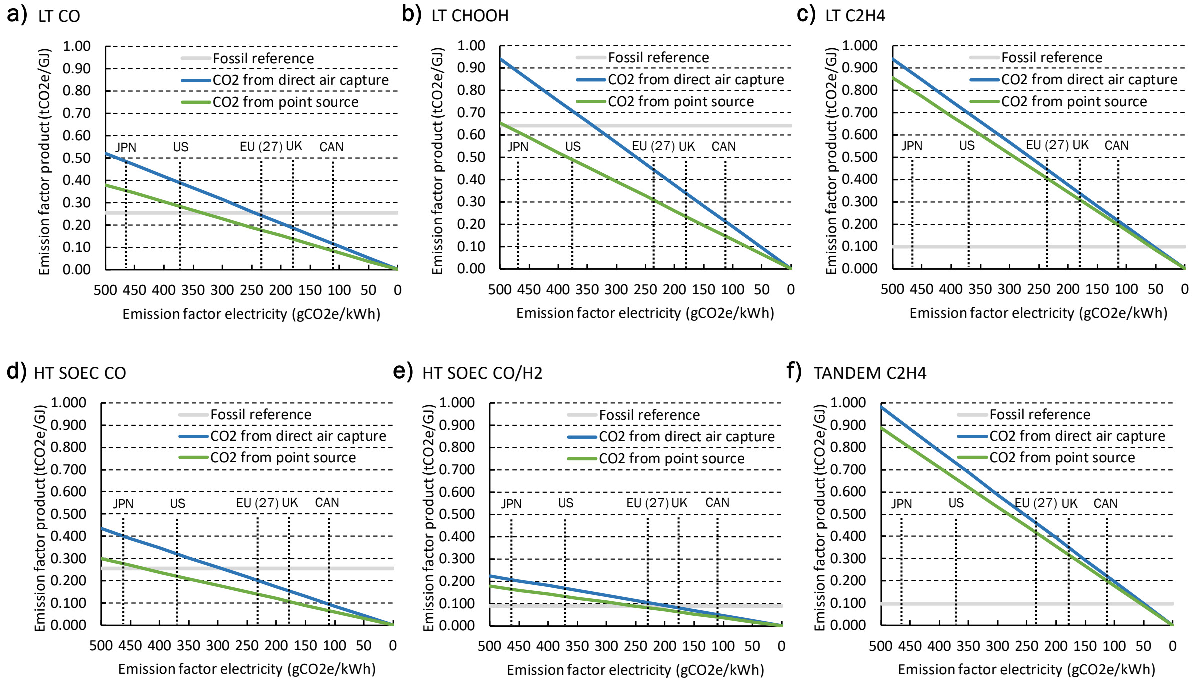

**Figure 6 Emissions from electricity for all six routes**

The LT route to produce CO can achieve similar emissions as the fossil reference when the emission factor of the grid is less than approximately 350 $gCO_2e/kWh$, which is currently the case in several countries, such as the United Kingdom (UK), Canada (CAN), and in the European Union (EU). To become a meaningful route to produce renewable fuels and chemicals, the emission factor of the products should, however, be significantly lower in comparison to fossil-based alternatives. European regulation for instance states that "the greenhouse gas emissions savings from the use of renewable liquid and gaseous transport fuels of non-biological origin (RFNBO's) shall be at least 70%" (REDII, 2018). To reach such a level of avoided emissions, the grid emission factor should be below 100 $gCO_2e/kWh$ for route 1. For formic acid production (route 2), the emission factor of the fossil reference is rather high and breakeven emissions can be realized with a grid emission of 500 $gCO_2e/kWh$, while a 70% reduction is realized with electricity that is generated with emissions of maximal 150 $gCO_2e/kWh$. In several countries, thanks to an increasing share of renewable electricity supply, the average grid emission factor is already approaching such a value and would thus afford the electrochemical production of these products at full annual capacity. The levelized costs would reduce from the base case value of 3.7 €/kg for 4000 full load hours (FLH) to 2.2 €/kg for 8000 FLH. A totally different situation occurs for production route 3 and 6 because the fossil reference emissions for ethylene production are relatively low and the electricity use of the electrochemical process is high. Only with a very low grid emission factor of around 50 $gCO_2e/kWh$, a product emission factor is obtained that is similar to the fossil reference. A >70% reduction target is within reach, but the grid emission factor should be close to zero.

The HT route 4 to produce CO is more efficient than the LT alternative and requires less electricity usage. The emission factor of the grid can be nearly 450 $gCO_2e/kWh$ for this route based on point source $CO_2$ to achieve an emission breakeven point with the fossil reference. To realize > 70% GHG savings, the difference between route 1 and 4 becomes smaller in absolute terms and emissions from the grid may amount to 125 $gCO_2e/kWh$ or 25 $gCO_2e/kWh$ more than for route 1. Syngas contains less carbon per GJ of product compared to pure CO and its associated emission factor is analogously lower, also for the fossil reference. With grid emissions below 250 $gCO_2e/kWh$, the electrochemical pathway can compete in emissions with the fossil-based alternative. From around 70 $gCO_2e/kWh$ and lower, substantial GHG savings ( > 70%) can be reached, purely based on electricity use of the process. Background emissions throughout the entire supply chains and other environmental aspects are not (fully) analysed and may have an impact on the preliminary conclusions on the competitivity of these routes with fossil refence pathways. Full life-cycle assessment can provide more detailed insights into these aspects but is not part of this study.

## Knowledge gaps

Knowledge gaps and research directions for LT routes:

- Roadmap for the future process performance indicators for the 2020 – 2030 decade is uncertain to be achieved. Important challenges in LT $CO_2$ electrolysis technology development need to be overcome to realise the stipulated roadmap. The most important one is to ensure long-term stable operation ( > 10,000 h) at high current densities and efficiencies, and low cell voltage (solving the problems of carbonates precipitation at the cathode).
- Costly purification unit for the HCOOH case. It is of paramount importance to highlight the necessity of selecting an energy and cost-efficient purification strategy for any LT $CO_2$ electrolysis products, and more importantly, for liquid products. Alternatives to the selected hybrid-extraction distillation system can already be found in the literature, as for instance a pervaporation-driven process with potential low capital and operational expenses.

- LT $CO_2$ electrolyser lifetime. Best state-of-the-art lifetime data for LT $CO_2$ electrolysis (for CO production) lifetime are ca. 5,000 h at low current densities and small scale. It is therefore important to understand that the LT $CO_2$ electrolysis process is a technology under development, and a special R&D emphasis on ensuring the long-term stability at high current densities is critical to make this concept industrially feasible.
- Required $CO_2$ purity and role of impurities for $CO_2$ electroreduction. The $CO_2$ stream supply to the electrochemical unit has been left out of the scope of the present work. The role of impurities and unwanted contaminants in the inlet $CO_2$ gas stream in the electrolysis operation has not yet received enough attention amongst researchers, even though these trace components can have significant consequences in the stability and lifetime of the electrochemical unit.
- $CO_2$ crossover towards the anode and associated costs for $CO_2$ recovery. The chosen $CO_2$ reclaiming process is based on an energy-intensive DAC technology that can work with $O_2$-rich inlets, and potential new solutions can be proposed for the $CO_2$ separation from this stream. In the literature, several approaches have been proposed to specifically tackle the $CO_2$ crossover challenge for LT electrolysis.
- Need for a $CO_2/H_2$ separation process in the LT route for HCOOH. A $H_2/CO_2$ separation process needs to be implemented in case the efficiency for the $CO_2$ to HCOOH reaction is not 100% (to be achieved by 2030). Industrially available technology using Palladium-based membranes can be adopted for this application, normally used for $H_2$ purification for $CO_2$-containing streams.
- Role of the anodic reaction in the economic feasibility for $CO_2$ electroreduction. The chosen anodic reaction for all proposed routes has been the Oxygen Evolution Reaction (OER), producing $O_2$, difficult to valorise economically (barely \$ 24 – 40/t $O_2$). Several authors have already pointed out the potential of the anodic oxidation reaction for alternative products or applications. By selecting a sensible anodic product that can easily be assimilated by the CCU value chain, the economic feasibility drastically improves.

Knowledge gaps and research directions for HT routes:

- Required purity of CO. Higher purity can be achieved with further down-stream processing at higher cost and vice versa. CO costs and emissions also strongly depend on the reference technology: coal gasification or steam methane reforming (SMR) with water-gas-shift (WGS).
- Required purity and composition of syngas. The application in which the syngas is applied determines the required composition of produced syngas from the SOEC system outlet. Hence, the ratio of steam and $CO_2$ feedstock must be changed to obtain a syngas with a specified $CO/H_2$ ratio. Moreover, in the case of syngas, separation technology costs for $CO/CO_2/H_2$ depend strongly on the intended end-use of the product.
- Separation of CO from $CO_2/CO$ stream. Currently, there is not enough data regarding separation technologies for a $CO/CO_2$ stream. Halder-Topsøe mentions use of a PSA unit to obtain a high purity CO stream. However, data regarding yield, purity, and costs of such PSA unit is not publicly available.
- Required purity of the $CO_2$ feed. Purity requirements of the $CO_2$ feed are usually considered out-of-scope in research projects and not reported in the published research. This will affect both the Capex for the purification unit and the associated energy consumption.
- From uninstalled cost to total plant cost. As most of the discussed technologies are at low and medium TRL, reported costs usually focus on stack costs. Real life total plant costs are

unknown yet. Hence, total plant costs are estimated based on assumptions for balance-of-plant costs and using installation factors based on comparable technologies. These assumptions introduce uncertainties in the assessment of the total CAPEX.

- Need for system level pilots. A general issue with all investigated pathways is that the research is usually limited to cell-level and stack-level research. Pilot projects in which the entire product chain from industrial $CO_2$ stream to final product is demonstrated are needed to accurately determine CAPEX and O&M costs in an industrial environment.
- Stack and system level research directions. On the solid oxide stack, several research directions are aimed at lowering cost. The FCH program aims at lowering stack cost to below 150 €/kW. Other research aims at reducing the dependence on raw materials on cell level. Upscaling beyond MW level requires optimal system design for better heat management. Lowering stack replacement costs by improving stack lifetime via reduction of degradation at the cell level may further reduce production cost.

## Expert Review Comments

9 reviewers were invited to review the draft report, of which 4 agreed to review and 2 submitted comments within the deadline. Overall, the reviewers recommended the report for being well written and for the high level of detail. One reviewer suggested renaming the report title from “Cost Curves for Electrochemical $CO_2$ Conversion Technologies”, as the report provides much more information that just those cost curves. As per the request of the reviewers, additional details and references were added and uncertainties related to the assessment of low TRL technologies were highlighted more.

## Conclusions

The analysis has shown that several electrochemical technologies are available to convert $CO_2$ into different products. All routes are currently significantly more expensive in comparison with fossil-based approaches, but stringent climate targets in combination with technology development may in the future favour the renewable alternative approaches. The chlor-alkali process, as an example of a mature electrochemical process, can function as a starting point for further experience and developments, especially for LT technology. The LT routes seem to be mainly based on membrane-type electrolyser systems and can benefit from developments in water electrolysis and fuel cell applications, e.g. PEM technology. HT systems are less comparable to membrane technology and are better compared with solid state fuel cell technology, such as SOFC and molten carbonate fuel cell (MCFC). Especially solid oxide technology seems most advanced and most applied in $CO_2$ electroconversion routes. The relatively high power density at which these systems operate, comparable to water electrolysis, provides them an advantage over LT technology. The investment costs per unit output are for HT systems significantly lower than those of their LT counterparts.

Besides this current advantage in investment costs, the projected costs also reduce faster for the HT $CO_2$ conversion routes. This is mainly because in the learning curve analysis the assumed learning rate, which is based on SOFC technology, is slightly higher compared to LT technology for which the LR is based on water electrolysis. The economic performance of all routes is mainly determined by the CAPEX component and thanks to steep learning of the HT pathways, these routes are likely first to reach break-even levelized production cost in comparison to the fossil reference. LT electrolysis processes still need a substantial reduction in investment costs to achieve break-even.

All electrochemical production routes to produce CO, formic acid, and syngas avoid or can soon avoid $CO_2$ emissions when compared to the fossil reference processes. $CO_2$ taxation can therefore play a substantial role in the competitivity of electrochemical $CO_2$ conversion routes. In the base case projections, for CO, formic acid, and syngas production, $CO_2$ taxation should range between at least 60 and 636 €/t$CO_2$ to break-even with the fossil reference price. A higher $CO_2$ price would be required if the electricity that is used in the electroconversion routes is accompanied by an emission factor higher than zero. For ethylene production, saving GHG emissions by the electrochemical routes (3 and 6) becomes difficult if the efficiency and power density cannot be substantially improved without increasing investment costs. The projections indicate that only with a $CO_2$ taxation of more than 2000 €/t$CO_2$ these routes may become competitive with the current fossil-based benchmark.

The early development stage of the investigated technologies also provides opportunity for improvements and innovation that can drastically increase the technological performance. Research gaps are identified on various levels: materials, catalysts, electrodes, lifetime and associated maintenance costs of the active materials. Purification of both the feedstock and product, and downstream processing costs depend on the feedstock and product requirements. The early research phase often does not focus on these up- and downstream processes and further study is necessary. Pilot projects in which the entire product chain from industrial or atmospheric $CO_2$ source to final product is demonstrated can help to more accurately assess the performance, total investment costs, and operating and maintenance costs in an industrial environment. More development and investments are deemed necessary to ensure technological learning effects and reduce costs of electrochemical $CO_2$ conversion routes. An advantage for these specific processes is that they can benefit from experience obtained in comparable technologies, such as water electrolysers and fuel cells.

## Recommendations

This study identified knowledge gaps and research directions on various levels. In general, more development and investments are necessary to enhance TRL and decrease costs of the investigated $CO_2$ electroconversion routes. For specific recommendations, the reader is referred to the section on ‘Knowledge gaps’ in the ‘Findings’ section.

Radarweg 60
1043 NT Amsterdam
The Netherlands

www.tno.nl

T +31 88 866 50 10

**TNO report**
**TNO 2022 R12194**

# Cost curves for electrochemical $CO_2$ conversion technologies

| | |
|---|---|
| Date | 10 November 2022 |
| Author(s) | R.J. Detz, C.J. Ferchaud, A.J. Kalkman, C. Sánchez Martínez, M. Saric, M.V. Shinde |
| Copy no | |
| No. of copies | |
| Number of pages | 73 (incl. appendices) |
| Number of appendices | 1 |
| Sponsor | IEA Environmental Projects Ltd |
| Project name | Cost curves for electrochemical CO2 conversion technologies |
| Project number | 060.50886 |

# Executive Summary

Electrochemical reduction of $CO_2$ to produce chemicals or fuels with a single (C1) or two (C2) carbon atoms is expected to contribute to the zero-emission goal of the petrochemical industry in 2050. Here we report the results of an investigation into the most promising products (CO, syngas, formic acid and ethylene) produced by either low-temperature electrolysis, high-temperature solid-oxide electrolysis, or tandem high/low temperature electrolysis. Of several possible pathways that are reported in literature, we identified six possible pathways that have reached a sufficient technology readiness level (TRL > 4 or are otherwise interesting to explore) and for which we can find sufficient data to allow for science-based extrapolation and conclusions. The current report focusses on the following six electrochemical pathways: low-temperature CO production, low-temperature formic acid production, low-temperature ethylene production, high-temperature CO production, high-temperature syngas production, and a tandem approach to produce ethylene.

We report the State-of-the-Art of the various pathways (e.g. energy & conversion efficiency, investment costs), including that of the chlor-alkali process. We use a learning curve method to project costs up to 2050. We calculate the economic performance of the various pathways in terms of levelized production costs and the greenhouse gas (GHG) performance for various scenarios of carbon intensity of the power, both compared to the current reference of production from fossil-based resources.

We conclude that high-temperature solid-oxide electrolysis to produce CO and syngas is closest to reaching break-even levelized production cost in 2050 in comparison to the fossil reference. Low-temperature electrolysis processes still need a substantial reduction in investment costs to achieve break-even, although the most promising process, formic acid production, can reach break-even costs in 2050 with a $CO_2$ taxation of 72 €/t $CO_2$.

The GHG emission performance is based on the emission factor of the electricity that is used to drive the processes, while we assume that the feedstock $CO_2$ can be derived from either a biogenic point source or direct air capture. Electrochemical production of formic acid, CO, and syngas results or can soon result in substantial GHG savings compared their fossil-based alternatives. The extent to which savings can be achieved depends merely on the carbon intensity of the local power grid, or more generally, the supplied electricity. Any reduction in electricity demand of the processes thanks to efficiency improvements would, thus, also be beneficial. Electrochemical $CO_2$ conversion to produce ethylene would require a very low emission factor of electricity (< 50 $gCO_2$/kWh) to be competitive with current production methods, and is therefore not likely to contribute significantly to the zero-emission goal of the petrochemical industry in the foreseeable future.

We conclude the report with an overview of knowledge gaps and research questions. Research gaps are identified on various levels: materials, catalysts, electrodes, lifetime and associated maintenance costs of the active materials. Purification and down-stream processing costs depend on the product requirements, and need further attention.

A general issue with all investigated pathways is that purity requirements of the $CO_2$ feed are not reported in the published research. Pilot projects, which demonstrate the entire product chain from industrial $CO_2$ stream to final product, are needed to accurately determine the performance, total investment costs, and operating and maintenance costs in an industrial environment.

# Contents

**1 Introduction 4**
1.1 General background 4
1.2 Scope of the study 4
1.3 Cost projection method and uncertainty 6

**2 Methodology 8**
2.1 System size and configuration 8
2.2 Energy and mass balances 8
2.3 Investment costs 9
2.4 Production costs 9
2.5 Cost projections through learning curve analysis 10
2.6 Environmental greenhouse gas performance 11

**3 Electrochemical $CO_2$ conversion: State-of-the-Art 12**
3.1 Chlor-alkali process 12
3.2 Low-temperature electroconversion to produce carbon monoxide 16
3.3 Low-temperature electroconversion to produce formic acid 21
3.4 Low-temperature electroconversion to produce ethylene 25
3.5 High-temperature solid oxide electroconversion to produce carbon monoxide 29
3.6 High-temperature solid oxide electroconversion to produce syngas 32
3.7 High-temperature molten carbonate electroconversion 36
3.8 Tandem electroconversion approach to produce ethylene 39
3.9 Technology and material summary of the different routes 42

**4 Techno-economic analysis 45**
4.1 Investment costs 45
4.2 Levelized production costs 46
4.3 Sensitivity analysis 48
4.4 Cost projections 50

**5 Environmental greenhouse gas performance results 56**

**6 Identified knowledge gaps and proposed research directions 58**
6.1 Knowledge gaps and research directions in the low-temperature $CO_2$ electrolysis routes 58
6.2 Knowledge gaps and research directions in the high-temperature $CO_2$ electrolysis routes 60

**7 Concluding remarks 62**

**8 References 63**

**9 Appendix 72**

# 1 Introduction

## 1.1 General background

The use of fossil resources provides the world with highly concentrated forms of energy, but additionally with an abundance of carbon. Due to fuel combustion and waste incineration, a substantial share of this carbon is emitted to the atmosphere as carbon dioxide ($CO_2$). Next to these undesirable $CO_2$ emissions, many materials that are used in society, for example bitumen, lubricants, plastics, and solvents, contain carbon as the main element. A vital climate change mitigation option encompasses the reduction of greenhouse gas (GHG) emissions of which fossil $CO_2$ emissions account for roughly 70% (Global Carbon Budget, 2021). Various technologies to provide renewable energy, such as solar photovoltaics and wind turbines, are currently being deployed to avoid and replace the use of fossil fuels. Abandoning the use of fossil resources will eventually also reduce the availability of carbon as a feedstock to produce fuels, chemicals, building materials, and polymers. To find alternatives for fossil carbon, the chemical industry is already exploring various pathways to use circular flows of carbon, originating from either biogenic or atmospheric sources, or waste streams (Detz & van der Zwaan, 2019).

Carbon capture and utilization (CCU) technologies show promise for providing valuable, cost-competitive products into the economy while simultaneously mitigating $CO_2$ emissions and climate change. Increased electrification and the rise of carbon-free, intermittent electricity has attracted global interest towards flexible CCU systems driven by electrical power. Electrochemical systems use electrons to reduce, for instance, $CO_2$ into a multitude of products. This variety in products mirrors the diversity of electrochemical systems under development. For example, proton exchange membrane (PEM) electrolyzers function at (near) ambient conditions, while solid-oxide systems can operate at temperatures above 700°C. Unfortunately, existing $CO_2$ conversion processes are energy-intensive and expensive. R&D efforts typically focus on improving the energy efficiency and selectivity of laboratory-scale demonstrations. More information is needed to understand the technical and economic hurdles that unique reactor systems may face when scaling from lab and bench scale projects to demonstration and pilot scale applications.

## 1.2 Scope of the study

The current study was assigned to TNO by IEA GHG and seeks to evaluate the economics of electrochemical processes for producing three major product types: gaseous single carbon products (C1G), liquid single carbon products (C1L), and multi-carbon products (C2+). Gaseous single carbon products (C1G) include products such as syngas ($CO + H_2$) or synthetic natural gas, that can be processed further downstream to products like methanol. The other two classes, liquid single carbon products (C1L) and multi-carbon products (C2+), encompass products like formic acid or ethylene, respectively, that are market ready commodities. To contextualize these evaluations, this study proposes to compare CCU electrochemical conversion economics and energy requirements with chloralkali production as an existing, industrial-scale electrochemical process. The industrial chloralkali process shows that it is possible to build and operate industrial scale electrochemical installations. Existing industry metrics can provide a qualitative comparison and potential price points to achieve commercial electrochemical production of CCU products.

The scope of the study consists of the following tasks:

1. Provide an overview of the CCU electrochemical conversion technologies that are currently at TRL $\geq$ 4 and track how the technology has developed and improved over the last several years.

2.a Use an established methodology to take developmental technology R&D data collected at the bench scale and project system-level performance and cost results at the industrial scale. Project expected future technology development trends for the next decade (e.g. performance improvements, cost reductions) and include this cost result in the mapping.
2.b. Conduct a similar analysis to determine cost of production and map the development of the State-of-the-Art technology for electrochemical chloralkali processes.

3. Evaluate the economics of electrochemical processes to establish stack-level performance metrics and identify R&D needs. Products should fall within the following three types: a. gaseous single carbon products (C1G), b. liquid single carbon products (C1L), and c. multi-carbon products (C2+)

4. Model the life cycle environmental greenhouse gas performance for each electrochemical process using various levels of a decarbonized electricity (DE)

5. Critically discuss the results and identify relevant research questions and gaps.

In this study, we review the use of $CO_2$ as feedstock, also known as carbon capture and utilization (CCU) routes, to produce carbon-based chemicals, with a focus on carbon monoxide (CO), syngas ($CO/H_2$), formic acid (CHOOH), and ethylene ($C_2H_4$). Different sources of $CO_2$ are available, such as from biomass, atmosphere, ocean, or fossil resources. The origin of the $CO_2$ feedstock is not part of this assessment but has important implications for, for instance, the costs, energy demand, accessibility, scale, societal acceptance, and sustainability of the route (IEAGHG, 2021a). CCU may have substantial market opportunities if it can replace part of the fossil fuels and chemicals industry and this prospect encourages several stakeholders to investigate different approaches to convert $CO_2$ into products (IEA, 2019; IEA, 2020; IEAGHG, 2021a). Many routes at various stages of technological maturity are being developed. The different approaches, such as biochemical synthesis (e.g., Jiang *et al.*, 2013), carbonation, electroconversion, photoreduction (e.g., Li *et al.*, 2019; Ng *et al.*, 2022), and thermocatalysis (e.g., IEAGHG, 2021b), are schematically depicted in Figure 1.

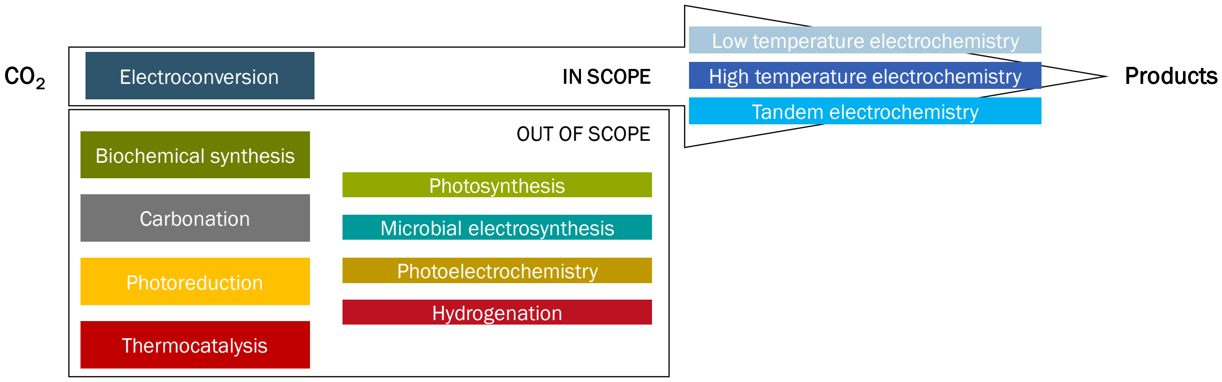

Figure 1. Overview of different approaches to convert $CO_2$ into products. The category 'Tandem electrochemistry' refers to a combination of high- and low-temperature electroconversion of $CO_2$ to products.

We will examine six electroconversion routes that apply electricity as energy carrier to directly convert $CO_2$ into products by electrochemical means. Such an approach has several advantages in that it can: 1) accelerate the uptake of renewable electricity supply thanks to increased demand; 2) reduce the reliance of industry on fossil fuels by enhancing industrial electrification; 3) result in more efficient (ideally) single step conversion processes that can lead to pure products and simplify purification steps. First we explain the methodology behind our techno-economic assessment. In chapter 3, we determine the State-of-the-Art in terms of development stage and performance metrics of direct electrochemical $CO_2$ conversion approaches. We have selected six routes, mainly based on technology readiness level (TRL>4: route 1-5) and a tandem approach (TRL 3: route 6), for further techno-economic assessment (Table 1). For these routes, we determine the current costs and apply learning curve analysis to project costs up to 2050. At that time, the technology needs to be competitive at an industrial scale in order to play a meaningful role in the energy transition. Next to costs, the environmental aspects (e.g. $CO_2$ emissions) are also important to understand the feasibility of this approach. We touch upon the environmental greenhouse gas performance of our six routes in chapter 5. We will discuss the results of our analysis and, in chapter 6, provide an overview of knowledge gaps and research questions before presenting the conclusions. We hope that the insight from our assessment helps people from knowledge institutes, industry, and governments to steer developments into the right directions and to accelerate industrial transformation.

Table 1. Scope overview with electrochemical $CO_2$ conversion technologies and products. Green ticks (✓) indicate routes that are in scope for this project and will be analysed in detail. Grey beaker symbols ( 🧪 ) indicate processes that are currently at a very early stage (TRL<4), making it difficult to draw science-based conclusions about their scale-up potential. EC=Electrochemical; LT=Low Temperature; HT=High Temperature; SOEC=Solid Oxide Electrolysis Cell; MCEC=Molten Carbonates Electrolysis Cell; FA=Formic Acid; MeOH=Methanol; OxA=Oxalic Acid; EtOH=Ethanol; PropOH=n-propanol; AcOH=Acetic Acid.

| Product type<br>Technology line | | | Gaseous single carbon ($C1_G$) | | | Liquid single carbon ($C1_L$) | | | Multi-carbon (C2+) | | | | |
|---|---|---|---|---|---|---|---|---|---|---|---|---|---|
| | | | CO | CO+$H_2$ | $CH_4$ | FA | MeOH | $CH_2O$ | $C_2H_4$ | OxA | EtOH | PropOH | AcOH |
| EC | LT | | ✓ (1) | 🧪 (2) | 🧪 (3) | ✓ (4) | 🧪 (5) | 🧪 (6) | ✓ (7) | 🧪 (8) | 🧪 (9) | 🧪 (10) | |
| | HT | SOEC | ✓ | ✓ | | | | | | | | | |
| | | MCEC | 🧪 | 🧪 | | | | | | | | | |
| | Tandem HT/LT | | | | | | | | ✓ | | | | |

[1] Liu *et al.* (2018); [2] Lu *et al.* (2020); [3] Sedighian Rasouli *et al.* (2020); [4] Yang *et al.* (2020); [5] Albo *et al.* (2015); [6] Nakata *et al.* (2014); [7] Dinh *et al.* (2018); [8] König *et al.* (2021); [9] Karapinar *et al.* (2021); [10] Wang *et al.* (2022)

## 1.3 Cost projection method and uncertainty

An important part of the assignment is to use an established methodology to take technology R&D data collected at the bench scale and estimate system-level performance and cost results for application at an industrial scale. It also includes a projection of expected future technology development trends for the next decade (incl. performance improvements and cost reductions) and incorporate the results in the mapping. The aim of this task is to assess whether and when a certain technology is expected to become economically feasible.

Projections on costs are very difficult to make, already for better established technologies. Therefore we highlight the strong uncertainty related to assessing early stage technologies which have never been built and operated in a commercial environment. The current report is not meant to guide investment decisions, but uses scientific best practices to extrapolate the available data to make informed predictions about the potential deployment of the discussed CCU technologies in the next decade. The extrapolation method used is the ‘Learning Curve method’, for which the underlying assumption is that through ‘learning-by-doing’ costs (excluding inflation) will decline proportional to the global total cumulative installed capacity of the technology. This method is well researched, and its limitations are well known (see section 2.5). The ‘learning-by-doing’ process may be influenced by external factors like, e.g., surges in commodity prices and energy prices, supply-demand dynamics and availability of resources, geopolitical choices, political tools like available R&D budgets, subsidies and regulations, and the decreasing availability of favorable locations. In general, the uncertainty in projected cost will be larger for technologies with lower TRL. The authors recommend that the current cost projections will be updated every couple of years with the most recent data.

# 2 Methodology

Electrochemistry may appear an attractive approach to convert a stable molecule like $CO_2$ into an array of carbon-based products, such as carbon monoxide (CO), formic acid (CHOOH), and ethylene ($C_2H_4$). Here we investigate six routes to electrochemically convert $CO_2$ to produce CO (2 routes), syngas (1 route), formic acid (1 route), and ethylene (2 routes). The two key technologies we investigate for these routes, i.e. low temperature electrolysis and high temperature electrolysis, are at a relatively low development level and we include the commercial chlor-alkali process as a reference and benchmark technology in our analysis. For each of the routes we determine the technical status of the involved technology in terms of system size and configuration, technology readiness level (TRL), energy and mass balances, current investment costs, and cumulative installed capacity.

## 2.1 System size and configuration

Today, no commercial $CO_2$ electroconversion routes are applied and we therefore base our process analysis on a (potential) demonstration facility. This plant at full load (8760 h/yr of operation) has an input capacity of around 1.0 kt$CO_2$ per year (Figure 2). This scale does approximately match the current development status of our key technology units but not the size of current fossil-based plants that produce for instance syngas or ethylene, which typically deal with feedstock flows that are three orders of magnitude larger (~1000 kt per year) (Petrochemicals Europe, 2022). To accommodate for this mismatch between our six routes and industrial facilities, we assume that scale-up occurs during the development towards TRL 9 and that cost reduction in response to economies-of-scale is an intrinsic element of our technology learning curve. Both the State-of-the-Art and the expected rates of development and system scale-up are discussed for each of the key technologies.

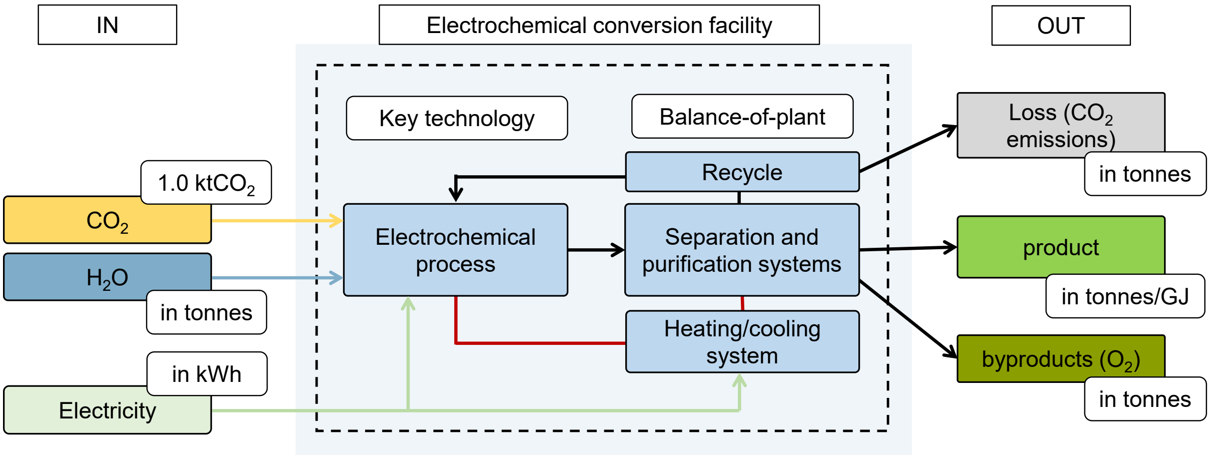

Figure 2. Schematic representation of a $CO_2$ electrochemical conversion route showing the system boundary (dashed box) and in- and outputs. Upstream $CO_2$ separation and purification steps are out-of-scope.

## 2.2 Energy and mass balances

The basic configuration as shown in Figure 1 indicates three different input streams: $CO_2$, $H_2O$, and electricity. If heat or steam is required, we assume it will be provided by an electric heating system, which operates at an efficiency of 95%. For each of the key technologies the stack efficiency is determined by dividing the energy of the desired product (in lower heating value (LHV)) by the electricity consumption of the key technology unit. The total energy efficiency of the route also includes the electricity used for balance-of-plant operation, such as electric heating, powering pumps, and energy use in buildings.

The conversion efficiency of the process is based on carbon in which we divide the amount of carbon in the product by the total amount of carbon in the $CO_2$ inlet stream (both in moles). Process selectivity, single pass conversion rates, and separation and recycling efficiencies together determine the losses and byproducts of the route. The portion of carbon that is not converted into the product and cannot be recycled results in a loss category, which includes for instance purge streams that are flared or vented and can result in $CO_2$ emissions, but also undesirable side products due to poor reaction selectivity. The byproducts category consists of compounds that are formed along with the desired product and cannot be avoided, e.g. oxygen. No value is attributed to the losses and byproducts.

As mentioned in the introduction, the source of $CO_2$ substantially contributes to the sustainability of the approach and the production costs of the different compounds. $CO_2$ input is considered to be supplied from a circular source, such as from biogenic point sources, waste streams, or direct air capture (DAC). The costs of these sources may vary significantly and we explore their impact in a sensitivity analysis (Table 2).

The energy source to drive the electrochemical $CO_2$ conversion process is electricity. The origin of this electricity determines largely the sustainability and environmental impact of the routes. Many aspects of the conversion route do rely on assumptions regarding the electricity source, such as the costs of the electricity, the intermittency and amount of full load hours (FLH) of electricity supply, and the $CO_2$ emission factor of the electricity. To illustrate the dependence on the electricity source, we investigate the electricity costs and amount of FLH in a sensitivity analysis (Table 2). In Section 2.6, we describe how the environmental greenhouse gas (GHG) performance of the different routes were assessed.

## 2.3 Investment costs

The electrochemical conversion facility consists of the core technology unit, for instance a low temperature electrolyzer, and the balance-of-plant equipment, such as the purification and heating/cooling systems. The total investment costs (CAPEX) are estimated for a 1.0 kt$CO_2$/yr plant and expressed in €(2020) (Table 2). The core technology and balance-of-plant equipment costs are determined based on literature sources (see Chapter 3) and expert judgement and sum up to the direct CAPEX. We apply an installation factor of 2 on top of the direct CAPEX to accommodate for indirect costs, such as for construction, design, engineering, buildings, permits, contingency, etc (Hydrohub, 2022). Direct and indirect CAPEX combined result in the total installed CAPEX of our plant design (see also Section 4.1). The operating and maintenance (O&M) costs (excl. electricity and $CO_2$ input) are set at 4% of the total installed CAPEX (typical between 2 and 5% as, e.g., described in Agora (2018) and Detz, *et al.* (2018)). Total replacement costs of key technology components are calculated for each of the routes separately, annualized over the total plant lifetime, and added to the O&M costs.

## 2.4 Production costs

The levelized production costs ($C_x$) are calculated with equation (1) in which the total annual costs are divided by the amount of product generated annually ($P_x$) (Blok & Nieuwlaar, 2016). The discounted annualized CAPEX (with α being the capital recovery factor), the annual O&M costs (including equipment replacement costs), and the annual feedstock costs $F$ (for $CO_2$, electricity and water) represent the total annual costs. The capital recovery factor (a) is determined by equation (2) and is a function of the discount rate ($r$) and the plant lifetime ($n$). We here use a typical discount rate of 10% and a plant lifetime of 20 years (based on IEA (2020); Detz, *et al.* (2018)) and vary these values in the sensitivity analysis. We assume that the operational capacity of the plant in FLH is steady over the plant lifetime. For our base case, the FLH amount to 4000, which is based on intermittent renewable electricity supply (e.g. from offshore wind, or a combination of solar and wind parcs), while we explore a range of 2000 to 8000 FLH in the sensitivity analysis. We investigate an

$$C_{\mathrm{x}} = \frac{\alpha \times \mathrm{CAPEX} + \mathrm{O\&M} + \mathrm{F}}{P_{\mathrm{x}}} \tag{1}$$

$$\alpha = \frac{r}{1 - (1 + r)^{-n}} \tag{2}$$

electricity cost range of 20 to 60 €/MWh of which 40 €/MWh is our base case value (IEA, 2020). The costs of $CO_2$ as a feedstock may, depending on the source, vary significantly. Capture of biogenic $CO_2$ at industrial fermentation processes can provide $CO_2$ for around 10 €/ton (IEAGHG, 2021a), while direct air capture technology, although currently still expensive, may in the future supply $CO_2$ for approximately 100-250 €/ton (Keith *et al.*, 2018). We apply for our base case a $CO_2$ feedstock cost of 50 €/ton, while a broader range (20-150 €/ton) is explored in the sensitivity analysis (Table 2). Water is supplied at 1 €/ton (Agora (2018)). Costs will be reported in €(2020), unless otherwise noted. Other currencies will be converted to € in the year under consideration, and subsequently corrected for inflation by converting them to our reference year (2020).

Table 2. Parameters for analysis of $CO_2$ electroconversion routes

| Parameter | Selected base value | Sensitivity range | Unit |
|---|---|---|---|
| **Production capacity** | 1 | 1 - 100 | kt$CO_2$ input/yr |
| **Plant lifetime** | 20 | 15 - 25 | years |
| **Annual operating time** | 4000 | 2000 - 8000 | h/yr |
| **Discount rate** | 10 | 5 - 15 | % |
| **Euro Reference year** | 2020 | | |
| **O&M cost factor** | 4 | 2 - 6 | % of initial CAPEX |
| **$H_2O$** | 1.0 | 0.5 – 2.0 | €/t$H_2O$ |
| **$CO_2$** | 50 | 20 - 150 | €/t$CO_2$ |
| **Electricity** | 40 | 20 - 60 | €/$MWh_e$ |

## 2.5 Cost projections through learning curve analysis

Estimates of today's production costs of our six routes are substantially higher compared to those of conventional processes that generate the same products from fossil resources (see section 4.2). The costs of these novel technologies are likely to decline significantly thanks to for instance scale-up, innovation, and learning-by-doing. These overall decline in costs of these phenomena together can be aggregated into a technology learning curve. A technology learning curve provides information on how fast costs (or another metric) decline in relation to the cumulative installed capacity (McDonald & Schrattenholzer, 2001; Ferioli *et al.*, 2009). Plotting empirical data of costs versus the cumulative installed capacity on two logaritmic axes generally results in a declining straight line. The slope of this line relates to the learning rate (LR), which specifies the rate (as a percentage) of cost reduction for each doubling in cumulative installed capacity. This relationship can be expressed by equation (3) in which $C_{X_t}$ represents the costs for a cumulative installed capacity $X_t$, , $C_{X_0}$ the initial costs at the initial cumulative installed capacity $X_0$, and b is the learning parameter from which the LR can be derived via equation (4).

$$C_{X_t} = C_{X_0}\left(\frac{X_t}{X_0}\right)^{-b} \qquad (3)$$

$$LR = 1 - 2^{-b} \qquad (4)$$

Many technologies, during their deployment, rather steadily follow their learning curve for many decades. Extrapolation of the historical learning curve can, thus, be a valuable tool to estimate future costs of a technology. For novel technologies a learning curve is generally non-existing or is not (yet) determined because barely any cumulative capacity has been installed and cost data is difficult to find. For such a technology, a learning curve can be estimated based on the State-of-the-Art and an assumed learning rate. A learning curve (or data) of comparable technologies might provide a good starting point for such assumptions.

We apply learning curve analysis to the direct investment costs of the technologies in our routes. We extrapolate historical learning curves of these technologies or, if no data is available, of comparable technologies to project the cost curves up to at least 2030 for different compound annual growth rates (CAGRs) for the analyzed technologies. We apply a low and high CAGR to explore a range in cumulative installed capacity in 2030. The CAGR values are based on various reported scenarios and existing plans and announcements for (comparable) technology deployment. We do not consider any limitations regarding annual capacity additions due to restrictions in market size of a specific product category because we foresee that until 2030 the share of electrochemical $CO_2$ conversion capacity remains relatively low compared to conventional capacity. Most of our core technologies are mainly developed for hydrogen or electricity production, i.e. water electrolyzers and solid oxide fuel cells. We postulate that the share of total capacity applied for electrochemical $CO_2$ conversion is relatively small in 2030. The specific amount of capacity employed for electrochemical $CO_2$ conversion cannot be deduced from the learning curves but will be discussed separately for each of the routes. We employ our CAPEX learning curves to calculate the future total investment costs (including indirect costs) and levelized production costs. We also project costs up to 2050. Although less reliable due to the many uncertainties regarding the successful scale-up of the conversion routes, such projections illustrate the possible trajectories of technology deployment and related cost reductions.

## 2.6 Environmental greenhouse gas performance

The sustainability of novel routes to convert $CO_2$ into various products is determined by their environmental impact over the total value chain. More detailed insight on several impact categories, such as climate change, ozone depletion, acidification, water use, and toxicity, requires extensive life-cycle analysis and is not the focus of this study. Here, we perform an analysis on the $CO_2$ emissions associated to each route to generate 1 GJ of product based on the emission factor of the electricity supply. The $CO_2$ feedstock is considered sustainable (i.e. originating from atmosphere, either directly via DAC or via biomass) and does not contribute to net emissions, not even when $CO_2$ is emitted again during the process via combustion of side products.

For each electrochemical route, we investigate the impact of the emission factor of electricity supply. We explore various levels of a decarbonized electricity: e.g. based on solar PV, wind turbines, fossil-based generators, or the average grid. The carbon intensity of the electrochemical processes is compared with the fossil reference (including end-of-life emissions) in terms of carbon footprint.

# 3 Electrochemical $CO_2$ conversion: State-of-the-Art

Here we describe the technical status of the chlor-alkali process and seven electrochemical $CO_2$ conversion approaches in terms of system size and configuration, technology readiness level (TRL), energy and mass balances, current investment costs, and existing projects.

## 3.1 Chlor-alkali process

The chlor-alkali electrolytic process is globally the main technology to produce chlorine and caustic soda. Three types of systems are widely applied: the mercury cell, diaphragm cell and membrane cell The first two have been commercialized in the late 19th century, while the membrane cell process is developed in the 1950s (O'Brien *et al.*, 2005; Crook & Mousavi, 2016). Due to concerns around the use of mercury and asbestos in respectively mercury and diaphragm cells, the membrane cell process has become the dominant technology, possessing a 60% share for chlorine production in 2012 in the EU-27 (Brinkmann *et al.*, 2014), and an 85% share in 2019 (Eurochlor, 2022). In all three processes, an electric potential is applied onto two electrodes to convert sodium chloride and water into sodium hydroxide, chlorine, and hydrogen.

$$2NaCl + 2H_2O \longrightarrow 2NaOH + Cl_2 + H_2$$

Another novel approach has recently entered the market, the so-called Oxygen Depolarised Cathode (ODC) cell, which is an update of the membrane cell approach. Rather than co-producing $H_2$, ODC cells consume $O_2$ at the cathode. This process benefits from a lower cell voltage (from around 3.0 V down to 2.0 V in the ODC process (Thyssenkrupp, 2020)) and thereby substantially reduces the total energy requirements (around 25% lower per kg $Cl_2$ produced).

$$2NaCl + H_2O + {}^1\!/_2\, O_2 \rightarrow Cl_2 + 2NaOH$$

Globally, around 90 Mt $Cl_2$ is annually produced next to around 100 Mt of caustic soda (Eurochlor, 2018). The total worldwide installed capacity for the membrane technology equals nearly 22-26 GW and will likely increase to fulfil chlorine demand of a growing chemical industry (Eurochlor, 2022). Chlor-alkali electrolysis produces as a by-product around 2% of total global hydrogen (IEA, 2019). The equipment is supplied by several manufacturers around the world, such as Thyssenkrupp. These companies will likely also provide equipment for the water electrolyzer industry and currently their combined annual equipment production capacity is roughly 2 GW/yr (NOW, 2018; IRENA, 2020). This capacity has substantially increased over the last years, because many companies prepare themselves for a rapidly increasing demand for electrolyzers.

### Mass and energy balances

The mass and energy balances of the current membrane electrolysis chlor-alkali process are summarised in the diagram from Figure 3.

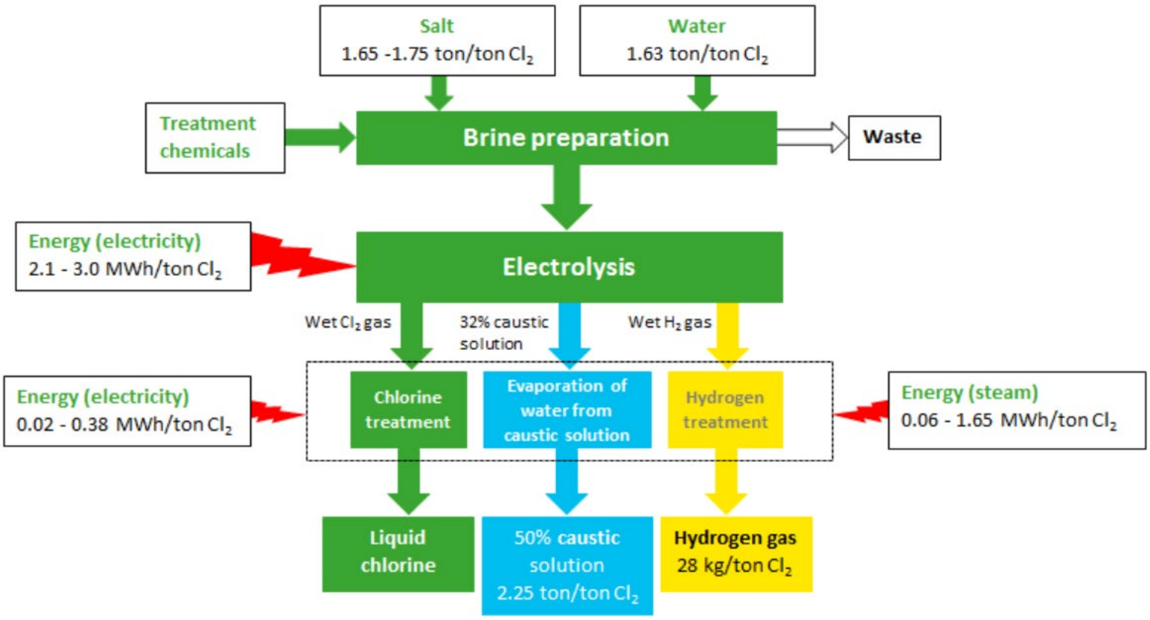

Figure 3. Overview of the chlor-alkali production process and the main material flows (reproduced from Eurochlor, 2018).

The complete chlor-alkali process starts from the NaCl salt and purified water. These two elements undergo a preparation process to produce the brine stream (concentrated aqueous salt solution) that will feed the electrolysis unit. The brine stream, along with the electricity input, yield the electrolysis process possible, producing a gaseous $Cl_2$ stream (anode side), $H_2$ (cathode side), and a concentrated aqueous caustic soda (NaOH) stream at the cathode. A post-treatment step for all three streams render the final $Cl_2$ product, a 50% NaOH (aq.) solution, and some $H_2$ gas.

The schematics of the electrolysis cells for both the $H_2$ co-production and the ODC system are given in Figure 4. The main particularity of the ODC system is the feeding of a gaseous $O_2$ stream to the cathode, and the suppression of the $H_2$ Evolution Reaction (HER). The final products of the electrolysis from the ODC system are as well $Cl_2$ and a concentrated NaOH solution.

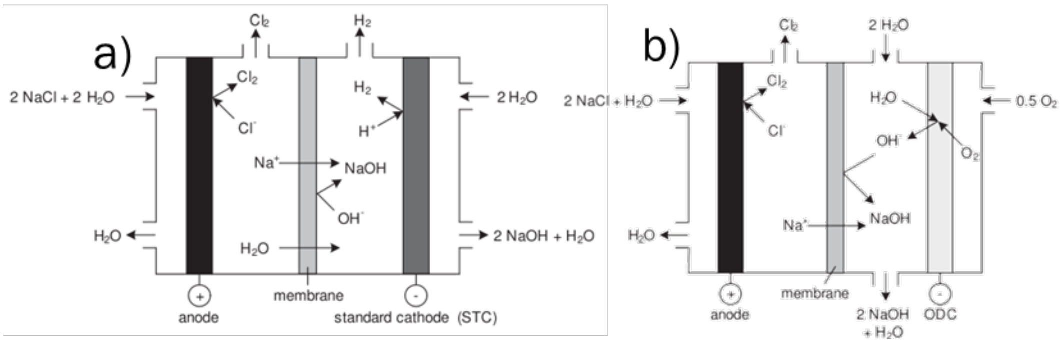

Figure 4. 1. Schematic design and operation of a single electrolysis cell a) with $H_2$ co-production and ;b) with an Oxygen Depolarised Cathode (ODC), with coupled $O_2$ consumption (reproduced from Jung *et al.*, 2014).

The complete mass and energy balances of both the $H_2$ co-production system and the ODC system for the chlor-alkali process are found in Table 3. The final purity of the $Cl_2$ gas is taken to be 98%vol., according to Thyssenkrupp (2015).

Table 3. Complete mass and energy balances for the chlor-alkali process, for $H_2$ co-production ($H_2$ co-p), and the Oxygen Depolarised Cathode (ODC) systems, based on the production of 1 kg $Cl_2$. Data retrieved from Jung *et al.*, 2014 and Eurochlor, 2018.

| **Flow** | | **Unit** | **$H_2$ co-p** | | **ODC** | |
|---|---|---|---|---|---|---|
| | | | Input | Output | Input | Output |
| **Electricity** | Stack | $kWh_{el}$ | 2.40 | - | 1.75 | - |
| | Post-treatment | $kWh_{el}$ | 0.08-2.03 | - | 0.08-2.03 | - |
| | Total | $kWh_{el}$ | 2.49-4.52 | - | 1.83-3.87 | - |
| **$H_2O$** | | kg | 1.65-1.75 | - | 1.65-1.75 | - |
| **NaCl** | | kg | 1.63-1.70 | - | 1.63-1.70 | - |
| **$O_2$** | | kg | - | - | 0.25 | - |
| **$Cl_2$ (>98%vol)** | | kg | - | 1 | - | 1 |
| **$H_2$ (>99,9%vol.)** | | kg | - | 0.03 | - | - |
| **NaOH (aq. 32%wt.)** | | kg | - | 1.13 | - | 1.13 |
| **NaOH (aq. 50%wt.)** | | kg | - | 2.25 | - | 2.25 |

The membrane electrolysis technology for the chlor-alkali process has undergone an optimisation process in terms of energy consumption, with new cell designs over the past 15 years. The new ODC design also represents a major improvement in the energy consumption for the chlor-alkali process. An overview of the Figure 5. The thermodynamic minimal energy requirements for both the $H_2$ co-production system and the ODC design are also plotted, showing the maximal optimisation potential of both technologies.

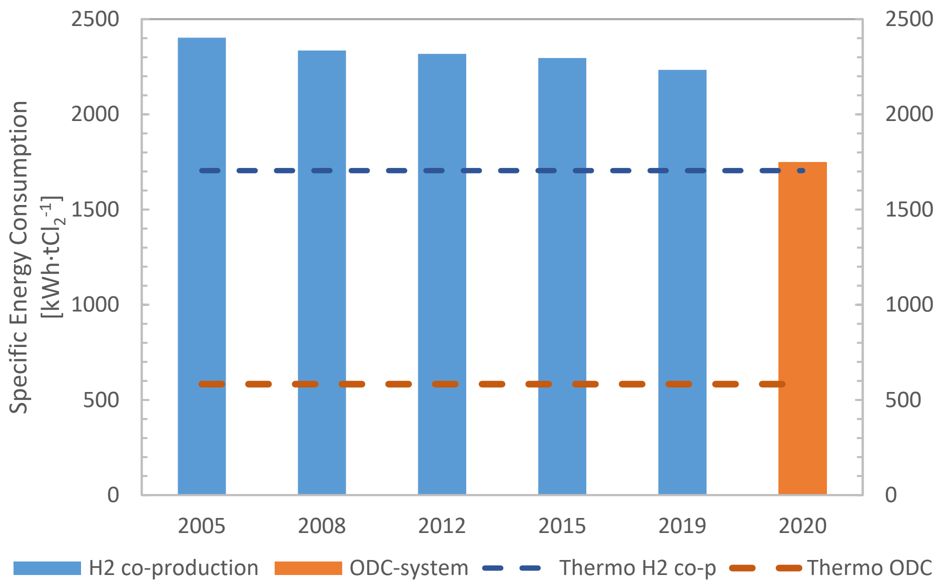

Figure 5. Evolution of the specific energy consumption for the production of $Cl_2$ through the membrane electrolysis technology since 2005. $H_2$ co-production is the technology seen in Figure 2 a), and Oxygen Depolarised Cathode (ODC), depicted in Figure 2 b). As well, the theoretical minimal energy requirements for both technologies are plotted, taking the thermodynamic

potentials for both electrochemical reaction mechanisms. Plot constructed with data from (Thyssenkrupp, 2015) and (Thyssenkrupp, 2020).

## 3.2 Low-temperature electroconversion to produce carbon monoxide

The low-temperature (LT) electrochemical reduction of $CO_2$ into carbon monoxide (CO) consists of the electrolysis unit, and a series of auxiliary units for the final production of a purified gaseous CO stream. A diagram of the complete process is shown in Figure 6.

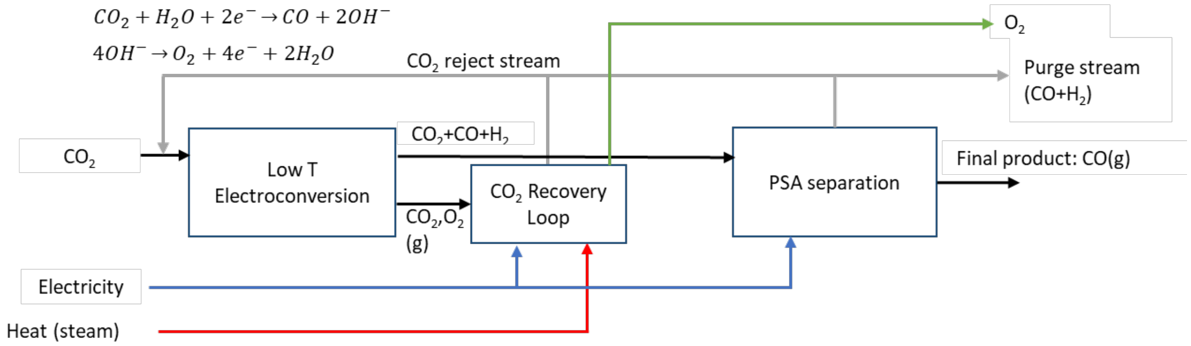

Figure 6. Process diagram of the LT $CO_2$ electrolysis towards CO.

The overall reaction of the process is displayed below. As it is shown, $CO_2$ is the only reactant in the process, yielding CO and $O_2$.

$$CO_2 \rightarrow CO + {}^1/_2\, O_2$$

The current state of development for the LT $CO_2$ conversion to CO technology is estimated to be at a TRL 5-6 (Nørskov et al., 2019). The most important project dealing with this process route is summarised in

Table 4.

Table 4. Summary of the most important development projects for LT $CO_2$ to CO.

| Project | Framework | Companies | Description |
|---|---|---|---|
| **Rheticus**[1] | Joint venture | Siemens Energy, Evonik | Joint Siemens-Evonik project with the aim of constructing and validating a 25 kW electrolyzer stack for the production of syngas ($CO+H_2$), the output of which will be then fed to a bio-reactor for the fermentation of this syngas into butanol and hexanol |

[1] (Siemens, 2020)

Current State-of-the-Art for LT electrolysis of $CO_2$ to CO involves the use of gas diffusion electrodes (GDEs) in a so-called Membrane Electrode Assembly (MEA) cell architecture, inspired by the PEM water electrolyzer design (Küngas, 2020). An Anion Exchange Membrane (AEM) is used to allow the ionic transport. A gaseous, humidified $CO_2$ stream is fed at the back of the cathode GDE, producing CO and unwanted $H_2$ through the HER. The cathode outlet stream contains $CO_2$, $H_2O$, CO and $H_2$. A depiction of the MEA cell for LT $CO_2$ to CO is shown in Figure 7.

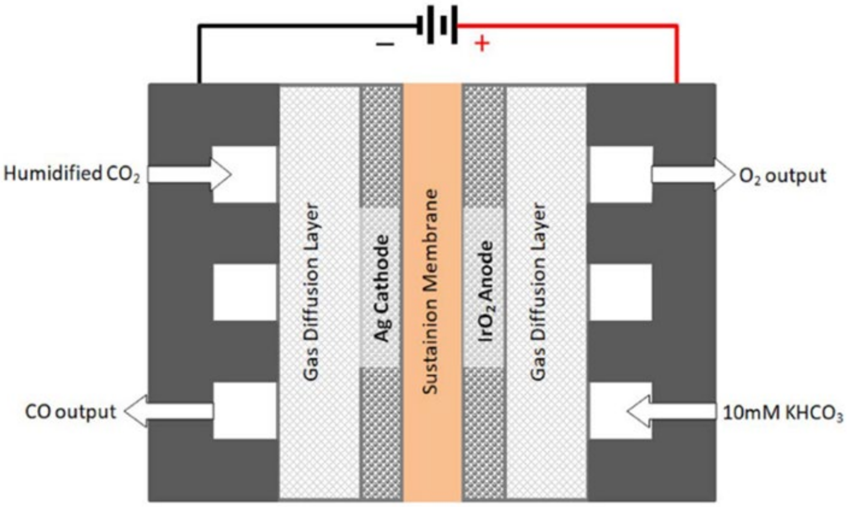

Figure 7. Schematics of a typical membrane electrode assembly (MEA) cell for $CO_2$ electrolysis to CO (reproduced from of Liu *et al.*, 2018). Nota bene: the anode side is shown in the right hand-side of the diagram, and the cathode side, on the left.

The alkaline nature of the cathode acts as a trap for the fed $CO_2$, converting it into carbonates. The negatively charged carbonates cross the AEM and end up in the anode compartment. There, given the acidic nature of the anode environment, carbonates are acidified and $CO_2$ is released, along with $O_2$, produced from the water oxidation reaction. A neutral anolyte can be used to provide water to the anode.

The $CO_2$ Utilisation Degree ($CO_2$UD) determines the extent to which $CO_2$ is effectively converted to the product of interest. It is defined as the ratio of the $CO_2$ converted to the product of interest and the total $CO_2$ inlet to the cathode. $CO_2$UD can be calculated as the ratio of the faradaic efficiency (FE), defined as the efficiency with which electrons participate in a given electrochemical transformation, towards the product and the total $CO_2$ consumed, as reported by Yang *et al.* (2021). A theoretical maximum of $CO_2$UD of 50% can be hypothesised for a 100% FE towards CO.

$$CO_2UD = \frac{FE_{product}}{CO_2\ consumed} \leq 50\%\ for\ CO_2 \rightarrow CO$$

The gas outlet from the anode side will contain $O_2$, $CO_2$ and some $H_2O$. Given the high $O_2$ concentration in this stream, $CO_2$ needs to be captured in an oxidation-resistant process, like a calcium caustic loop, used for DAC. Data was retrieved from Keith *et al.* (2018) for a caustic loop consisting of three steps: a pellet reactor, calciner, and slaker. The modelled loop for $CO_2$ reclaiming has electric energy as input for the high-temperature steps, and has as outputs a gas stream of $CO_2$, that is recycled back to the cathode inlet of the LT electrolyzer, and an $O_2$ gas stream.

On the cathode outlet, a mixture of $CO_2$ and CO (and traces of $H_2$ and $H_2O$), is sent to a pressure swing adsorption (PSA) unit for CO purification. The PSA unit delivers a commercial grade 98%vol CO stream (Air Products, 2022) as final output and a reject stream with $CO_2$ and CO, which can be recycled back to the $CO_2$ inlet stream towards the electrolyzer unit. The energy for this process is provided by electricity.

Current State-of-the-Art process performance indicators for the LT electrolysis of $CO_2$ to CO are reported in Table 5. As well, the prospects and targets for LT $CO_2$ electrolysis of towards different products, in terms of current density, cell voltage, and power density for the 2020 – 2030 decade are plotted in Figure 8. As it can be seen, the expected performance of LT $CO_2$ electrolysis by 2030 will approach that of the current PEM water electrolysis technology in terms of current density and power density. The power density variable is the product of the cell voltage and the partial current density (FE times total current density) towards the product of interest, and is a measure of the productivity of the cell in terms of delivered power per unit of electrode area.

Table 5. State-of-the-Art process performance parameters for the LT electrolysis of $CO_2$ to CO.

| **Parameter** | **Unit** | **Value** | **Reference** |
|---|---|---|---|
| **Current density** | A/m$^2$ | 2000 | Liu *et al.*, 2018 |
| **Cell voltage** | V | 3.0 | Liu *et al.*, 2018 |
| **Faradaic efficiency CO** | - | 98% | Liu *et al.*, 2018 |
| **$CO_2$ utilisation degree** | mole product/mole $CO_2$ in | 49% | Yang *et al.*, 2021 |
| **Carbon yield to product** | mole C-product/mole $CO_2$ reacted | 100% | Assumed |
| **Power density** | kW/m$^2$ | 6.00 | Calculated |

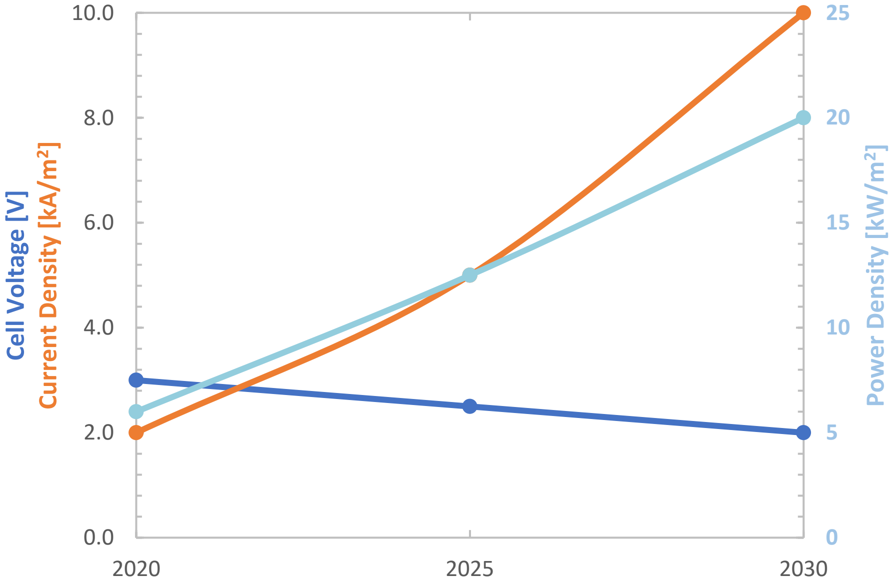

Figure 8. Roadmap for different process performance indicators for the LT $CO_2$ electrolysis for the 2020 decade. Considered products from the LT $CO_2$ electrolysis are CO, formic acid, and ethylene. Reproduced from Nørskov *et al.*, 2019.

The complete mass and energy balances for the LT electrolysis of $CO_2$ to CO process is shown in Table 6.

Table 6. Complete mass and energy balances for the LT electrochemical reduction of $CO_2$ to CO. The category '*Aux.+DSP*' corresponds to the energy requirements of the PSA unit for CO purification (data from Jouny *et al.*, 2018a) and the calcium caustic recovery loop for the $CO_2$ recovery in the anode side (data from Keith *et al.*, 2018). $CO_2$ emissions would correspond to the $CO_2$ content in the reject stream from the PSA unit.

| **Flow** | | **Unit** | **LT-CO** | |
|---|---|---|---|---|
| | | | **Input** | **Output** |
| **Electricity** | Stack | kWh$_{el}$ | 5.68-5.98 | - |
| | Aux.+DSP | kWh$_{el}$ | 1.29-1.36 | - |
| | Total | kWh$_{el}$ | 6.97-7.33 | - |

| **Flow** | **Unit** | **LT-CO** | |
|---|---|---|---|
| | | **Input** | **Output** |
| **$CO_2$** | kg | 1.60-1.69 | - |
| **$H_2O$** | kg | 0.01 | - |
| **CO (98%vol.)** | kg | - | 1 |
| **$O_2$** | kg | - | 0.58-0.61 |
| **$CO_2$ emissions** | kg | - | 0.00-0.05 |
| **$H_2$** | kg | - | 0.00 |

The estimation of the CAPEX investment costs for LT $CO_2$ electrolyzers must be done taking as starting point the most similar commercial technology available: water PEM electrolysis. The electrolysis unit investment costs are reported as a function of the total electrical installed capacity. The stack lifetime for the LT $CO_2$ electrolysis stacks is taken from the PEM water electrolysis technology, given the lack of data on long-term testing of this process at industrially relevant conditions. An overview of long-term performance data for several electrolysis technologies is given by Küngas, reporting > 4,000 h of operation for a LT $CO_2$ electrolysis unit for CO production . A summary of the different cost indicators is found in Table 7.

Table 7. Approximate uninstalled investment costs for a PEM electrolysis unit (stack and auxiliary equipment) for a 1 MW electrolysis unit in 2019. The cost share of the different components reported by Böhm *et al.* refer to the '*Total electrolysis system uninstalled costs'* row of the table. The '*power density'* factor for PEM electrolysis is reported by Mayyas *et al.* (2019) for a PEM system with a performance of 1.70 kA/m$^2$ at 1.7 V total cell voltage.

| **Parameter** | **Unit** | **Value** | **Reference** |
|---|---|---|---|
| **Total PEM electrolysis system uninstalled costs** | €/kW | 667 – 1450 | Patonia *et al.*, 2022 |
| **Stack costs share** | - | 60% | Böhm *et al.*, 2019 |
| **Power electronics cost share** | - | 15% | Böhm *et al.*, 2019 |
| **Gas conditioning cost share** | - | 10% | Böhm *et al.*, 2019 |
| **Balance of plant cost share** | - | 15% | Böhm *et al.*, 2019 |
| **Power density PEM electrolysis** | kW/m$^2$ | 28.9 | Mayyas *et al.*, 2019 |
| **Stack lifetime** | h | 40,000 | Tichler *et al.*, 2018 |

Given the different power density for the water PEM electrolysis and the LT $CO_2$ electrolysis, the reported values for investment costs for the PEM systems need to be adapted to the performance indicators for LT $CO_2$ electrolysis. This can be done with the following equation, using the power density for both water PEM electrolysis and LT $CO_2$ electrolysis (see Table 5), as indicated by Barecka *et al.* (2021):

$$CAPEX(LT-CO_2)\left[\frac{€}{kW_{LT-CO_2}}\right] = CAPEX(PEM)\left[\frac{€}{kW_{PEM}}\right]\cdot\frac{PD(PEM)\left[{kW_{PEM}}/{m^2}\right]}{PD(LT-CO_2)\left[{kW_{LT-CO_2}}/{m^2}\right]}$$

The investment costs for the calcium caustic recovery loop for the $CO_2$ recovery from the anode side and the PSA unit for the CO purification must also be taken into consideration to estimate the total system costs for the LT $CO_2$ electrolysis to CO. These data can be found in Table 8.

Table 8. Summary of the different CAPEX contributions for the LT $CO_2$ electrolysis to CO system in terms of the $CO_2$ recovery loop from the anode, and the CO purification section.

| Parameter | Unit | Value | Reference |
|---|---|---|---|
| **Calcium caustic recovery loop investment costs (reference capacity)** | M€ | 235.4<br>(122.5 t $CO_2$/h) | Keith *et al.*, 2018 |
| **PSA CO /$CO_2$ separation investment costs (reference capacity)** | M€ | 1.70<br>(1000 $Nm^3$/h) | Jouny *et al.*, 2018a<br>Paturska *et al.*, 2015 |
| **Scaling factor** | - | 0.7 | Jouny *et al.*, 2018a |

### 3.3 Low-temperature electroconversion to produce formic acid

The LT electrochemical reduction of $CO_2$ into formic acid (FA or CHOOH)/formate consists of the electrolysis unit, and a series of auxiliary units for the final production of a purified aqueous FA stream. A diagram of the complete process is shown in Figure 9.

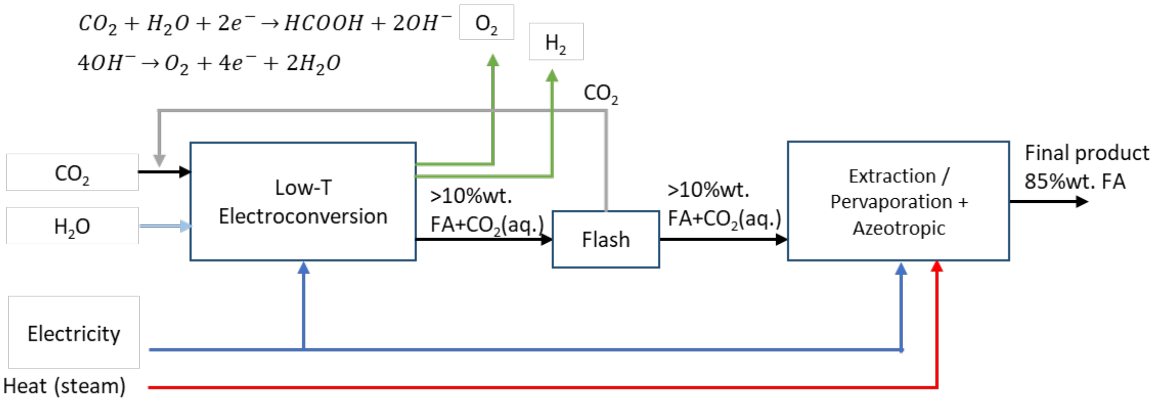

Figure 9. Process diagram of the LT $CO_2$ electrolysis towards FA.

The overall reaction of the process is displayed below. As it is shown, $CO_2$ and $H_2O$ are the reactants of the process, yielding FA and $O_2$.

$$CO_2 + H_2O \rightarrow FA + {}^{1}/_{2}\,O_2$$

The current development stage for the LT $CO_2$ conversion FA is claimed to be at a TRL 3-5 (Schuler *et al.*, 2020). The most important projects dealing with this process route are summarised in Table 9.

Table 9. Summary of the most important development projects for LT $CO_2$ to FA.

| Project | Framework | Companies | Description |
|---|---|---|---|
| **OCEAN**[1] | A.SPIRE | AVANTIUM, ERIC, IIT, Gaskatel, Politecnico di Torino, RWE, Universiteit Amsterdam | Achieve a TRL 6 development stage for the electrochemical conversion of $CO_2$ to formate (250 g/h at 1500 A/m$^2$) |
| ***e*2C**[2] | Interreg 2-Seas | TNO, VITO, Universiteit Antwerp, Lille University, University of Sheffield, University of Exeter, TU Delft | Build a pilot demonstrator for the LT $CO_2$ conversion to FA and validate the technology at TRL 6 |
| **ECFORM**[3] | - | DNV GL | Semi-pilot ECFORM demonstration reactor with a 600 cm$^2$ surface area and a capacity of reducing approximately 1 kg $CO_2$/d. From 1 t of $CO_2$, the process produces 1.04 t of formic acid in the form of a minimum 85 wt% distillate. |

[1] OCEAN (2022); [2] e2C (2022); [3] Zhu (2019)

Current State-of-the-Art for LT electrolysis of $CO_2$ to FA involves the use of GDEs and a special electrochemical cell design with an acidic centre compartment for the direct production of FA and not the deprotonated formate ($HCOO^-$), which would lead to a costly downstream protonation step with an electrodialysis process for FA production, as reported by Ramdin *et al.*, 2019.

An electrochemical cell design that is reported to directly produce a diluted (up to 10%w/w) FA aqueous stream is reported by Yang *et al.* (2020). The cell is a 3-compartment electrolyzer, featuring a cathode GDE for the conversion of gaseous $CO_2$ to $HCOO^-$, a AEM directly attached to the cathode GDE that allows for the direct migration of $HCOO^-$ anions towards a centre compartment. In this middle compartment, acid cation exchange media are present to provide both electrical conductivity and protons to form FA from $HCOO^-$. At the other side, an anode GDE is fed with liquid water for $O_2$ production. This GDE is directly attached to a CEM to allow for the transport of protons from the Oxygen Evolution Reaction (OER) at the anode. The sketch of said cell design is shown in Figure 10.

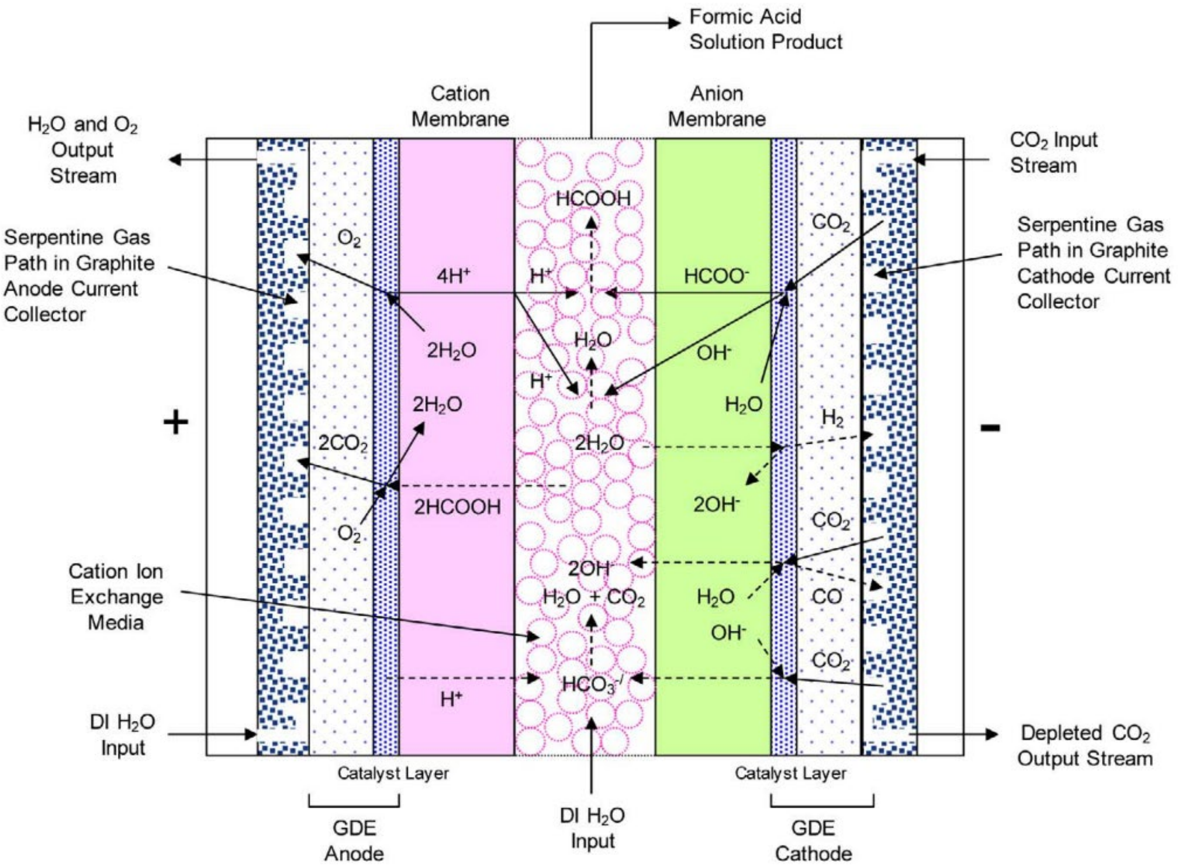

Figure 10. Depiction of the 3-compartment electrochemical cell for the direct production of FA through a LT $CO_2$ electrolysis process, showing proposed electrochemical reactions and ion transport. Reproduced from Yang *et al.*, 2017. Nota bene: the anode side is shown in the left hand-side of the diagram, and the cathode side, on the right.

Analogously as for the LT $CO_2$ to CO route, some $CO_2$ will migrate from the gas compartment to the electrolyzer in the form of bicarbonates. The $CO_2$UD can also be assumed as half of the FE towards FA. The bicarbonate anions will cross towards the middle compartment, and, given the acidic nature of the latter (as reported by Yang *et al.*, 2020, they can reach a 10%wt. FA concentration, with a pH of ca. 1.0), $CO_2$ will be stripped out from this compartment, which can be easily separated from the aqueous FA stream with a flash unit, as seen in Figure 9. Therefore, there is no need of adding a $CO_2$ recovery loop for the anode outlet stream, as for the LT $CO_2$ to CO route.

The outlet FA stream from the middle compartment is an aqueous solution with a concentration up to 10%wt. (as reported by Yang *et al.*, 2020), and that can be fed to a hybrid extraction-distillation process to achieve industrially relevant concentrations of FA, >85%wt. (aq.), as proposed by Ramdin *et al.* (2019). The simplified process flow diagram of this purification section is depicted in Figure 11.

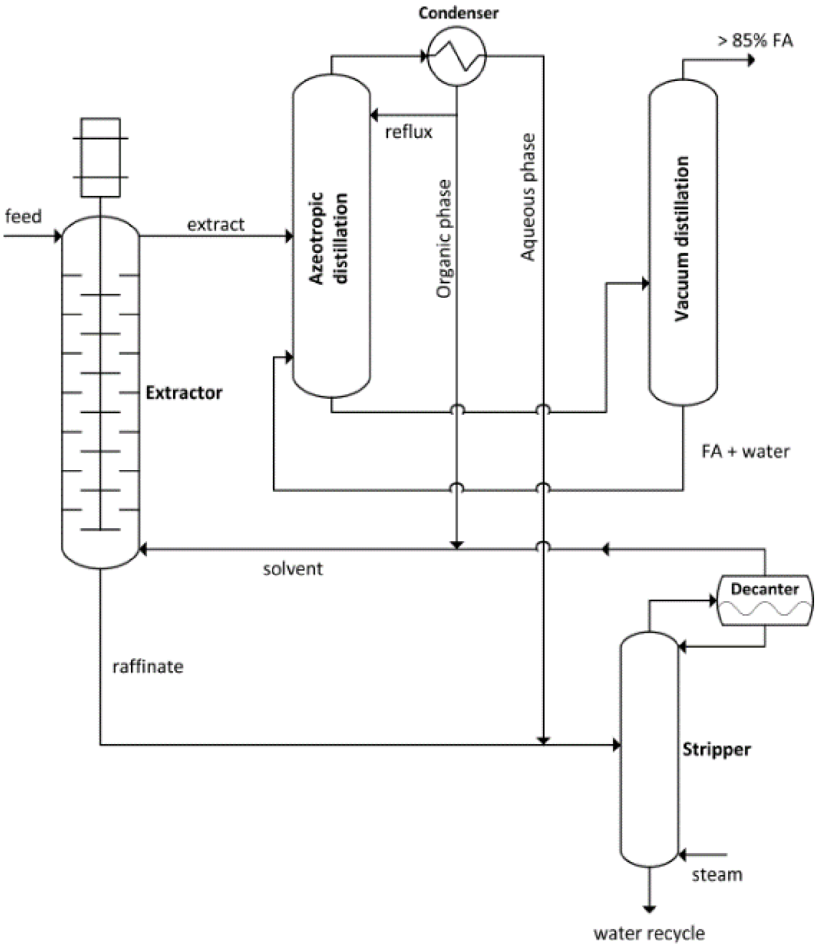

Figure 11. Hybrid extraction + azeotropic distillation strategy for the purification of an aqueous FA solution with a low boiling solvent. In the extractor, this solvent removes FA from water. The extract is sent to an azeotropic distillation column, recovering the azeotrope water-solvent at the top, and a highly concentrated FA stream at the bottom. The top fraction, biphasic, is split into two phases, being the organic phase (rich in solvent) partly recycled back to the azeotropic distillation column, and the rest being sent to a stripper to remove all water, along with the aqueous phase of the azeotropic distillation column. The bottom of this column is sent to a vacuum distillation column, in which an 85%wt. FA solution is recovered at the top. Reproduced from Ramdin *et al.*, 2019.

Current State-of-the-Art process performance indicators for the LT electrolysis of $CO_2$ to FA are reported in Table 10. The $CO_2$ utilisation degree is dependent on the FE towards the desired product (FA). In this case, the FE values are taken from the row above, and the displayed range is a function of the range for FE towards FA

Table 10. State-of-the-Art process performance parameters for the LT electrolysis of $CO_2$ to FA.

| Parameter | Unit | Value | Reference |
|---|---|---|---|
| **Current density** | $A/m^2$ | 2000 | Yang *et al.*, 2020 |
| **Cell voltage** | V | 3.75 | Yang *et al.*, 2020 |
| **Faradaic efficiency FA** | - | 73 – 91% | Yang *et al.*, 2020 |

| Parameter | Unit | Value | Reference |
|---|---|---|---|
| **$CO_2$ utilisation degree** | mole product/mole $CO_2$ in | 37 – 46% | Yang *et al.*, 2021 |
| **Carbon yield to product** | mole C-product/mole $CO_2$ reacted | 100% | Assumed |
| **Power density** | kW/m$^2$ | 7.50 | Calculated |

The complete mass and energy balances for the LT electrolysis of $CO_2$ to FA process is shown in Table 11.

Table 11. Complete mass and energy balances for the LT electrochemical reduction of $CO_2$ to CO. The category '*Aux.+DSP*' corresponds to the energy requirements of the hybrid extraction and azeotropic distillation for the purification of an aqueous FA stream up to 85%wt. (data from Ramdin *et al.*, 2019).

| Flow | | Unit | LT-FA | |
|---|---|---|---|---|
| | | | Input | Output |
| **Electricity** | Stack | kWh$_{el}$ | 4.08 – 5.09 | - |
| | Aux.+DSP | kWh$_{el}$ | 1.42 | - |
| | Total | kWh$_{el}$ | 5.50 – 6.51 | - |
| **$CO_2$** | | kg | 0.81 | - |
| **$H_2O$** | | kg | 0.58 – 0.79 | - |
| **FA (85%wt. aq.)** | | kg | - | 1 |
| **$O_2$** | | kg | - | 0.33 – 0.41 |
| **$CO_2$ emissions** | | kg | - | - |
| **$H_2$** | | kg | - | 0.00 – 0.01 |

The estimation of the investment costs for the electrolysis unit for the LT $CO_2$ electrolysis to formic acid is done analogously as with the LT $CO_2$ to CO case (see Table 7), with the power density of both water PEM electrolysis and the one for formic acid (see Table 10). To have a comprehensive analysis of the overall investment costs for the LT $CO_2$ to formic acid route, the downstream hybrid extraction and distillation train for the formic acid purification has also to be taken into account. Data for the estimation of the investment costs for this section can be seen in Table 12.

Table 12. Total uninstalled investment costs for the hybrid extraction and distillation unit for the recovery of formic acid.

| Parameter | Unit | Value | Reference |
|---|---|---|---|
| **Hybrid extraction + distillation train investment costs (reference capacity)** | M€ | 7.88<br>(1000 kg $CO_2$/h) | Ramdin *et al.*, 2019 |
| **Scaling factor** | - | 0.7 | Assumed |

### 3.4 Low-temperature electroconversion to produce ethylene

The LT electrochemical reduction of $CO_2$ into ethylene ($C_2H_4$) consists of the electrolysis unit, and a series of auxiliary units for the final production of a purified gaseous $C_2H_4$ stream. A diagram of the complete process is shown in Figure 12.

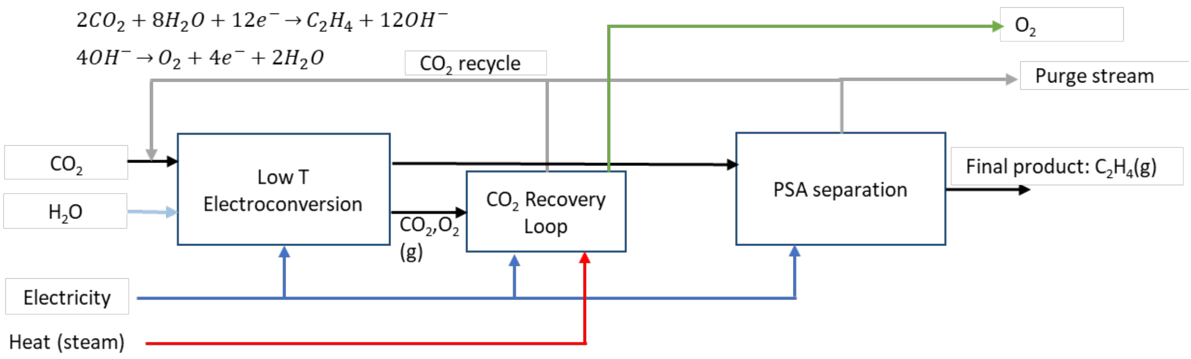

Figure 12. Process diagram of the LT $CO_2$ electrolysis towards $C_2H_4$.

The overall reaction of the process is displayed below. As it is shown, $CO_2$ and $H_2O$ are the reactants of the process, yielding $C_2H_4$ and $O_2$.

$$2CO_2 + 2H_2O \rightarrow C_2H_4 + 3O_2$$

The current development stage for the LT $CO_2$ conversion $C_2H_4$ is claimed to be at a TRL 3-4 (Schuler *et al.*, 2020). The most important projects dealing with this process route are summarised in Table 13.

Table 13. Summary of the most important development projects for LT $CO_2$ to $C_2H_4$.

| Project | Framework | Companies | Description |
|---|---|---|---|
| **SELECT $CO_2$[1]** | EU Horizon 2020 | TU Berlin, EPFL, TU Delft, RINA, DTU, De Nora, Pretexo, University of Surrey, SLAC | Development of the LT $CO_2$ electrolysis technology to achieve TRL 4 for $C_2H_4$ production |
| **Electrochemical $CO_2$ reduction to Ethylene for industrial applications[2]** | Energi forskning | Siemens, DTU | Joint Siemens & DTU project for large-scale production of a generic electrode platform for electrochemical reduction of $CO_2$ to ethylene |

[1] SELECT $CO_2$ (2022); [2] Energiforskning (2022)

Current State-of-the-Art for LT electrolysis of $CO_2$ to $C_2H_4$ involves the use of GDEs and a MEA-type of cell design, analogous to that for the LT CO production (see Figure 7). In the LT $C_2H_4$ case, a humidified $CO_2$ gas stream is fed to the cathode GDE gas side, that is separated with an AEM from the anode GDE side. In the anodic side, an alkaline aqueous stream is fed to sustain the OER. The cathode outlet stream contains $CO_2$, $H_2O$, $C_2H_4$, other C-gaseous products, possible C-liquid products, and $H_2$. A depiction of the MEA cell for LT $CO_2$ to $C_2H_4$ is shown in Figure 13.

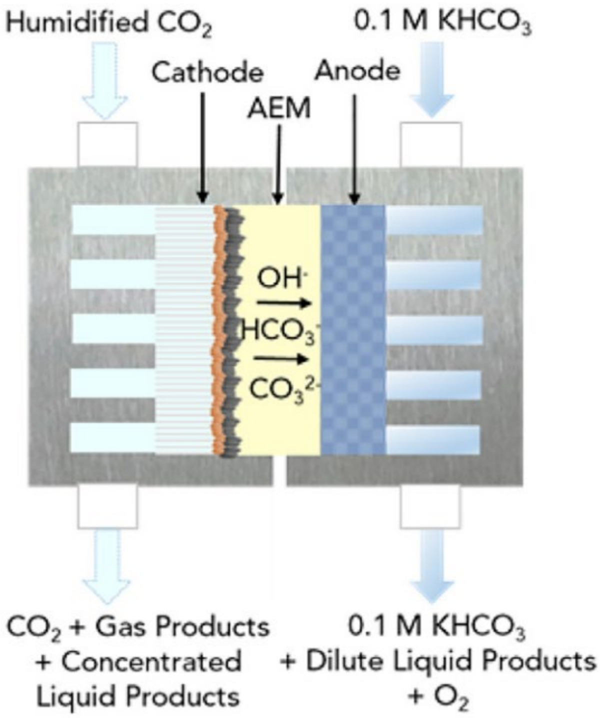

Figure 13. Schematic diagram of the MEA cell for the LT electrolysis of $CO_2$ to $C_2H_4$. Reproduced from Gabardo *et al.* (2019). Nota bene: the anode side is shown in the right hand-side of the diagram, and the cathode side, on the left.

As for the LT CO production case, the alkaline nature of the cathode acts as a trap for the fed $CO_2$, converting it into carbonates, migrating through the AEM towards the anode side. For the $C_2H_4$ reaction, given the high electron exchange and high $OH^-$ anions produced at the cathode per $C_2H_4$ molecule produced (12 electrons and 12 $OH^-$ molecules per $C_2H_4$ produced), the $CO_2$ lost to $CO_2$ reacted ratio is even higher than for the LT CO scenario, given the high local alkalinity at the vicinity of the cathode surface, acting as a 'trap' for the supplied CO2 in the form of carbonates. Gabardo *et al.* (2019) report a 4:1 ratio for the $CO_2$ lost to $CO_2$ reacted (i.e., $CO_2$UD = 20%). Sisler *et al.* (2021) report a more optimistic scenario of a 2:1 ratio ($CO_2$UD = 33%).

Due to the $CO_2$ crossover from the cathode to the anode the gas outlet from the anode side will contain $O_2$, $CO_2$ and some $H_2O$. A calcium caustic recovery loop for $CO_2$ reclaiming will be considered, as it was done for the LT CO case. The recovered $CO_2$ from this loop will be fed back to the cathode inlet of the LT electrolyzer, as well, a gaseous $O_2$ stream will come as an outlet of the $CO_2$ recovery loop.

On the cathode outlet, a mixture of $CO_2$, $C_2H_4$, and traces of $H_2$ and $H_2O$ is sent to a PSA unit for $C_2H_4$ purification. The final outputs from this PSA unit will be a commercial grade 99.9%wt. $C_2H_4$ stream (NIH, 2022), and a reject stream with $CO_2$ and $C_2H_4$. A simplified process diagram of the complete LT $C_2H_4$ production process is shown in Figure 14.

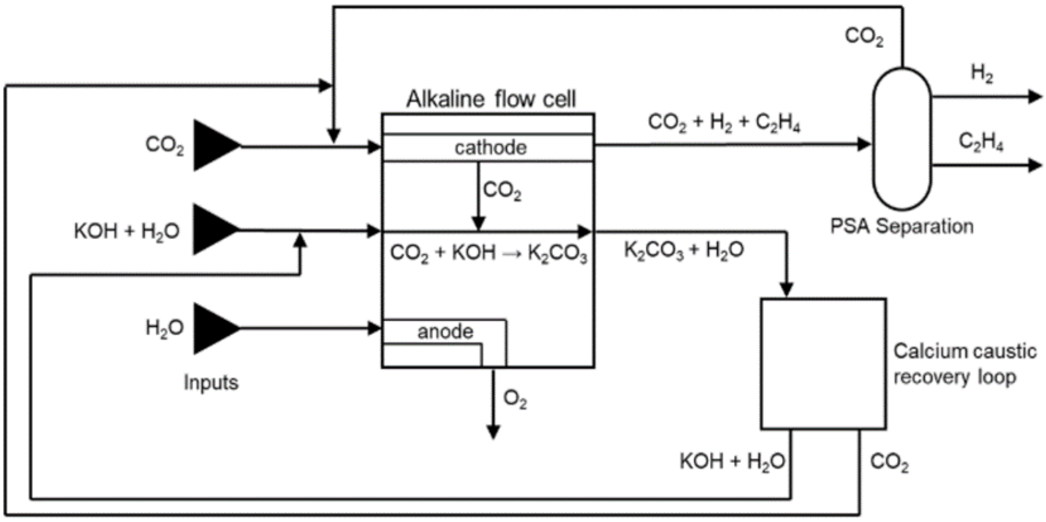

Figure 14. Process flow diagrams for each electrolyzer cell and cascade considered for $CO_2$ reduction towards ethylene in an alkaline flow cell. Reproduced from Sisler *et al.* (2021).

Current State-of-the-Art process performance indicators for the LT electrolysis of $CO_2$ to $C_2H_4$ are reported in Table 14.

Table 14. State-of-the-Art process performance parameters for the LT electrolysis of $CO_2$ to $C_2H_4$. The carbon yield to product is calculated as the ratio between the Faradaic Efficiency (FE) towards the final product, $C_2H_4$, and the FE towards all carbon-products (incl. $C_2H_4$).

| Parameter | Unit | Value | Reference |
|---|---|---|---|
| **Current density** | A/m$^2$ | 1200 | Dinh *et al.*, 2018 |
| **Cell voltage** | V | 3.70 | Dinh *et al.*, 2018 |
| **Faradaic efficiency $C_2H_4$** | - | 64% | Dinh *et al.*, 2018 |
| **$CO_2$ utilisation degree** | mole product/mole $CO_2$ in | 20% | Dinh *et al.*, 2018 |
| **Carbon yield to product ($C_2H_4$)** | mole C-product/mole $CO_2$ reacted | 86% | FE($C_2H_4$)=64%; FE(C-products)=74%* |

*FE(C-products) refer to all $CO_2$-derived products converted electrochemically, incl. $C_2H_4$.

The complete mass and energy balances for the LT electrolysis of $CO_2$ to $C_2H_4$ process is shown in Table 15.

Table 15. Complete mass and energy balances for the LT electrochemical reduction of $CO_2$ to $C_2H_4$. The category '*Aux.+DSP*' corresponds to the energy requirements of the PSA unit for $C_2H_4$ purification (data from Jouny *et al.*, 2018a) and the calcium caustic recovery loop for the $CO_2$ recovery in the anode side (data from Keith *et al.*, 2018). $CO_2$ emissions would correspond to the $CO_2$ content in the reject stream from the PSA unit.

| Flow | | Unit | LT-$C_2H_4$ | |
|---|---|---|---|---|
| | | | Input | Output |
| **Electricity** | Stack | kWh$_{el}$ | 75.7 – 79.7 | - |
| | Aux.+DSP | kWh$_{el}$ | 2.89 – 3.05 | - |
| | Total | kWh$_{el}$ | 78.6 – 82.7 | - |

| **Flow** | **Unit** | **LT-$C_2H_4$** | |
|---|---|---|---|
| | | **Input** | **Output** |
| **$CO_2$** | kg | 4.62 – 4.78 | - |
| **$H_2O$** | kg | 2.85 – 2.92 | - |
| **$C_2H_4$ (99.9%wt.)** | kg | - | 1 |
| **$O_2$** | kg | - | 5.36 – 5.55 |
| **$CO_2$ emissions** | kg | - | 0.00 – 0.05 |
| **CO (side product)** | kg | | 0.94 |
| **$H_2$** | kg | - | 0.17 |

The estimation of the investment costs for the electrolysis unit for the LT $CO_2$ electrolysis to ethylene is done analogously as with the LT $CO_2$ to CO case (see Table 7), and for the LT $CO_2$ to formic acid route, with the power density of both water PEM electrolysis and the one for formic acid (see Table 7). With respect to the estimation of the investment costs for the PSA unit, data from the LT $CO_2$ to CO case (see Table 8) can be taken and adapted to the present route.

## 3.5 High-temperature solid oxide electroconversion to produce carbon monoxide

High-temperature (HT) electrolysis in a solid oxide electrolyzer (SOE) is the only $CO_2$ electrolysis technology that is approaching commercialization (TRL 8) (Küngas, 2020). The technology is based on solid oxide cells (SOC) technology presented in Figure 15, composed of ceramic-based components (cathode and anode electrodes and electrolyte) able to produce CO via the electrolysis of $CO_2$ at elevated temperatures (600-800°C). In the SOC principle, $CO_2$ is fed to the cathode side of the cell via gas channels, which helps to distribute the gas across the cell. In the porous cathode (fuel electrode) $CO_2$ is reduced to CO. The electrons for the reaction are provided by an external power supply. The oxide ions ($O^{2-}$) formed in the reaction are incorporated into the electrolyte and traverse through the electrode into the anode, where the ions are oxidized into molecular oxygen (Küngas, 2020).

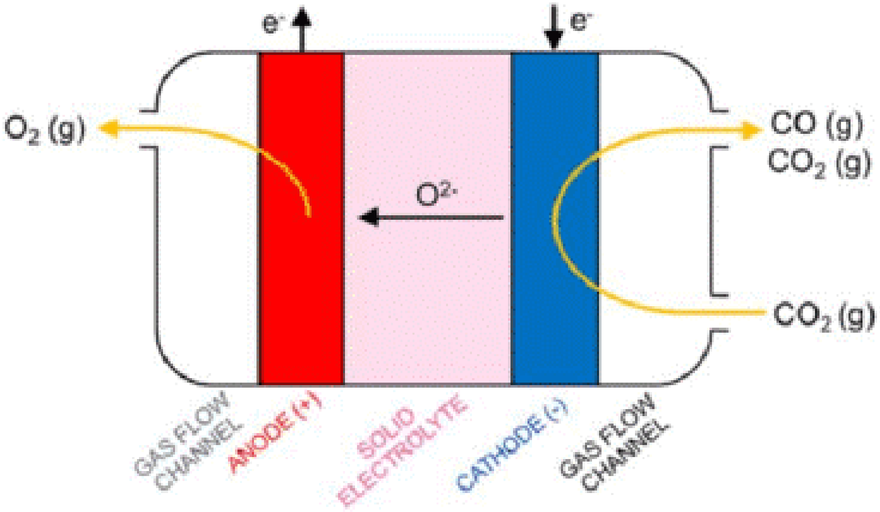

Figure 15: Principle of CO production in a Solid Oxide Cell (Küngas, 2020)

State-of-the-art on $CO_2$-SOE technology

The SOE concept for CO production has been exclusively developed on the system scale by the technology supplier Topsøe (Küngas, 2020). Topsøe technology is based on electrode supported SOC technology (Figure 16-1), operating at the temperature of 700°C, thanks to the thin Yttria-stabilized zirconia (YSZ) electrolyte design allowing the conduction of $O^{2-}$ ions at this temperature with a low internal resistance, a Ni-YSZ fuel electrode cermet (cathode) able to convert CO into $CO_2$ and a perovskite-based anode La0.6Sr0.4Co0.2Fe0.8O3- (Ce0.9Gd0.1)O1.95 (LSCF-CGO) able to reconvert $O^{2-}$ ions into $O_2$. All layers constitute the core of the single repeating SOC units (Figure 16-2) assembled in a stack design (Figure 16-3), with the addition of metallic-based bipolar separators and end plates enabling gas and current transfer through the cell and stack and sealing components next to each bipolar separator plate to prevent gas-crossing between the anode and cathode sides.

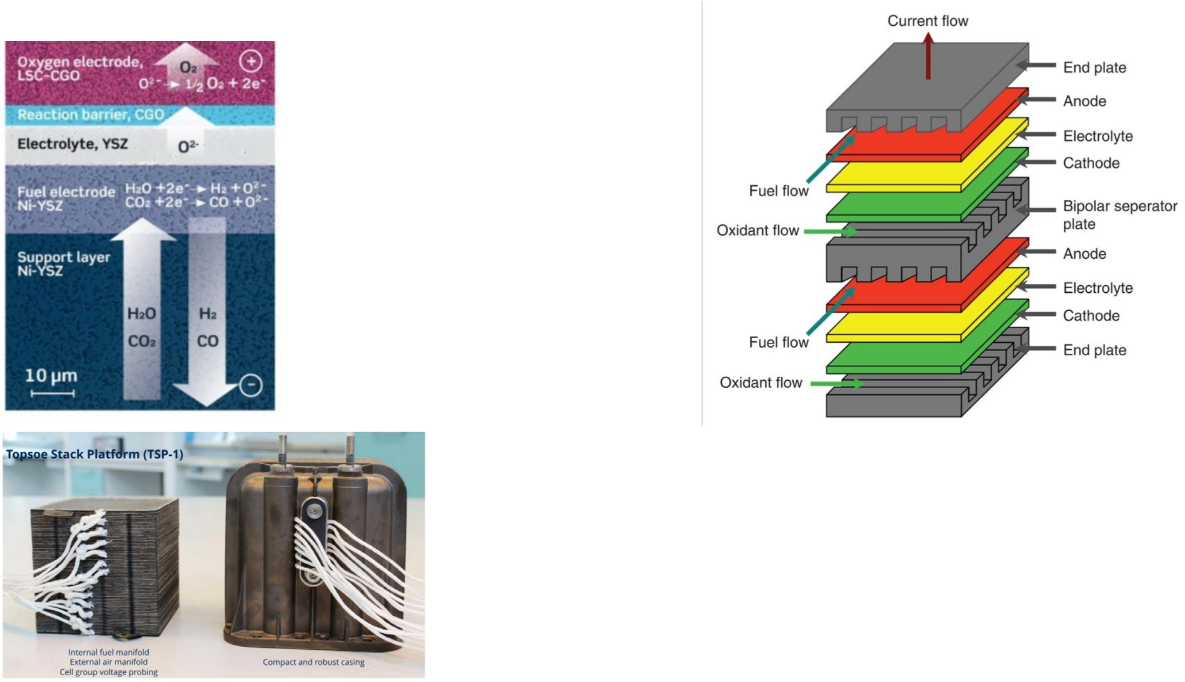

Figure 16. Top left: Electrode supported Solid Oxide Cell design developed by Haldor Topsøe (2022), Right: Scheme of two single repeating SOC units design in a SOE stack (Singhal, 2014), Bottom left: Topsøe stack design developed for CO production (Topsøe, 2022).

Topsøe developed this stack technology for direct implementation on the system level for CO production on an industrial site, in a stand-alone unit connected with power, $CO_2$, and product gas, as shown in Figure 17. It can produce on-demand at capacities ranging from 1 to 250 kg/h of CO.

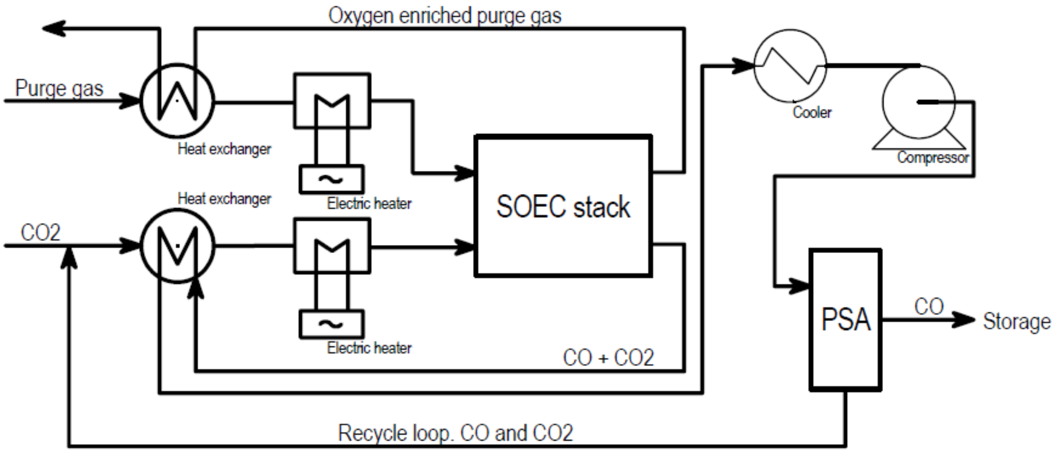

Figure 17. Block flow diagram for Topsøe's eCOS unit for the SOE $CO_2$ to CO process (Duhn, 2017).

Single-pass conversion of $CO_2$ to CO depends on the operating temperature of the SOE stack (Duhn, 2017). The limitation for high single-pass conversion of $CO_2$ is due to carbon formation by the Boudouard reaction and resulting degradation of the cell. For the base case, single-pass $CO_2$ conversion of 50% is assumed and the overall conversion is assumed to be 100%. Hence, on a system level, 1 mole of $CO_2$ will produce 1 mole of CO. The electric power consumption for the stack varies between 2.6 to 2.8 kWh/kg of CO and depends on the operating voltage (Küngas *et al.*, 2019). Total system energy consumption depends on the level of heat integration and single-pass $CO_2$ conversion. The total energy consumption for system will be in between 4.7 to 6.3 kWh per kg CO produced. Based on stoichiometry, for 1 mole of CO produced, 0.5 mole of oxygen will be produced (produced oxygen has to be diluted with sweep air due to safety issues in the stack). Assumed commercial grade CO product purity is around 98% (volume), as specified in section 3.2 for LT CO production (Air Products, 2022). Moreover, in the PSA unit, there will be a trade-off between yield and purity of CO (Kasuya & Tsuji, 1991). Current process performance parameters for CO production are as shown in Table 16.

Table 16. State-of-the-Art process performance parameters for the HT electrolysis of $CO_2$ to CO.

| **Parameter** | **Unit** | **Value** | **Reference** |
|---|---|---|---|
| **Current density** | $A/m^2$ | 7500 | Foit,*et al.*, 2020 |
| **Cell voltage** | V | 1.4 | Foit,*et al.*, 2020 |
| **Faradaic efficiency CO** | - | 100% | Küngas, 2020 |
| **$CO_2$ utilisation degree** | mole product/mole $CO_2$ in | < 60% | Duhn, 2017 |
| **Carbon yield to product** | mole C-product/mole $CO_2$ reacted | 100% | Assumed |
| **Power density** | $kW/m^2$ | 11.0 | Calculated |

Here, the system capacity is assumed to be 1 $MW_e$. Total uninstalled CAPEX for the system is calculated based on the steam electrolysis data taken from Hydrogen Europe targets. The split of CAPEX was assumed to be 30% for the cell stack, 30% for the power electronics, 6% for the gas conditioning, and 34% for the balance of plant (Böhm *et al.*, 2019). CAPEX for $CO_2$ electrolysis is scaled based on the ratio of power density ($kW/m^2$) for steam and $CO_2$ electrolysis. Further, $CO_2$ electrolysis will require an additional separation unit (PSA) compared with steam electrolysis. CAPEX for the PSA unit has been calculated by taking the total flow rate of $CO_2$ and CO entering the PSA unit as basis (Paturska *et al.*, 2015). Table 17 shows the overall mass and energy balance for $CO_2$-SOE production system.

Table 17. Complete mass and energy balance for the $CO_2$- SOE to CO production.

| **Flow** | | **Unit** | | |
|---|---|---|---|---|
| | | | **Input** | **Output** |
| | | | | |
| **Flow** | | **Unit** | | |
| | | | **Input** | **Output** |
| **Electricity** | Stack | $kWh_{el}$ | 2.6 – 2.8 | - |
| | Balance of plant | $kWh_{el}$ | 2.1 - 3.5 | - |
| | Total | $kWh_{el}$ | 4.7 – 6.3 | - |
| **$CO_2$** | | kg | 1.57-1.65 | - |
| **$H_2O$** | | kg | - | - |
| **CO** | | kg | - | 1 |
| **$O_2$** | | kg | | 0.54 – 0.57 |
| **$CO_2$ emissions** | | kg | - | - |
| **Heat** | | GJ | - | - |

The estimation of the CAPEX investment costs for $CO_2$-SOE electrolyzers can be done by taking CAPEX values of steam electrolysis as a starting point. The electrolysis unit investment costs are reported as a function of the total electrical installed capacity. A summary of the different cost indicators is presented in Table 16.

Table 18. Cost indicators for SOE HT $CO_2$ electrolyzer system for CO production for a 1 MW electrolysis unit.

| Parameter | Unit | Value | Reference |
|---|---|---|---|
| **Total SOEC electrolysis system uninstalled costs** | €/kW | 520-2130 | Hydrogen Europe, 2020 |
| **Stack costs share** | - | 30% | Böhm *et al.*, 2019 |
| **Power electronics cost share** | - | 30% | Böhm *et al.*, 2019 |
| **Gas conditioning cost share** | - | 6% | Böhm *et al.*, 2019 |
| **Balance of plant cost share** | - | 34% | Böhm *et al.*, 2019 |
| **Power density SOEC electrolysis** | $kW/m^2$ | 11.0 | Foit *et al.*, 2020 |

Although achieving high TRL completion (TRL8) for CO production, SOE technology remains in a constant development on the cell, stack and system levels to reduce system costs for viable commercial implementation in the industrial sector (TRL9).

CAPEX costs reduction can be achieved through the reduction of Critical Raw Materials (CRM) content (e.g. Co, Sr, Y…) in the SOE cells manufacturing (European Commission, 2020; NewSoc, 2022), reduction of stack (<150 k€/kW) and system (<500 k€/kW) costs (CHJU, 2021) and improvement of the yield of production for mass integration in the industry (Frøhlke, 2021), while improving efficiency of the SOE cell (high current density operations), stack (high fuel utilization) and system (heat & gas recycling) components.

OPEX reduction is aimed for by increase of the SOE cells and stack lifetime (>> 8000 h) with the prevention of the coking process (Boudouard reaction) and sulfur poisoning at the fuel electrode (cathode) side. This can be realized through optimization of the robustness of the cell and stack components & design, with development of alternative materials compared to the highly reactive State-of-the-Art Ni-YSZ cermet fuel electrode (Riegraf *et al.*, 2016). Tuning of the operating conditions of the SOE stack (temperature, pressure, current density) and integration of purification systems (desulfurization) (Hauch *et al.*, 2021) in the BoP of the SOE system are also under development to prevent the poisoning issues at the fuel side of the stack.

## 3.6 High-temperature solid oxide electroconversion to produce syngas

Syngas ($H_2$/CO) of tunable ratios can be produced in one single electroconversion process step with HT with a similar operating principle in Solid Oxide Cell as used for CO production (as shown in Figure 18 ). The operating concept of the SOE for syngas production consists of a co-electrolysis (co-SOE) of water and $CO_2$, able to produce variable $H_2$ and CO compositions, for further process applications, as for instance, production of green fuels and chemicals such as methane and methanol. Steam and $CO_2$ are reduced in SOEC according to the following equations, with $H_2$/CO ratio in the syngas modified by variations of the steam and $CO_2$ flows.

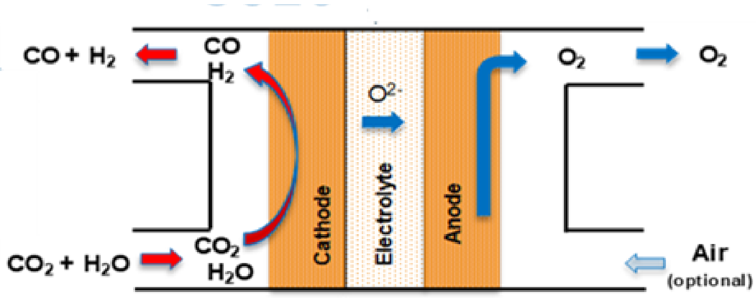

$$CO_2 + 2e^- \rightarrow CO + O^{2-}$$

$$H_2O + 2e^- \rightarrow H_2 + O^{2-}$$

$$2O^{2-} \rightarrow + 0.5\, O_2 + 2e^-$$

$$Overall\ reaction\ anode\ and\ cathode{:}\ \ CO_2 + H_2O + \Delta H \rightarrow CO + H_2 + O_2$$

Figure 18 Schematical concept of Solid Oxide Cell Electrolysis (SOEC) for high temperature co-electrolysis of steam and $CO_2$ on cell level.

State-of-the-art on co-SOE technology

The production of syngas ($H_2$/CO) using co-SOE is in the development phase with an achieved TRL of 5 to 6. The German system supplier Sunfire is the world leader and known as the only system supplier for co-SOE systems (Sunfire, 2021). Sunfire system is based on high-temperature operation system (850°C), with electrolyte supported cells and stack technology (Figure 19). Actual system is developed on a 150 kW scale, with the so-called name Syn-Link (Figure 20).

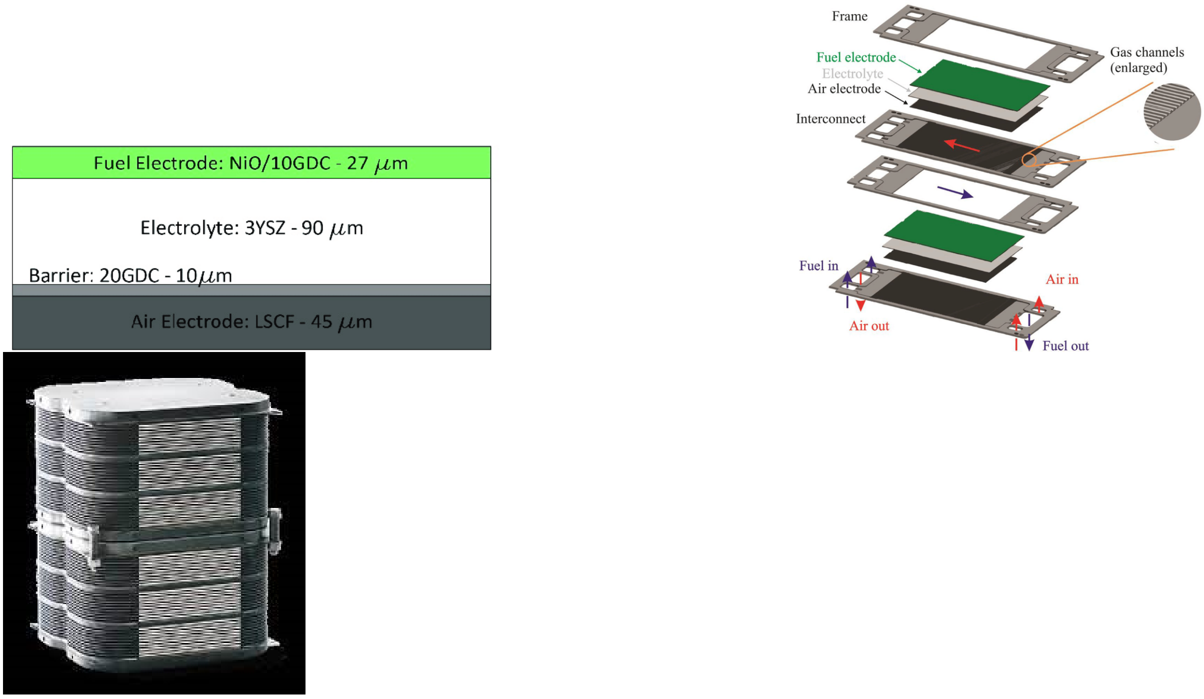

Figure 19: Sunfire Solid Oxide Cell and stack technology for co-SOE electrolyzers (Masini *et al.*, 2019; Sunfire, 2022a),

Figure 20: 150kW co-SOE prototype and system (Syn-link) developed at Sunfire (Sunfire, 2022b)

The co-SOE technology has been developed within multiple European research projects. To the best of our knowledge, the past and on-going projects for the development of co-SOE systems from kW to MW scale are summarized below in Table 19.

Table 19. Summary of the most important development projects for HT $CO_2$ electrochemical conversion.

| Project | Period | Involvement | Description |
|---|---|---|---|
| **Eco project**[1] | 2016-2019 | | co-SOE concept for methane production |
| **Kopernikus**[2] | 2016-2019 | Sunfire | Development of 10 kW co-SOE system by Sunfire |
| **Norsk e-fuel**[3] | 2019-2025 | | Development of the co-SOE technology for production of green-fuel for aviation & maritime transport, from $CO_2$ captured from the air and renewable energy sources |
| **MegaSyn** [4] | 2021-2025 | FCHJU project | Demonstration of large-scale co-electrolysis for the Industrial Power-to-X market: first demonstration of syngas production by co-electrolysis on the mega-watt scale in an industrial environment at the Schwechat Refinery in Austria, with Sunfire technology |

[1] Eco (2019); [2] Kopernikus (2019); [3] Norsk e-fuel (2022); [4] MegaSyn (2022)

Co-SOE system boundaries considered for the current TEA study

Syngas composition of $H_2$:CO = 2:1 is assumed for the calculations. This syngas ratio corresponds approximately to the ratio required for fuels production through the Fischer-Tropsch process and methanol synthesis. The mass balance for the base case is based on stoichiometry calculations. The single-pass conversion of $CO_2$ and $H_2O$ for the base case is assumed to be 80% (van Berkel *et al.*, 2021). Figure 21 shows the conceptual block flow diagram for syngas production using an HT SOE system. The outlet gas mixture produced from SOE systems ($H_2$:CO:$CO_2$: steam) requires additional separation processes to feed clean syngas ($H_2$/CO) for the sub-mentioned fuels and chemicals production processes (depending on the end use of syngas). Steam is commonly removed by a condensation process and recycled to the steam system. $CO_2$ can be separated from the ($H_2$:CO:$CO_2$) gas stream by absorption, adsorption, or membrane-based separation methods. Moreover, absorption-based separation with amine solutions is commercially available. Separated $CO_2$ is recycled to the inlet of the SOE system. However, separation of $CO_2$ from syngas depends on the end-use of the produced syngas (for instance, for methanol production, the syngas inlet feedstock can contain $CO_2$). Heat from SOE outlet gases is recovered using heat exchangers to increase the overall system energy efficiency.

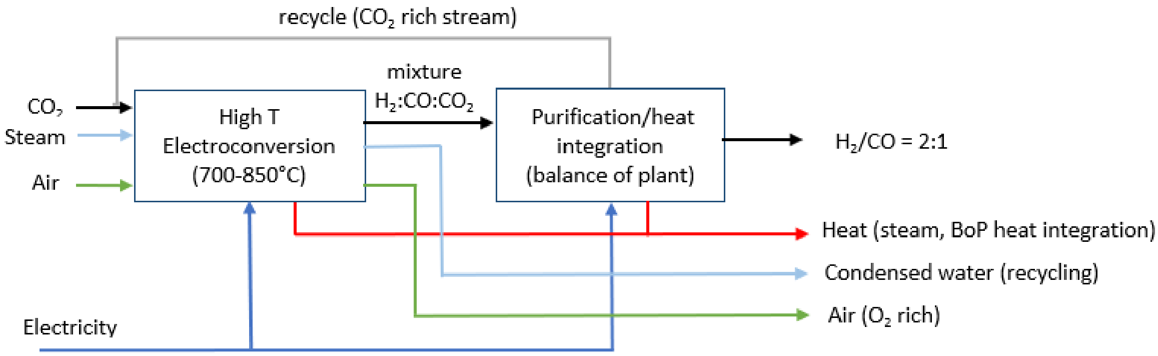

Figure 21. Conceptual block flow diagram for the HT co-electrolysis process for syngas production.

Total uninstalled CAPEX for the system is calculated based on the steam electrolysis data taken from Hydrogen Europe targets. The split of CAPEX was assumed to be 30% for the cell stack, 30% for the power electronics, 6% for the gas conditioning, and 34% for the balance of plant (Böhm *et al.*, 2019). CAPEX for syngas production through SOE is scaled based on the ratio of power density for steam and co-electrolysis. Syngas electrolysis will require additional separation compared with steam electrolysis. CAPEX for the separation unit has not been included and, if deemed necessary, may increase the overall investment and production costs of route 5.

Current process performance parameters for the co-electrolysis are reported in Table 20.

Table 20. State-of-the-Art process performance parameters for the HT co-electrolysis process for syngas production.

| Parameter | Unit | Value | Reference |
|---|---|---|---|
| **Current density** | $A/m^2$ | 7500 | van Berkel *et al.*, 2020 |
| **Cell voltage** | V | 1.32 | van Berkel *et al.*, 2020 |
| **Faradaic efficiency syngas** | - | 100% | Assumed |
| **$CO_2$ and steam utilisation (single pass)** | mole product/mole $CO_2$ in | 80% | van Berkel *et al.*, 2020 |
| **Carbon yield to product** | mole C-product/mole $CO_2$ reacted | 100% | Assumed |
| **Power density** | $kW/m^2$ | 9.9 | Calculated |

| Parameter | Unit | Value | Reference |
|---|---|---|---|
| **Stack Lifetime** | h | 40000 | Posdziech, 2021 |

The overall mass balance for syngas production is given in the Table 21.

Table 21. Complete mass and energy balance for the HT co-electrolysis process for syngas production.

| **Flow** | | **Unit** | | | **Reference** |
|---|---|---|---|---|---|
| | | | **Input** | **Output** | |
| **Electricity** | Stack | $kWh_{el}$ | 7.87 | - | |
| | Balance of plant | $kWh_{el}$ | 1.04 | - | |
| | Total | $kWh_{el}$ | 8.91 | - | |
| **$CO_2$** | | kg | 1.36 | - | |
| **$H_2O$** | | kg | 1.16 | - | |
| **Syngas ($H_2$/CO) ($H_2$:CO = 2:1)** | | kg | - | 1 | |
| **$O_2$** | | | | 1.50 | Schreiber *et al.*, 2020 |
| **$CO_2$ emissions** | | kg | - | - | |
| **$H_2$** | | kg | - | | |
| **Heat** | | GJ | - | - | |

## 3.7 High-temperature molten carbonate electroconversion

Molten Carbonate Electrolysis Cell (MCEC) is a high temperature electroconversion technology (600-900°C) able to produce carbon monoxide (CO) or syngas (CO/$H_2$) (Hu, 2016). MCEC operating concept is based on the reversible operation of Molten Carbonate Fuel Cell (MCFC) technology, where the direction of the redox reactions is inversed (Figure 22). CO and syngas can respectively be produced by electrochemical conversion in a molten carbonate salt electrolyte ($CO_3^{2-}$) by feeding $CO_2$ or a mixture of steam and $CO_2$ streams at the fuel electrode (Monforti Ferrario *et al.*, 2021).

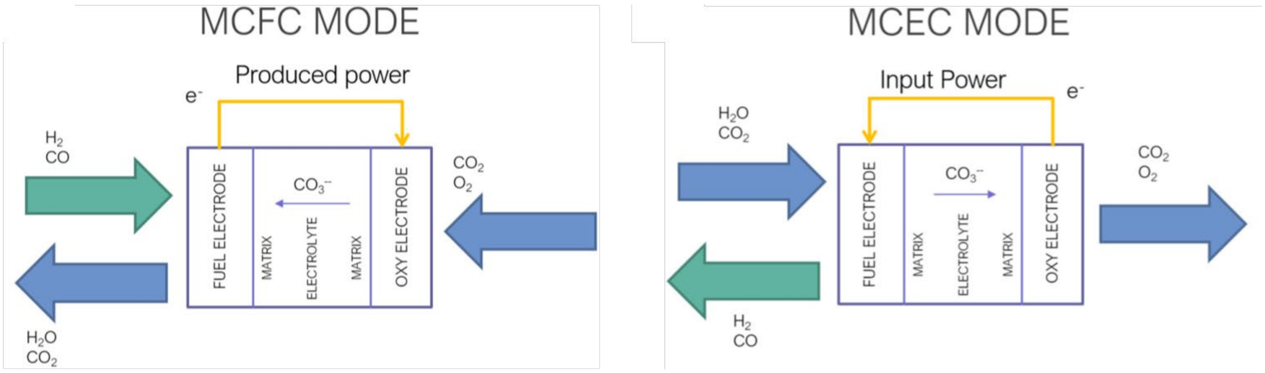

Figure 22. Scheme of the two operation modes of a Molten Carbonate Cells (MCC): (Right) MCC in the electrolysis (MCEC) mode and (Left) MCC in the FC (MCFC) mode (Monforti Ferrario *et al.*, 2021).

The MCEC technology has seen an increase of its development in the last few years, demonstrating the feasibility of both CO and syngas production processes at the lab-scale level (TRL 2-3), with experiments using button cells (Kaplan *et al.*, 2010; Kaplan *et al.*, 2014), planar single cells (Hu, 2016; Hu *et al.*, 2014; Meskine *et al.*, 2021), and numerical models (Perez-Trujillo *et al.*, 2018; Perez-Trujillo *et al.*, 2020). An overview of the MCEC operating conditions and performance are presented in Table 22.

Table 22. Overview of MCEC systems properties for CO and syngas production.

| | Unit | CO production[1] | Syngas production[2] |
|---|---|---|---|
| **Fuel electrode reactions** | | $2CO_2 + 2e^- \rightarrow CO_2^{3-} + CO$ | $H_2O + CO_2 + 2e- \rightarrow CO_3^{2-} + H_2$<br>$CO_2 + H_2 \leftrightarrow H_2O + CO$ (RWGS) |
| **Oxygen electrode reactions** | | $CO_2^{3-} \rightarrow CO_2 + 1/2\ O_2 + 2e^-$ | $CO_2^{3-} \rightarrow CO_2 + 1/2\ O_2 + 2e^-$ |
| **Operating temperature** | °C | 900 | 600-680°C |
| **Current density** | $A/m^2$ | 1000 | 1000 – 1600 |
| **Cell voltage** | V | 0.87 | 1.15 - 1.4 |
| **Faradaic efficiency** | - | 100% | 100% |
| **$CO_2$ utilisation degree** | mole product/mole $CO_2$ in | 85% | 80% |
| **Power density** | $kW/m^2$ | 0.87 | 1.12 – 2.24 |

[1] Kaplan *et al.*, 2010; Kaplan *et al.*, 2014; Küngas, 2020. [2] Monforti Ferrario *et al.*, 2021; Kaplan *et al.*, 2010; Kaplan *et al.*, 2014. (*) most of the CO2 is converted to CH4

The MCEC concept used for **syngas production** is based on the same system components as those used for the MCFC operating at in the temperature range of 600-680°C. In the reference studies on the topic (Hu, 2016; Monforti Ferrario *et al.*, 2021; Kaplan *et al.*, 2014), the fuel electrode is made of porous nickel and/or alloyed with Cr and/or Al, the oxygen electrode of porous lithiated nickel oxide (NiO) and an electrolyte composed of a eutectic mixture of lithium, potassium, and/or sodium carbonate ($Li_2CO_3$, $K_2CO_3$, and $Na_2CO_3$), which remains liquid at the operating temperature (600-680°C). A porous matrix, commonly made of g-$LiAlO_2$, is used to retain the electrolyte, besides conducting the carbonate ions between the electrodes as well as separating the fuel and oxidant gases. A MCEC system based on this concept can operate at current density of 0.1 to 0.16 $A/cm^2$ for operating voltage between 1.15V and 1.4V, but the production of CO is rather limited (max 3%), about 30% of the $CO_2$ is converted to $CH_4$. (Monforti Ferrario *et al.*, 2021).

For **CO production**, the reversible MCFC technology based on Ni electrodes or Li-Na-K carbonate eutectic electrolytes was demonstrated to not be suitable under MCEC operations for this application (Kaplan *et al.*, 2010; Kaplan *et al.*, 2014). The Ni fuel electrode used in MCFC systems was shown to coke almost instantaneously and a mixture of alkali metals subsequently intercalates the resulting surface graphite layer, leading to complete deactivation of the electrode. An alternative concept of MCEC technology for CO production, based on molten $Li_2O/Li_2CO_3$ electrolyte, a titanium fuel electrode and a graphite oxygen electrode has been shown to give promising results. The new concept operating at higher temperature (900°C) is able to deliver an efficiency of 85% at 0.1$A/cm^2$ for an operating voltage of 0.87V.

Regarding MCEC system integration, a system integration analysis at 1 MWe system scale has been carried out by Monforti Ferrario *et al.* (2021) in 2021 to integrate MCEC technology for the decarbonization of the reforming process of an oil refinery factory. The integrated system design presented in figure 19, aims to reuse 10-25% of the plant reformer off-gas in the MCEC stack, with intermediate gas processing with a PSA unit to achieve an equimolar $H_2O$:$CO_2$ ratio at the inlet of the MCEC stack needed for syngas production (Table 22). To optimize the efficiency of the system, a recycling of the off gas on the fuel outlet of the MCEC is aimed and the $CO_2$ stream outlet on the oxygen electrode side is also used for a process of Oxy-combustion integrated in the overall reforming process of the plant. With the MCEC stack integration with the following stack characteristics (650°C, 0.15 A/cm$^2$, 80% fuel utilization, 1 MWe, 490 m$^2$ cell area), several beneficial effects results for the operation of the refinery plant. The $H_2$ yield is increased by 3.06% with the recirculation of around 10% of the upgraded off-gas and an increase in the hydrogen yield up to 12% can be potentially achieved by increasing the installed power of the MCEC unit (4 MWe) to process the totality of the off-gas. The off-gas flow to the combustor is reduced by 7.93% at constant heat duty at the reformer combustor by increase of the integrated system efficiency (LHV of the upgraded off-gas). The MCEC integration also contribute to the reduction of $CO_2$ emissions with $CO_2$ reuse in the Oxy-combustion process. Last but not least, an electrochemical Specific Energy Consumption for the $H_2$ production of 3.24 kWh/Nm$^3$ $H_2$, which is a promising value in comparison with the competing low-temperature electrolysis technologies (between 5 and 6 kWh/Nm$^3$ $H_2$).

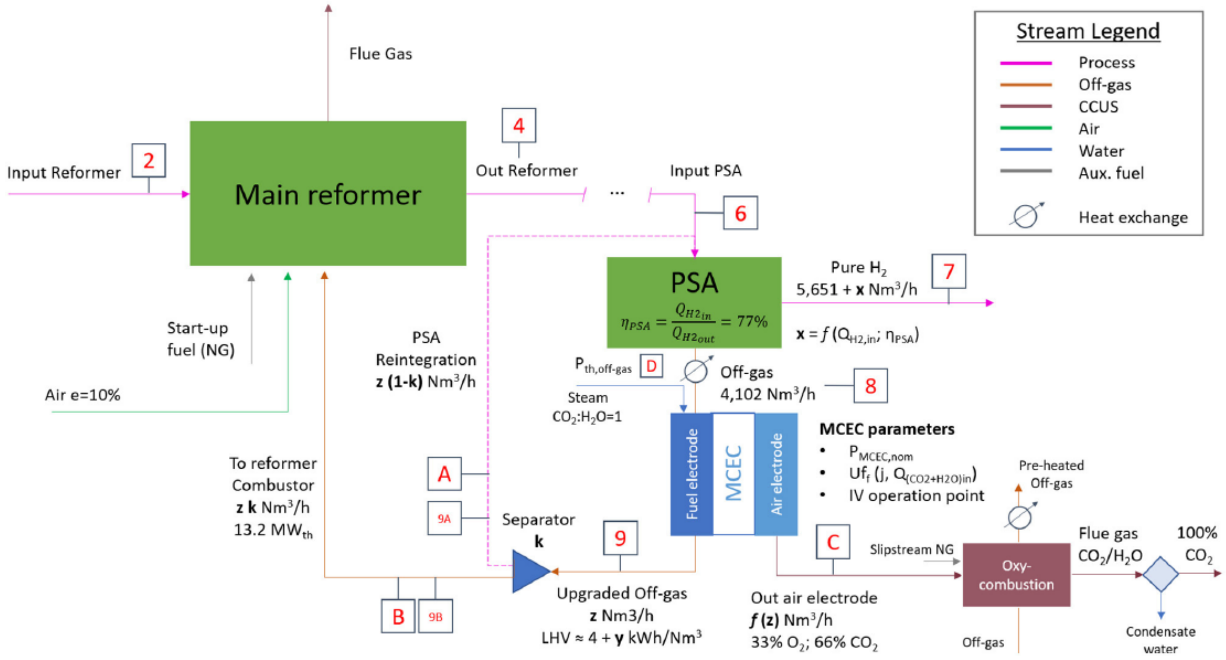

Figure 23: Integrated system scheme and effects of the MCEC unit on a plant scheme (Monforti Ferrario *et al.*, 2021).

Although MCEC system development has only reached a TRL of 4, use of this technology for syngas and CO production has a promising perspective for industrial implementation as MCFC technology, the reversible MCEC concept, is already commercialized on industrial scale (TRL 9) for power and heat generation with units of up to 3.7 MW sold by Fuel Cell Energy (Fuel Cell Energy, 2022) and POSCO (POSCO, 2022) and several power plants of 10–60 MW are already installed worldwide (Bove *et al.*, 2008).

In the subsequent techno-economic analysis (Chapter 4), the MCEC concept is nevertheless not included as separate route because, due to the development at low TRL, information on the system development (stack cost, effective operation) is lacking.

## 3.8 Tandem electroconversion approach to produce ethylene

The tandem process for the production of $C_2H_4$ consists of the combination of a HT electrolysis unit for $CO_2$ electrolysis towards CO (and the subsequent downstream processes for CO purification), followed by a LT electrolysis step for the conversion of the intermediate CO into $C_2H_4$, including auxiliary units for the purification and separation of $C_2H_4$. A diagram of the complete process is shown in Figure 24.

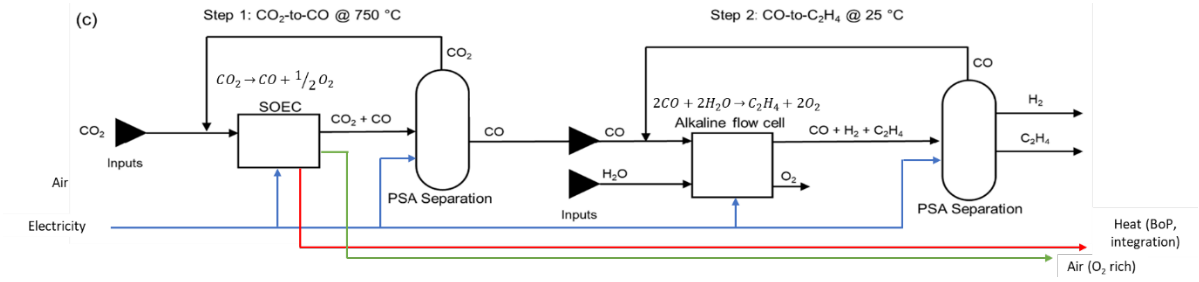

Figure 24. Process diagram of the tandem HT $CO_2$ electrolysis to CO and LT CO electrolysis towards $C_2H_4$, the so-called Tandem process. Adapted from Sisler *et al.*, 2021.

The individual reactions of the HT step and the LT step are displayed below.

Step 1: HT $CO_2$ electrolysis: $$2CO_2 \rightarrow 2CO + O_2$$

Step 2: LT CO electrolysis: $$2CO + 2H_2O \rightarrow C_2H_4 + 2O_2$$

The overall reaction of the tandem process is displayed below. As it is shown, the reaction is equivalent to that from the LT route of $CO_2$ towards $C_2H_4$.

$$2CO_2 + 2H_2O \rightarrow C_2H_4 + 3O_2$$

The current development stage of the tandem route for $C_2H_4$ synthesis is limited by the LT conversion step, given that the HT step has already achieved a TRL 8-9 (section 3.5). The LT CO electrolysis to products ($C_{2+}$, specifically $C_2H_4$) has been explored experimentally, and can be considered to be at a TRL 3 (Jouny *et al.*, 2018b; Jouny *et al.*, 2019).

State-of-the-Art of the HT step for $CO_2$ electrolysis towards CO has already been discussed in section 3.5. Current State-of-the-Art for LT electrolysis of CO to $C_2H_4$ comprises the use of a MEA cell design, in which a gaseous CO stream is fed to the electrolyzer, to the gas side of the cathode GDE. The cathode is separated from the anode with an ion exchange membrane (either CEM or AEM). In the anode compartment, an alkaline anolyte is fed as a reactant for the OER. The cathode outlet stream contains CO, $H_2O$, $C_2H_4$, other C-gaseous products, possible C-liquid products, and $H_2$. A depiction of the MEA cell for LT CO to $C_2H_4$ is shown in Figure 25.

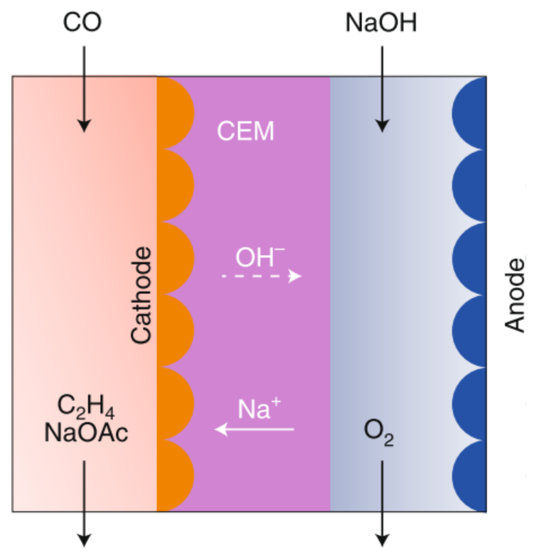

Figure 25. CO electrolyser design for the production of C2H4, with a CEM and an alkaline anolyte for OER. Reproduced from Jouny *et al.*, 2019. Nota bene: the anode side is shown in the right hand-side of the diagram, and the cathode side, on the left.

In the HT step for $CO_2$ electrolysis towards CO, a PSA unit is included in the process diagram to allow for CO purification (see section 3.5). in the LT step for CO electrolysis, a PSA unit is included as well to ensure the required purity for the $C_2H_4$ gas stream (99.9%wt., according to the NIH, 2022).

Contrary to the LT $CO_2$ electrolysis routes, the nature of the LT CO electrolysis process does not allow for the formation of bicarbonates or any crossover of the cathodic reactant towards the anode, as Sisler *et al.* (2021) claim. The fed CO in the Step 2 of LT CO electrolysis will react electrochemically to form different CO reduction products, or it will leave the electrolyzer unreacted, but it will not end up in the anode side. Therefore, there will be no need of implementing a (CO) recovery loop in contrast to the $CO_2$ recovery step that is required for the LT $CO_2$ electrolysis towards $C_2H_4$ (see section 3.4).

State-of-the-Art process performance for the first step of the HT $CO_2$ electrolysis towards CO has been described in section 3.5. Current State-of-the-Art process indicators for the LT electrolysis of CO to $C_2H_4$ are reported in Table 23.

Table 23. State-of-the-Art process performance parameters for the LT electrolysis of CO to $C_2H_4$. The Carbon (carbon monoxide) yield to product is calculated as the ratio between the Faradaic Efficiency (FE) towards the final product, $C_2H_4$, and the FE towards all carbon-products (incl. $C_2H_4$).

| Parameter | Unit | Value | Reference |
|---|---|---|---|
| **Current density** | A/m$^2$ | 1440 | Ripatti *et al.*, 2019 |
| **Cell voltage** | V | 2.32 | Ripatti *et al.*, 2019 |
| **Faradaic efficiency $C_2H_4$** | - | 35% | Ripatti *et al.*, 2019 |
| **CO utilisation degree** | mole product/mole CO in | 100% | Sisler *et al.*, 2021 |
| **Carbon yield to product** | mole C-product/mole CO reacted | 63% | FE($C_2H_4$)=35%; FE(C-products)=56% |
| **Power density** | kW/m$^2$ | 3.34 | Calculated |

The complete mass and energy balances for the tandem process of $CO_2$ to $C_2H_4$ process is shown in Table 24. The energy requirements for the HT step are adjusted as to produce enough CO for the LT conversion to ensure the production of a final 1 kg $C_2H_4$ in this second step.

Table 24. Complete mass and energy balances for the tandem route for the combination of HT CO production and LT CO conversion to $C_2H_4$. The energy requirements corresponding to the HT step (‘*HT*’), both for the stack and for the auxiliaries, are referred to the production of 1 final kg $C_2H_4$. The category ‘*CO (HT intermediate)*’ is the final CO stream coming from the HT step as input for the LT step. The category ‘*Aux.+DSP LT*’ corresponds to the energy requirements of the PSA unit for $C_2H_4$ purification (data from Jouny *et al.*, 2018a). ‘*$CO_2$ emissions (HT)*’ would correspond to the $CO_2$ content in the reject stream from the PSA unit in the HT step. ‘*CO emissions (LT)*’ would correspond to the CO content in the reject stream from the PSA unit in the LT step.

| **Flow** | | **Unit** | **Tandem HT-CO + LT-CO-$C_2H_4$** | |
|---|---|---|---|---|
| | | | Input | Output |
| **Electricity** | Stack HT | $kWh_{el}$ | 4.78 – 5.09 | - |
| | Stack LT | $kWh_{el}$ | 51.1 – 53.8 | - |
| | Aux.+DSP HT | $kWh_{el}$ | 3.91 – 6.48 | - |
| | Aux.+DSP LT | $kWh_{el}$ | 0.51 – 0.54 | - |
| | Total | $kWh_{el}$ | 60.3 – 65.9 | - |
| **$CO_2$ (HT)** | | kg | 5.03 – 5.47 | - |
| **$H_2O$ (LT)** | | kg | 5.73 – 5.80 | - |
| **CO (HT intermediate)** | | kg | 3.20 – 3.31 | |
| **$C_2H_4$ (99.9%wt.)** | | kg | - | 1 |
| **$O_2$ (HT+LT)** | | kg | - | 8.41 – 8.50 |
| **$CO_2$ emissions (HT)** | | kg | - | 0.00 – 0.34 |
| **CO emissions (LT)** | | kg | - | 0.00 – 0.05 |
| **$H_2$ (side product LT)** | | kg | - | 0.37 |
| **EtOH (side product LT)** | | kg | - | 0.99 |

For the tandem route, there will be two major components for the investment costs: the HT $CO_2$ to CO electrolyzer (incl. the PSA unit), and the LT CO electrolyzer to produce $C_2H_4$, with the downstream PSA unit. For the estimation of the HT electrolyzer investment costs, data on uninstalled investment costs and energy efficiency must be taken and adapted to the required CO demand for the LT CO electrolyzer: ca. 3.2 kg CO need to be produced in the upstream HT electrolysis unit and be fed to the LT CO electrolyzer to produce 1 kg $C_2H_4$ (see Table 24). For the second step LT electrolyzer, the method for estimating the investment costs is analogous to that for the rest of the LT routes: use the data for water PEM electrolysis (see Table 7), and scale it down using the power density factors (see Table 23). With respect to the estimation of the investment costs for the PSA unit, data from the LT $CO_2$ to CO case (see Table 8) can be taken and adapted to the present route.

### 3.9 Technology and material summary of the different routes

The different design aspects and materials used for each technology covered in the present chapter are displayed on Table 25.

Table 25. Compendium of the materials, catalysts and cell designs used for the different electrochemical routes covered in chapter 3. Disclaimer: CER: Chlorine Evolution Reaction; HER: Hydrogen Evolution Reaction; OER: Oxygen Evolution Reaction; Aq.: aqueous; DI: de-ionised water.

| Route | Cell reactor design | Membrane/separator | Electrolyte | Cathode catalyst material | Anode catalyst material |
|---|---|---|---|---|---|
| **Chlor-alkali (co-produced $H_2$)** | MEA with electrode foams in close contact with membrane[2] | Cation Exchange Membrane for $Na^+$ crossover<br>Double-layer: sulfonic acid-based layer + carboxylic acid-based layer[1] | ***Anolyte***: concentrated brine (aq. NaCl solution);<br>***Catholyte***: concentrated aq. NaOH solution[1] | Low-carbon steel; Ni foams for HER[1] | $IrO_2$, $RuO_2$ for CER<br>Dimensionally Stable Anode (DSA) [1] |
| **Chlor-alkali (ODC)** | Semi-MEA: DSA foam in contact with membrane; cathode GDE to reduce $O_2$[2] | | | Ag-based catalyst for ODC[1] | |
| **LT CO** | MEA cell with 2 GDEs and feeding at the back of the electrodes[3] | AEM Sustainion for anion crossover[3] | ***Anolyte***: aq. solution (can be alkaline);<br>***Catholyte***: absent; a humidified gaseous $CO_2$ stream is fed at the back of the cathode | Ag-based catalyst[3] | $IrO_2$-based catalyst for OER[3] |
| **LT FA** | 3-compartment cell with 2 membranes and GDEs[4] | AEM Sustainion (formate crossover) + CEM Nafion (for proton crossover)[4] | ***Anolyte***: aq. solution (can be alkaline);<br>***Centre compartment electrolyte***: DI water taking up produced FA;<br>***Catholyte***: absent; a humidified gaseous $CO_2$ stream is fed at the back of the cathode | Sn-based catalysts[4] ; $Bi_2O_3$-based catalysts[5] | $IrO_2$-based catalyst for OER[3] |
| **LT $C_2H_4$** | MEA cell with 2 GDEs and feeding at the back of the electrodes[6] | AEM Sustainion for anion crossover[6] | ***Anolyte***: aq. solution (can be alkaline);<br>***Catholyte***: absent; a humidified | Cu-based catalysts[6] ; | $IrO_2$-based catalyst for OER[3] |

| Route | Cell reactor design | Membrane/separator | Electrolyte | Cathode catalyst material | Anode catalyst material |
|---|---|---|---|---|---|
| | | | gaseous $CO_2$ stream is fed at the back of the cathode | | |
| **HT CO** | Cell with three layers(Cathode, electrolyte, Anode) and one compartment for CO2 and one compartment for Air[9] | | solid ceramic material such as yttria-stabilized zirconia (YSZ), scandia stabilized zirconia (ScSZ)[3] | Ni-YSZ cermet [3] | perovskites materials based on lanthanides and transition metals, such as Sr-doped LaMnO3(LSM),Sr-doped La(Fe,Co)O3 (LSCF),Sr-doped SmCoO3 (SSC)[3] |
| **HT syngas** | Cell with three layers(Cathode, electrolyte, Anode) and one compartment for mixed stream of CO2 and steam and one compartment for Air[9] | | solid ceramic material such as yttria-stabilized zirconia (YSZ), scandia stabilized zirconia (ScSZ)[3] | | perovskites materials based on lanthanides and transition metals, such as Sr-doped LaMnO3(LSM),Sr-doped La(Fe,Co)O3 (LSCF),Sr-doped SmCoO3 (SSC)[3] |
| **MC CO** | Porous electrode immersed in a molten carbonate salt | | electrolyte composed of a eutectic mixture of lithium, potassium, and/or sodium carbonate($Li_2CO_3$, $K_2CO_3$, and $Na_2CO_3$) | porous nickel and/or alloyed with Cr and/or Al | porous lithiated nickel oxide (NiO) |
| **Tandem $C_2H_4$ (HT-step)** | (same as HT-CO) | | | | |
| **Tandem $C_2H_4$ (LT-step)** | MEA cell with 2 GDEs and feeding at the back of the electrodes[8] | CEM Nafion (for $Na^+$ crossover)[8] | ***Anolyte***: aq. solution (can be alkaline);<br>***Catholyte***: NaOH and other C2+ products are collected in the | Cu-based catalysts[7]; | $IrO_2$-based catalyst for OER[3] |

| Route | Cell reactor design | Membrane/separator | Electrolyte | Cathode catalyst material | Anode catalyst material |
|---|---|---|---|---|---|
|  |  |  | ‘wept’ electrolyte through the membrane; a humidified gaseous CO stream is fed at the back of the cathode[8] |  |  |

[1] Li *et al.* (2021); [2] Thyssenkrupp (2020); [3] Küngas (2020); [4] Yang *et al.* (2017); [5] Yang *et al.* (2020); [6] Gabardo *et al.* (2019); [7] Jouny *et al.* (2019); [8] Ripatti *et al.* (2019)

# 4 Techno-economic analysis

Here we report the results of our production cost assessment of the six routes. The routes consist of three LT electrochemical conversion routes that either produce CO, formic acid, or ethylene, two HT routes to produce CO or syngas, and one tandem approach (combination of LT and HT technology) to produce ethylene. The sensitivity analysis and cost projections up to 2050 are presented and discussed.

## 4.1 Investment costs

A more detailed description of the investment costs for the different routes is provided in Chapter 3. In Figure 26, we compare the cost breakdown of the total investment costs (CAPEX) for each of the routes for 1 MW scale plants. The LT conversion technology is currently significantly more expensive per kW of electricity input compared to the HT routes (4 and 5). This is also observed for the tandem process (route 6) in which the contribution of the first HT step (HT CO production system, dark green area) is barely noticeable. The stack costs for LT systems are based on PEM technology for hydrogen production (see Table 7). For $CO_2$ reduction, the stack is operated at a lower power density, which results in significantly higher costs per kW electricity input. Next to relatively high specific stack costs, the presence of the $CO_2$ recovery loop, along with the purification unit for the end-product (PSA for gaseous products, and distillation for formic acid), represent a large contribution to the high total investment costs.

The system and operating power density for our HT $CO_2$ reduction routes are fairly similar to those of HT steam electrolysis for hydrogen production. This allows us to base our cost calculations on steam electrolysis data, which is reported in more detail. For route 4, we add the costs of a PSA unit to separate CO from $CO_2$ of which the latter is recycled to the stack. For syngas production (route 5), we assume the synthesis gas that is produced is ready for use in, for instance, a methanol synthesis reactor, and does not require any further purification step. Such a step might appear necessary if the product gas is not directly suitable for follow-up chemical processes.

Our total investment costs cover nearly all project costs to build a $CO_2$ electrochemical conversion plant. Next to direct equipment costs, the installation and owner’s costs are also included and represent roughly half of the total plant costs. In the refining and petrochemical industries, typically an installation factor is used of around 3-5 to acquire a rough estimate of the total project costs based on the costs for the main equipment (Lang, 1948; Wain, 2014). If we only consider the electrolyzer stack and power electronics as main equipment, our estimates correspond reasonably well with this factor. If other balance of plant costs, gas conditioning, and purification units (e.g., PSA/$CO_2$ recovery loop) are included in the main equipment costs, our applied installation factor (~2) seems relatively low for a chemical process plant. We justify our choice by using a similar installation factor as applied for capital cost calculations for large electrolytic hydrogen production plants (Hydrohub, 2022).

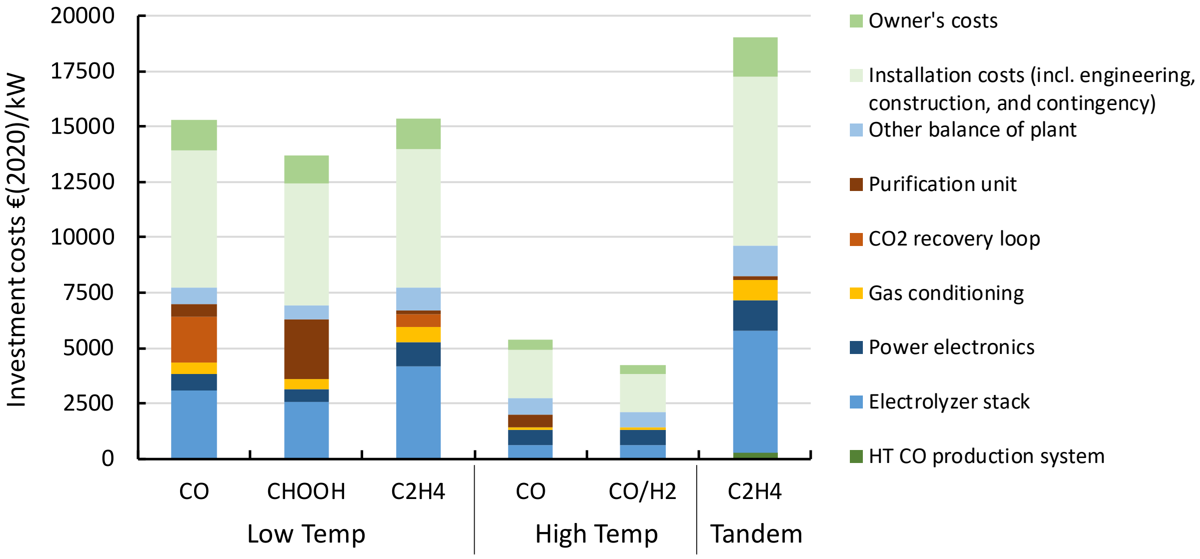

Figure 26. Cost breakdown of the total investment costs for each of the six electrochemical conversion routes for a fixed 1 MW capacity. Note the strong uncertainty related to CAPEX assessment of early stage technologies which have never been built and operated in a commercial environment.

In comparison to specific investment costs of other chemical processes, such as water electrolysis (Glenk & Reichelstein, 2019; Hydrohub, 2022; Detz & Weeda, 2022) or methanol synthesis (Detz *et al.*, 2018; Nyari *et al.*, 2020), the costs correspondent to electrochemical $CO_2$ conversion processes are relatively high, especially the LT routes. This can be expected of technologies at a low TRL because these do find themselves still at the start of their learning curve and significant cost reductions can be expected as soon as these technologies are further developed and scaled up. The effect of the investment costs on the levelized production costs is explained in the next section.

## 4.2 Levelized production costs

Current market prices of the products can provide a reasonable indication of the possible competitiveness of our routes. For bulk syngas and CO, it is difficult to estimate such a price because a market is non-existing. These gases are highly toxic and generally produced and directly converted into other products on site. To approximate a fossil-based reference price, a figure between the price of natural gas and methanol is chosen, ranging in 2019 between 7 and 12 €/GJ (Detz & van der Zwaan, 2022). To accommodate for recent volatility in natural gas and methanol prices (Methanex, 2022), we increased our high estimates with approximately 50%. Our reference price is, thus, fixed at 7–18 €/GJ or 0.07–0.18 €/kg CO or 0.17-0.43 €/kg syngas. As a specialty chemical in gas cylinders, CO sells at a price that is an order of magnitude higher. Formic acid is mainly produced through the reaction of methanol with CO to form methyl formate, which is subsequently hydrolysed. Market prices varied approximately from 130 to 150 €/GJ or 0.70-0.80 €/kg CHOOH in early 2022 (ChemAnalist, 2022a). Ethylene is typically produced via steam cracking of naphtha or natural gas liquids. The market price in the first quarter of 2022 varied between around 16 to 27 €/GJ or 0.70-1.30 €/kg $C_2H_4$ (ChemAnalist, 2022b).

As described in the methodology section (2.4), our levelized production costs calculations rely on investment costs, operating and maintenance (O&M) costs (of which we separately specify the stack replacement costs), and feedstock costs (incl. electricity, $CO_2$, and $H_2O$). The total investments for each of the routes, as presented in the previous section, are annualized by multiplying with the capital recovery factor using a discount rate of 10% and a plant lifetime of 20 years. The annual O&M costs are a fixed percentage of the initial total investment costs. We average out the replacement costs for the stack as a separate annual O&M cost component.

Figure 27 shows the results of the levelized costs calculations. From the figure it is clear that the stack replacement, O&M and investment costs are driving the levelized costs of all products and routes.
For LT electrochemical $CO_2$ conversion, the levelized costs to produce CO amount to approximately 500 €/GJ or 5.1 €/kg (Figure 27). Investment costs contribute more than 60%, O&M costs (incl. stack replacements) cover just above 30%, and the feedstocks, electricity and $CO_2$, together less than 10%.

The investment costs dominate the LT CO production costs. This effect is typically exaggerated for low TRL technologies because several parameters (indirect investment costs and O&M cost components) are related to the main equipment costs.

Formic acid can be produced for almost 700 €/GJ or 3.7 €/kg (Figure 27). The distribution of the costs over the different components is nearly identical to that of the LT CO production route. The costs per GJ of CHOOH are slightly higher compared to those of CO. This can be explained by the lower energy efficiency of the formic acid production process with respect to CO production (resp. 26% vs. 40%). This difference in cost per GJ product becomes more apparent for $C_2H_4$ production for which the energy efficiency is only 16%. The lower the efficiency, the more capacity in kW is required to produce a GJ of product, next to additional expenses for electricity. Together this results for the direct process (route 3) in levelized costs of nearly 1270 €/GJ or 60 €/kg ethylene of which the feedstock costs (electricity, $CO_2$, and $H_2O$) only represent 6% in total, while the rest is for CAPEX (60%), O&M (20%), and stack replacement costs (14%). The tandem process (route 6), which is slightly less efficient and has higher CAPEX, is even more expensive as route 3 and costs amount to more than 1600 €/GJ or 76 €/kg ethylene. The ethylene production costs are approximately two orders of magnitude higher as our fossil reference price.

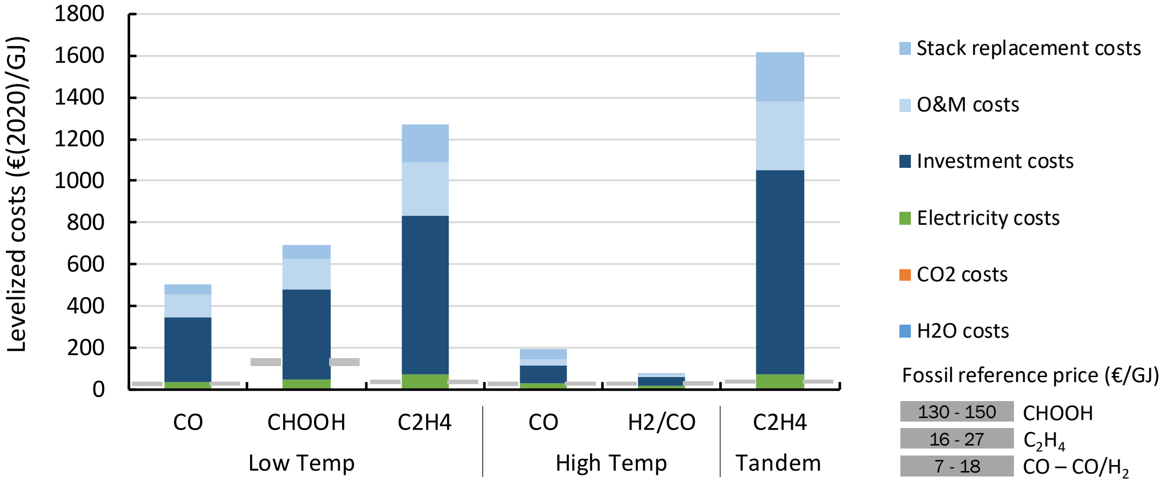

Figure 27. Levelized production costs of different $CO_2$ electrochemical conversion routes. A breakdown of the costs is indicated by the coloured areas for each of the key cost components. Note the strong uncertainty related to CAPEX assessment of early stage technologies which have never been built and operated in a commercial environment.

The HT processes benefit from relatively lower investment costs and higher energy efficiency. The levelized costs to produce CO are for route 4 slightly below 200 €/GJ or 1.9 €/kg (Figure 27). Nearly a quarter of these costs comes from the stack replacement costs, which are relatively high due to the low stack lifetime of only 8000 hours. Despite having an advantage in costs over the LT route (route 1), our fossil reference price is still at least ten times lower. Syngas production via HT route 5 results in levelized costs of around 80 €/GJ or 1.9 €/kg syngas. This route is currently the closest to its fossil reference of 7-18 €/GJ, and may under specific conditions already be competitive.

## 4.3 Sensitivity analysis

The levelized production costs, as presented in the previous section, are our base case estimates. Most parameters are not fixed values and are better described as a range. To illustrate the dependence of the total production costs on a single parameter, we have performed a sensitivity analysis for each of the routes. The low temperature routes, as well as the tandem route, rely mainly on CAPEX and, as a result, all parameters that are correlated to CAPEX have a substantial impact on the levelized production costs. This is shown for route 1 in Figure 28. The uncertainty in current CAPEX estimates has a substantial impact on the range of levelized production costs. Our base case value of 5.1 €/kg of CO may reduce to approximately 4 €/kg for our optimistic CAPEX value or increase to more than 6 €/kg if the investment costs approach 19000 €/kW. If the amount of full load hours (FLH) are either doubled or halved compared to our base case of 4000 FLH, the installed capacity also doubles or halves. The production costs almost linearly follow this trend and at nearly full load (8000 FLH), the levelized CO production costs go down to 3.0 €/kg. Currently, in most countries the intermittency of renewable electricity supply results in boundary conditions for the operation of processes to produce renewable products to avoid the use of fossil-based electricity (see also Section 2.6). At some locations or in the future, to drive these processes for more than 4000 FLH seems possible and, especially as long as CAPEX is a dominant cost factor, this may have a substantial impact on the levelized production costs. The stack lifetime is important to assess the costs associated to maintenance (i.e. stack replacement costs). Our base case value of 40000 hours is based on PEM electrolyzer stacks and improvements (e.g., up to 60000 hours) have a clear, but limited, positive effect on the production costs. A reduced stack lifetime (e.g., down to 20000 hours) has, however, a larger negative impact and achieving a certain level of stack lifetime, thus, seems an important development target. The O&M costs are a constant percentage of the CAPEX in our analysis and, as a consequence, their impact is high as long as the investment costs dominate the total production costs. Also the discount rate directly affects the investment cost component and, because CAPEX is currently so high for LT routes, resembles an important parameter. The plant lifetime influences our CAPEX component in that it is used to calculate the capital recovery factor (Section 2.4, equation 2) and its impact on the production costs remains rather low if the lifetime is at least 20 years.

The electricity use and costs are at this stage not so relevant for the levelized CO production costs. Even electricity costs as low as 20 €/MWh do not lead to a substantial cost reduction. The same holds for $CO_2$ costs because varying those from 20 to 150 €/t$CO_2$ only results in a difference in production costs of 0.2 €/kgCO, which is relatively a minimal impact. For route 2, 3, and 6, the sensitivity analysis tells a nearly identical story as for route 1 and we refer to the Appendix for more information (Figure A37, A38, and A40).

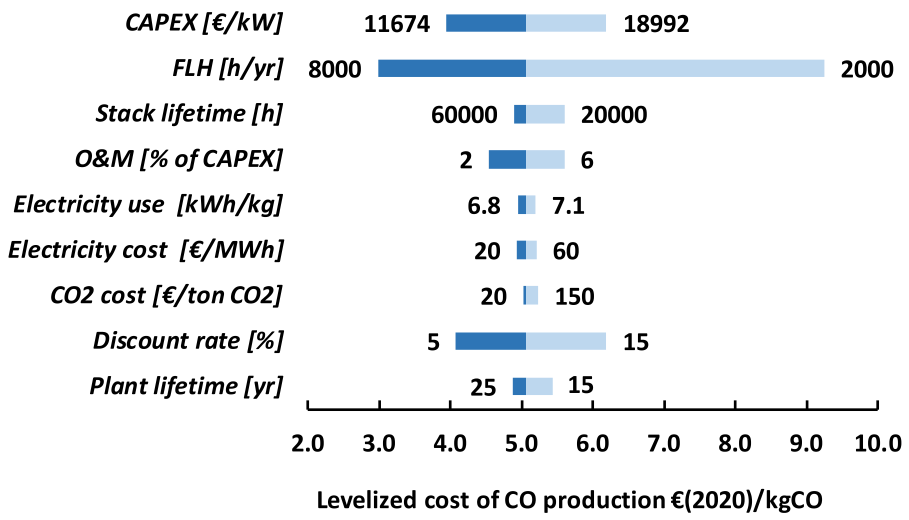

Figure 28. Sensitivity analysis for route 1 – LT electrochemical conversion of $CO_2$ to CO. Nine parameters are varied to explore their effect on the current levelized cost of CO production. The fossil reference CO price amounts to 0.07–0.18 €/kgCO.

The specific investment costs for our two HT routes are significantly lower compared to the LT routes and the results of our sensitivity analysis for route 4 is presented in Figure 29 (see Figure A39 in Appendix for route 5). When CAPEX is less dominant, also the role of other parameters becomes more apparent. Our variation in electricity use has for HT route 4, for instance, a similar influence on the levelized cost of CO production as has our investment costs range. The explored range in feedstock costs (electricity and $CO_2$) provides a more than 10% difference of levelized costs, which is much higher compared to the LT route (<5%).

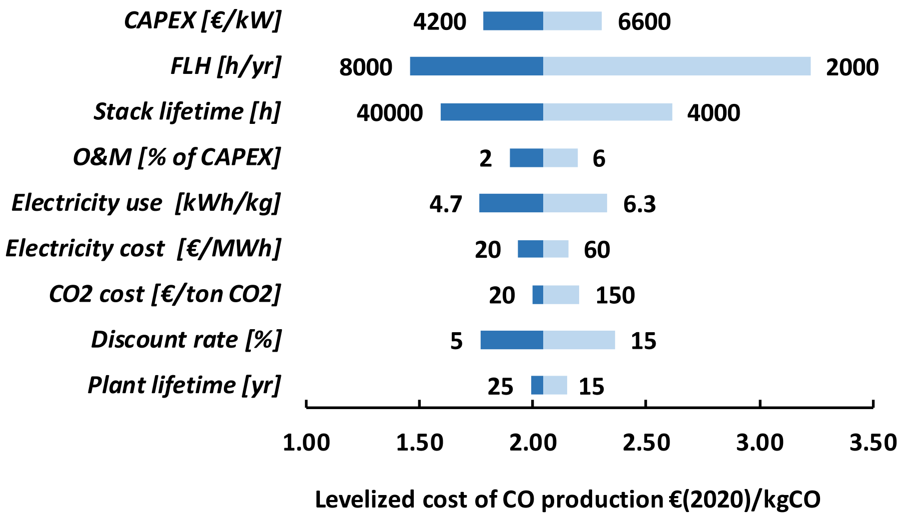

Figure 29. Sensitivity analysis for route 4 – HT electrochemical conversion of $CO_2$ to CO. Nine parameters are varied to explore their effect on the current levelized cost of CO production. The fossil reference CO price amounts to 0.07–0.18 €/kgCO.

For all routes, investments costs are an important component as can be expected for low TRL technologies. It is however likely that these costs can reduce substantially during scale-up and deployment. In the next section, we explore how such cost reductions may influence the competitivity of our routes in the future.

## 4.4 Cost projections

As indicated in the previous sections, the current costs to electrochemically convert $CO_2$ into products are high compared to fossil-based alternatives. The costs may reduce substantially thanks to, for instance, learning-by-searching, learning-by-doing, economies-of-scale, and lower material costs. We apply a learning curve analysis on the CAPEX component of our six conversion routes to explore how several of these phenomena affect the future investment costs. The insights from these learning curves are used to project the production costs for 2030, 2040, and 2050, taking into account several performance improvements of the electrochemical conversion processes.

### *4.4.1 Investment costs learning curves*

A technology learning curve is generally based on empirical data of observed cost reductions in the past (see also section 2.5). The curve generally resembles a declining straight line if costs are plotted against the cumulative installed capacity (CIC) on two logarithmic axes. By extrapolation of a historical learning curve, cost reductions can be projected if the cumulative installed capacity is increased. The learning rate for various energy technologies ranges typically between 10 and 30% (Ferioli *et al.* 2009). As an example, the LR for solar PV amounts to 24% (ITRPV, 2022), while an average LR of 12% is reported for onshore wind (Rubin *et al.*, 2015). To assess new technology, for which empirical data is often lacking, an estimate can be made of the learning curve based on the current technology status and analysis of comparable technology. Here we assess two key systems: low temperature $CO_2$ electrolyzer plants and high temperature $CO_2$ electrolyzer plants.

Low temperature systems to convert $CO_2$ into products are still at a pilot stage (kW scale systems) and current installed capacity is low (<MW). High temperature processes are slightly further in TRL but their cumulative installed capacity is also low (few MW) because the largest projects are currently developing MW systems. To project their learning curves, we base our initial cumulative experience and learning rate on that of comparable technology.

For LT $CO_2$ conversion, the technology is fairly similar to the chlor-alkali electrolytic process. The electrolyzer stack, as well as the power electronics and other balance-of-plant equipment are basically the same. Some pre-treatment and purification steps differ because these have to deal with other starting materials and products. The same manufacturers supply equipment for both the chlor-alkali, the electrolytic hydrogen, as well as the electrochemical $CO_2$ conversion industry. This justifies the use of existing experience and learning curve data of electrolytic production of chlor-alkali and hydrogen. To our knowledge, no learning curve has been reported for chlor-alkali investment costs. For electrolytic hydrogen production, several contributions report about a historical learning curve for electrolyzers (Schoots *et al.*, 2008; Schmidt *et al.*, 2017; Krishnan *et al.* 2020), and projections of cost reductions based on a learning curve (Detz *et al*, 2018; Detz and Weeda, 2022; Böhm *et al.* 2019; IEA, 2021). The results and assumptions of these studies have been summarized in Table 26. An important parameter for our projections is the initial cumulative installed capacity on which we base the existing experience because this value determines the amount of novel capacity that has to be installed before another doubling in cumulative capacity is reached. The value varies slightly among the studies but in each case seems to be based on the total capacity of both electrolytic chlor-alkali and hydrogen production systems. For our analysis, we assume that all experience gained in the chlor-alkali, water electrolysis, and PEM fuel cell industries is both part of the historical learning but also for future learning effects. This means that the total cumulative installed capacity for low temperature electrochemical conversion technology represents a substantially higher figure as used in most previous studies. The total production capacity of the chlor-alkali industry is currently around 22 GW and cumulatively approximately 40 GW of capacity (including replacements) has been installed over time. Together with water electrolysis and PEMFC systems, we arrive at an initial CIC of 45 GW for LT electroconversion routes. Historical learning curves for LT electrochemical devices have been reported for water electrolysis and PEM fuel cells (PEMFC) (Schoots *et al.* 2008; Schmidt *et al.* 2017; Krishnan *et al.* 2020; Schoots *et al.* 2010; Wei *et al.* 2017). The learning rates vary between 16 and 21%. Many of these learning rates are based on the (manufacturing) costs of the system and do not include other costs that contribute to the construction of an entire chemical plant. Several of these other components are more mature as the electrolyzer stack and benefit less from learning effects. We therefore apply to the total investment costs a conservative LR range of 10-20% with 15% as base case value.

HT electroconversion systems differ substantially from their LT counterparts. The stacks contain no liquids and consist of solid ceramic materials, while the balance-of-plant equipment has to deal with gasses and steam throughput and high process temperatures. We therefore select our starting point based on both SOFC and SOEC technology. The total CIC of such systems is estimated on approximately 0.5 GW, mainly SOFCs. As far as we know, two learning curve analyses have been reported for SOFC technology, but the learning rates vary significantly from 0 to 35% (Rivera-Tinoco *et al.*, 2012; Wei *et al.*, 2017). Such a broad range is illustrative for the high uncertainty with which assessment of technologies at an early development stage is typically accompanied. For instance, a lack of markets and competition can reduce the urgency for a manufacturer to produce and sell cheaper systems. We apply for our HT routes a slightly higher LR range compared to the LT systems, of 15-25%, with 20% as base case value.

Table 26. Learning curve parameters for electrochemical conversion technology. Onshore wind and Solar PV are included for reference.

| Study | Technology | CIC | LR (applied) | Year(s) |
|---|---|---|---|---|
| **This study** | LT $CO_2$ Electroconversion | 45 GW (2020) | 15 ± 5 | 2020 - 2050 |
| **This study** | HT $CO_2$ Electroconversion | 0.5 GW (2020) | 20 ± 5 | 2020 - 2050 |
| | | | | |
| **Rubin *et al.* 2015** | Onshore wind | 837 GW (2021) [1] | 12 | 1979 - 2010 |
| **ITRPV 2022** | Solar PV | 972 GW (2021) | 24 | 1976 - 2021 |
| **Schoots *et al.* 2008** | LT Electrolysis | 15 GW (2006) | 18 ± 13 | 1956 - 2006 |
| **Schmidt *et al.* 2017** | LT Electrolysis | 20 GW (2014) | 18 ± 6 | 1956 - 2014 |
| **Krishnan *et al.* 2020** | LT Electrolysis | 20 GW (2016) | 16 ± 6 | 1956 - 2016 |
| **Schoots *et al.* 2010** | PEMFC | 0.3 GW (2008) | 21 ± 4 | 1995 - 2006 |
| **Rivera-Tinoco *et al.* 2012** | SOFC | 0.05 GW (2009) | 35 | 1986 - 2009 |
| **Wei *et al.* 2017** | PEMFC | 0.8 GW (2015) | 18 | 2005 - 2015 |
| **Wei *et al.* 2017** | SOFC | 0.1 GW (2015) | ~0 | 2001 - 2015 |
| **Detz *et al.* 2018** | LT Electrolysis (AE) | 21 GW (2015) | 18 | 2015 - 2050 |
| **Detz *et al.* 2018** | LT Electrolysis (PEM) | 0.8 GW (2015, PEMFC) | 21 (PEMFC) | 2015 - 2050 |
| **Detz *et al.* 2018** | HT Electrolysis | 0.2 GW (2015, SOFC) | 27 (SOFC) | 2015 - 2050 |
| **Bohm *et al.* 2019** | LT Electrolysis (AE) | 20 GW (2015) | 18 | |
| **Bohm *et al.* 2019** | LT Electrolysis (PEM) | 1 GW (2015) | 18 | |
| **Bohm *et al.* 2019** | HT Electrolysis | 0.1 GW (2015) | 18 | |
| **Detz & Weeda 2022** | Electrolysis | 20 GW (2020) | 9 - 20 | 2020 - 2050 |
| **IEA, 2021** | Electrolysis | 0.3 GW (2020) | 15 (stack) | 2020 - 2050 |
| | | | | |

---

[1] https://gwec.net/global-wind-report-2022/

| Study | Technology | CIC | LR (applied) | Year(s) |
|---|---|---|---|---|
| **Calculated in this study** | Chlor-alkali | 40 GW (2020) | | |
| **Calculated in this study** | LT Electrolysis | 3.3 GW (2020) | | |
| | | | | |

The projected learning curves for all our routes are depicted in Figure 30 to Figure 35. For LT CO production route 1, the total investment costs reduce from currently approximately 11700–19000 €/kW$_{el}$ to 3700–11000 €/kW$_{el}$ after around five doublings in CIC (Figure 30). If 1.6 TW of LT electrochemical devices has been installed in 2050, our base case projection amounts to 6600 €/kW$_{el}$, which is nearly a 60% reduction in CAPEX compared to 2020. This cost reduction is through our applied learning curve induced by multiple factors, such as economies-of-scale, manufacturing improvements, process optimization, among others. We indicate our specific CAPEX in kW$_{el}$ input and improvements in the power density of the process have a tremendous impact on the output per kW$_{el.}$ This effect has not been investigated separately but the indirect consequence of our analysis implies that it is not straightforward that CAPEX scales linearly down with increasing power density. In other words, we assume that raising the power density goes paired with an increase in CAPEX. Notably, if in reality the power density can be improved without affecting the investment costs, cost may reduce faster as projected here. From section 4.2 it became clear that CAPEX resembles the key cost component for our routes. Lower investment costs, thus, have a substantial impact on the levelized production costs, which in our base case scenario reduce from 2020 to 2050 with nearly 65% to 175 €/GJ (1.75 €/kg). A small contribution to the observed cost reduction comes from improvements in energy efficiency. In comparison to our fossil benchmark of below 18 €/GJ, these costs are still high. Only with a CO$_2$ tax of at least more than 600 €/tCO$_2$, the production costs of route 1 can reach a breakeven point with the fossil reference price. On the specialty chemicals market with prices around 3 €/kg (van Rooij *et al.*, 2018), the LT CO production route might become competitive already in 2030, even without CO$_2$ taxation.

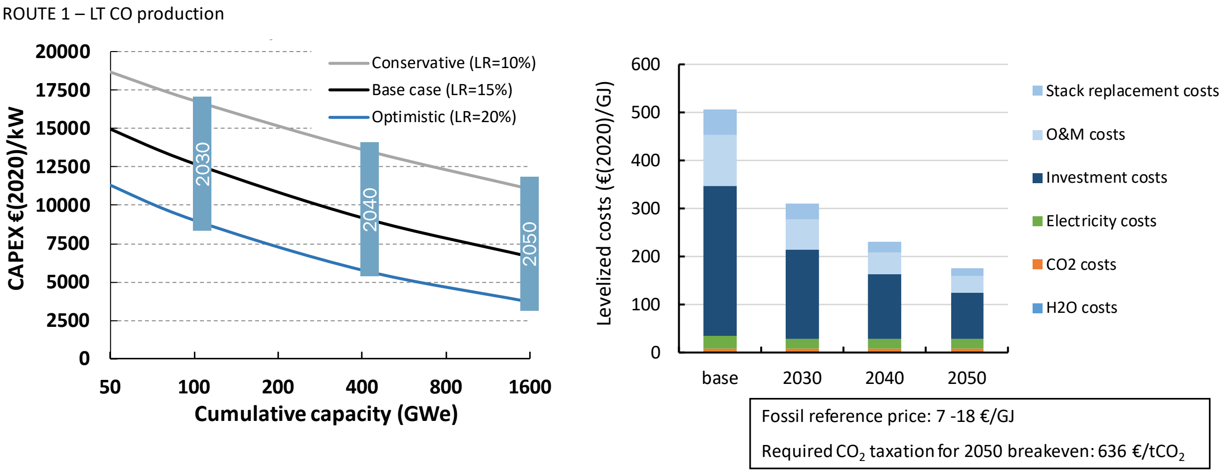

Fossil reference price: 7 -18 €/GJ
Required CO$_2$ taxation for 2050 breakeven: 636 €/tCO$_2$

Figure 30. Route 1 cost projections of the CAPEX (left) and the base case levelized CO production costs (right) for LT electrochemical CO$_2$ conversion to carbon monoxide. The CIC of LT electroconversion processes in 2020 is 45 GWe.

The investment cost projection for LT formic acid production (route 2) follows a similar pattern as for route 1. CAPEX reduces from currently 10700-16700 €/kW$_{el}$ to 3400–9700 €/kW$_{el}$ going up in CIC to 1600 GW$_e$ (Figure 31). This has a positive effect on the projected levelized cost as these go down from nearly 700 €/GJ today, to below 200 €/GJ in 2050. Such a cost level is already close to our fossil reference price and, for breakeven, a CO$_2$ taxation of approximately 70 €/tCO$_2$ should be sufficient.

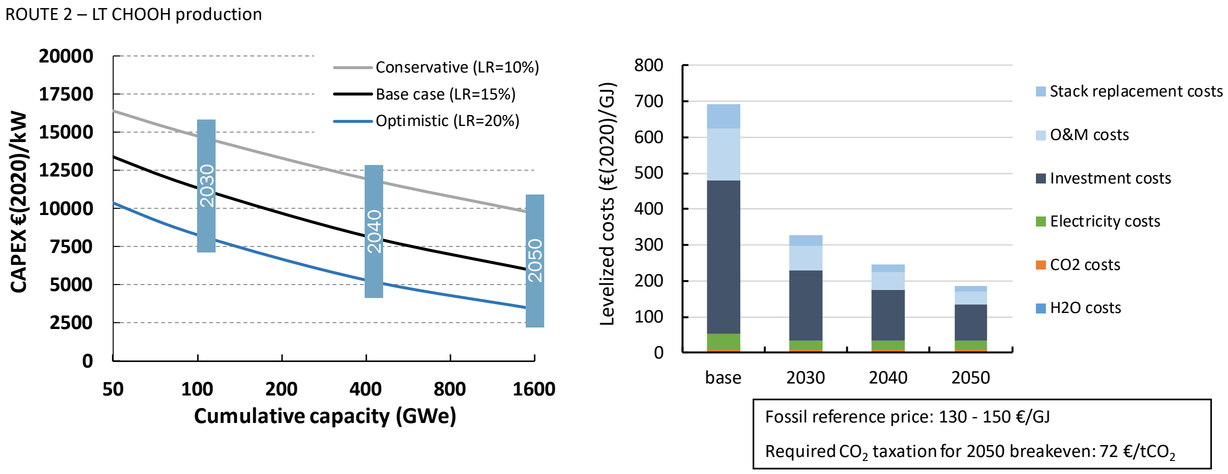
ROUTE 2 – LT CHOOH production

Fossil reference price: 130 - 150 €/GJ

Required $CO_2$ taxation for 2050 breakeven: 72 €/$tCO_2$

Figure 31. Route 2 cost projections of the CAPEX (left) and the base case levelized CHOOH production costs (right) for LT electrochemical $CO_2$ conversion to formic acid. The CIC of LT electroconversion processes in 2020 is 45 GWe.

The investment cost projection for LT ethylene production (route 3) reduce from an initial 10700-16700 €/kW$_{el}$ to 3400–9700 €/kW$_{el}$ for a CIC of 1600 GW$_e$ (Figure 32). The positive effect of a lower CAPEX on the levelized production costs of ethylene is further enhanced by a higher conversion and energy efficiency of the process. Together these developments result in a cost decline of 80% compared to our current base case costs by 2050. The levelized costs of 250 €/GJ ethylene in 2050 are a factor of ten higher than our fossil reference price. Only with a very high $CO_2$ tax of more than 2300 €/t$CO_2$, which may be unrealistic, a cost-breakeven point can be reached.

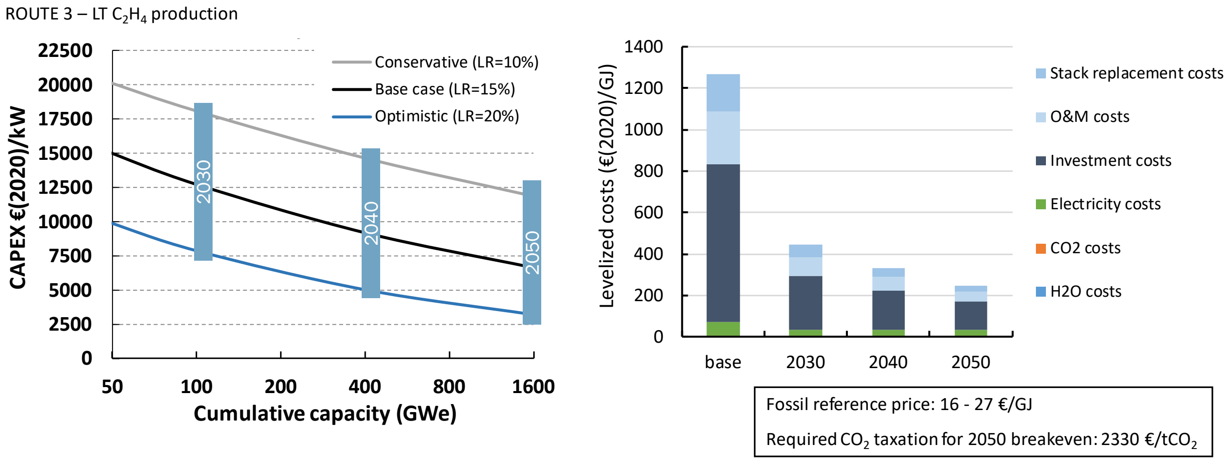
ROUTE 3 – LT $C_2H_4$ production

Fossil reference price: 16 - 27 €/GJ

Required $CO_2$ taxation for 2050 breakeven: 2330 €/$tCO_2$

Figure 32. Route 3 cost projections of the CAPEX (left) and the base case levelized $C_2H_4$ production costs (right) for LT electrochemical $CO_2$ conversion to ethylene. The CIC of LT electroconversion processes in 2020 is 45 GWe.

The specific investment costs for HT $CO_2$ electrochemical conversion (route 4 and 5) are significantly lower in comparison to LT routes. For CO production, CAPEX ranges currently between 4200-6600 €/kW$_{el}$, which is already close to the 2050 projections for our LT routes. Descending its learning curve, the costs go down rapidly thanks to the relatively high LR of 20% for the base case compared to 15% for our LT routes. We project that around 0.5 TW of cumulative capacity will be installed in 2050. As mentioned, this value includes the installed capacity of solid oxide water electrolyzers and fuel cells. In such a scenario, the investment costs reduce to 240-1300 €/kW$_{el}$ (Figure 33). This CAPEX reduction, together with improvements in energy efficiency and prolonged stack lifetime, result in levelized production costs for CO of 28 €/GJ or 0.28 €/kg in 2050. This is close to the fossil reference price of 7-18 €/GJ and a $CO_2$ tax of 60 €/t$CO_2$ would already induce a point of breakeven.

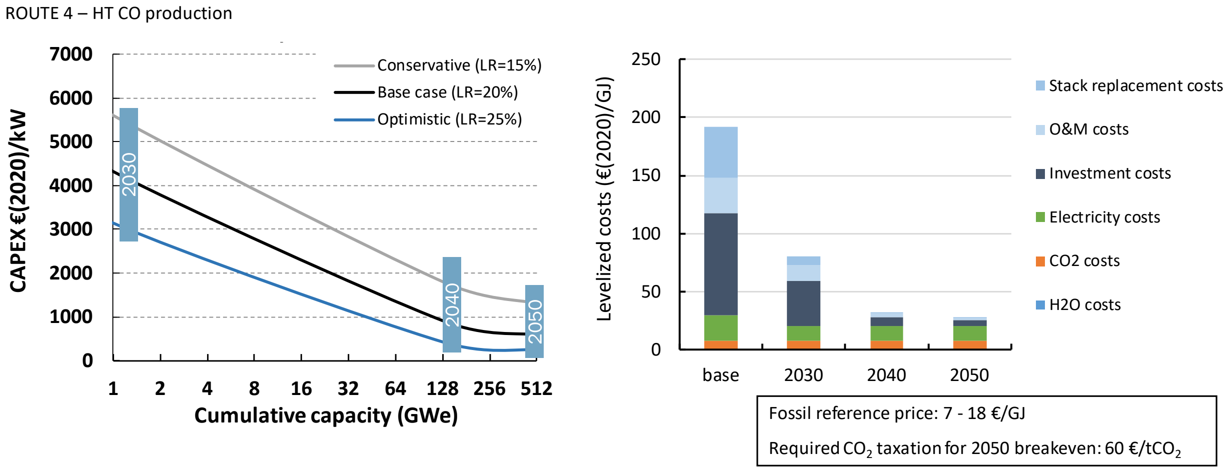
ROUTE 4 – HT CO production

Fossil reference price: 7 - 18 €/GJ

Required $CO_2$ taxation for 2050 breakeven: 60 €/t$CO_2$

Figure 33. Route 4 cost projections of the CAPEX (left) and the base case levelized CO production costs (right) for HT electrochemical $CO_2$ conversion to carbon monoxide. The CIC of HT electroconversion processes in 2020 is 0.5 GWe.

The investment costs for HT syngas production currently amount to 3000-5400 €/kW$_{el}$ and our projection indicates costs may go down to 170-1060 €/kW$_{el}$ (Figure 34). This is the main driver for a significant reduction of the levelized costs to produce syngas via this route towards 2050. In 2050, the dominant cost component are the electricity costs, which represent nearly 60% of the total production costs of 22 €/GJ or 0.53 €/kg. To become competitive with the fossil reference price of 7-18 €/GJ, a $CO_2$ taxation of at least 100 €/t$CO_2$ would be required.

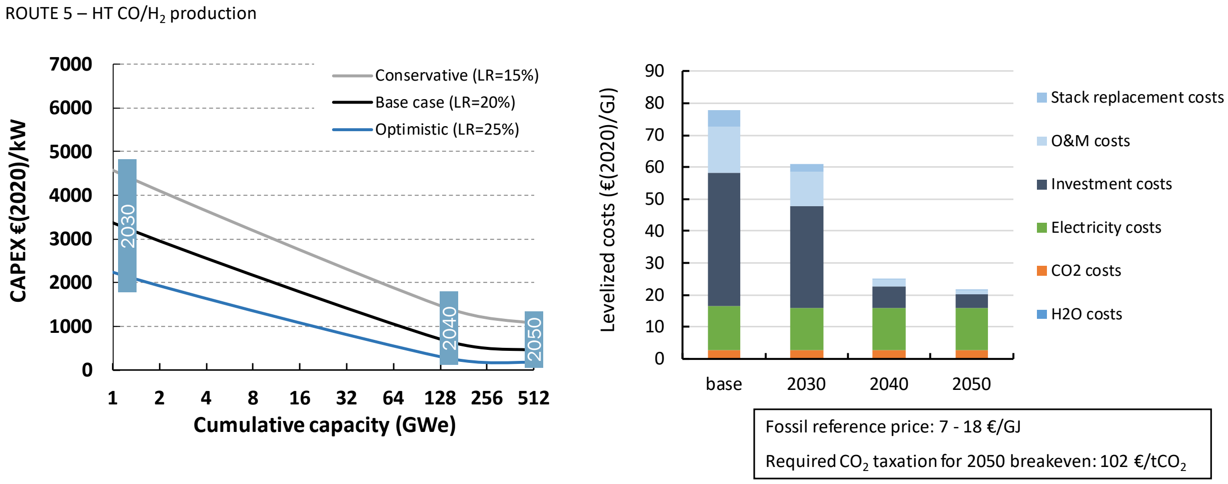
ROUTE 5 – HT CO/$H_2$ production

Fossil reference price: 7 - 18 €/GJ

Required $CO_2$ taxation for 2050 breakeven: 102 €/t$CO_2$

Figure 34. Route 5 cost projections of the CAPEX (left) and the base case levelized syngas production costs (right) for HT electrochemical $CO_2$ conversion to syngas. The CIC of HT electroconversion processes in 2020 is 0.5 GWe.

In the tandem process (route 6), first $CO_2$ is converted by a HT system into CO, which is the feed for a LT electrolyzer in which ethylene is produced. The current investment costs heavily rely on the costs of the LT system (>95%). This justifies the application of the learning curve parameters for the LT technology to the total investment costs. Our learning curve indicates that costs go down from to 12300-25700 €/kW$_{el}$ now to 5300-11100 €/kW$_{el}$ in 2050 (Figure 35). For our base case in 2050, this means that investment costs still dominate the ethylene production costs, which more than halve to 743 €/GJ or 35 €/kg ethylene. In our projections, any improvements in selectivity and efficiency of the process are excluded. These developments would further reduce the production costs because of lower energy usage and potentially less required capacity to produce a certain amount of ethylene. Compared to the fossil reference price of 16-27 €/GJ, such a cost is very high and only with exceptionally high $CO_2$ pricing (> 7000 €/t$CO_2$) a point of breakeven can be reached.

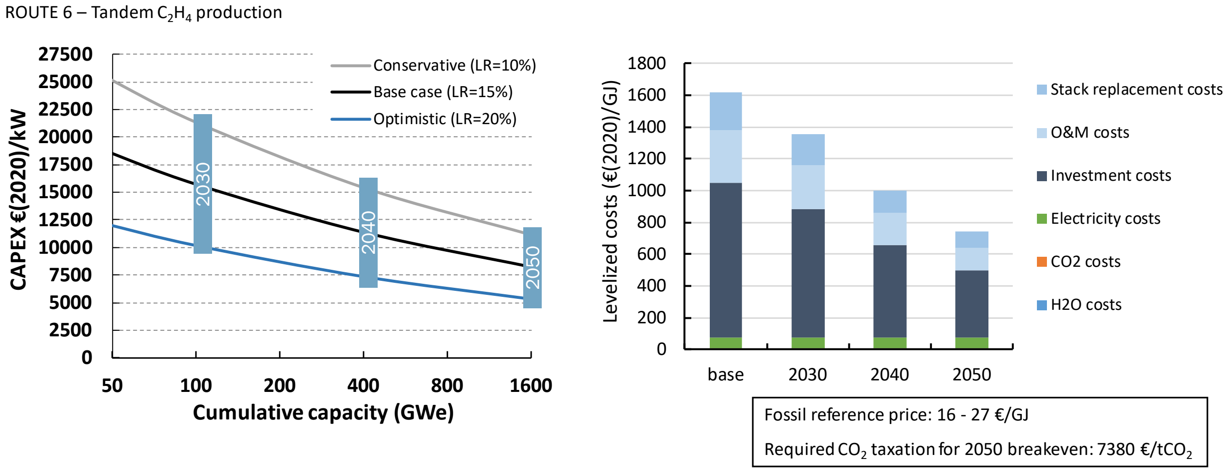
ROUTE 6 – Tandem $C_2H_4$ production

Fossil reference price: 16 - 27 €/GJ

Required $CO_2$ taxation for 2050 breakeven: 7380 €/t$CO_2$

Figure 35. Route 6 cost projections of the CAPEX (left) and the base case levelized $C_2H_4$ production costs (right) for Tandem electrochemical $CO_2$ conversion to ethylene. The CIC of LT electroconversion processes in 2020 is 45 GWe.

# 5 Environmental greenhouse gas performance results

The prospect of novel technologies to produce fuels and chemicals depend largely on their competitiveness with conventional pathways. We indicated in the previous chapters that if learning-by-doing proceeds as expected, some $CO_2$ electrochemical conversion routes may become economically competitive with alternative approaches based on fossil resources. Notably, this only seems possible if sufficient $CO_2$ taxation is in play, ranging from 60 to more than an unrealistically high 7000 €/t $CO_2$. It will be important that the GHG emissions associated to our routes are significantly lower compared to their fossil reference. Here we calculate a first estimate of the $CO_2$ emissions for each of the six routes by comparing the indirect emissions from electricity use of the processes (Figure 36). The emission factor of the electricity supply clearly affects the total emissions of the route. Our routes start from $CO_2$ as feedstock, while not taking into account the origin of this $CO_2$. To indicate the difference in energy regarding indirect emissions between point source capture and DAC, we show both scenarios, i.e., the emission factor of the product based on either point source capture (green lines) or DAC (blue lines). The energy use of point source capture depends on the type of point source and gas stream and, thus, varies significantly. We take a value (0.3 MWh/t$CO_2$) at the lower side of reported figures and assume that this energy can be supplied as electricity, either direct or via electric heating. (IEA, 2016; Irlam, 2017). For DAC, we use similar assumptions, but the electricity use is determined to be at the high end of the reported range (2.0 MWh/t$CO_2$) (Fasihi *et al.*, 2019). By this we cover more or less the entire range of emissions related to the electricity use for our $CO_2$ supply. The results are compared with the emissions related to the fossil reference pathway, which is based on average 100 year global warming potential values from the SimaPro database. In Figure 36, the emission factor of the products of all routes (route 1-6: a-f) has been displayed versus the emission factor of the electricity that is used for the process.

**a)** LT CO **b)** LT CHOOH **c)** LT C2H4

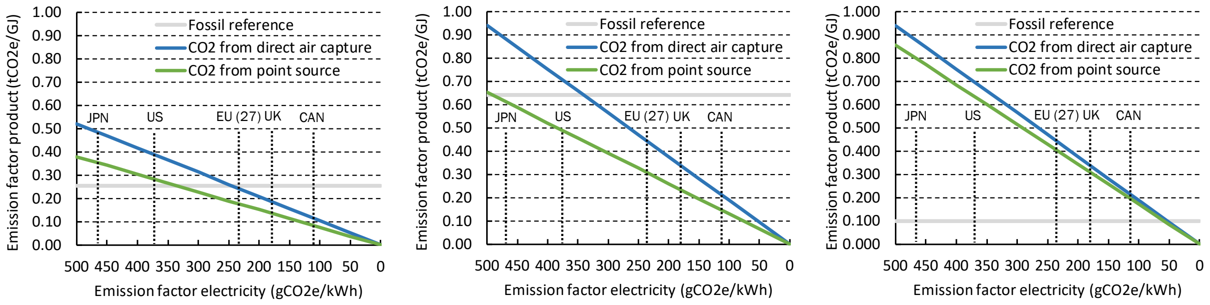

**d)** HT SOEC CO **e)** HT SOEC CO/H2 **f)** TANDEM C2H4

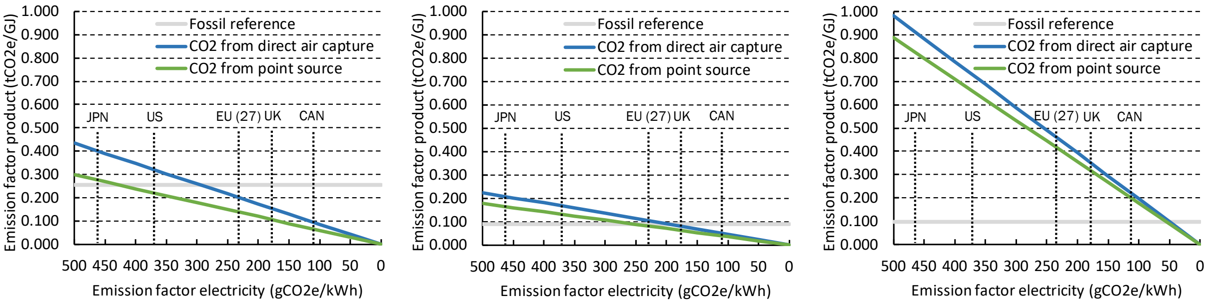

Figure 36. Emissions from electricity use for the six electrochemical $CO_2$ conversion routes. The vertical dotted lines indicate the emission factor of the grid in a specific country/region in 2020.

The LT route to produce CO can achieve similar emissions as the fossil reference when the emission factor of the grid is less than approximately 350 $gCO_2e/kWh$, which is currently the case in several countries, such as the United Kingdom (UK), Canada (CAN), and in the European Union (EU). To become a meaningful route to produce renewable fuels and chemicals, the emission factor of the products should, however, be significantly lower in comparison to fossil-based alternatives. European regulation for instance states that "the greenhouse gas emissions savings from the use of renewable liquid and gaseous transport fuels of non-biological origin (RFNBO's) shall be at least 70%" (REDII, 2018). To reach such a level of avoided emissions, the grid emission factor should be below 100 $gCO_2e/kWh$ for route 1. For formic acid production (route 2), the emission factor of the fossil reference is rather high and breakeven emissions can be realized with a grid emission of 500 $gCO_2e/kWh$, while a 70% reduction is realized with electricity that is generated with emissions of maximal 150 $gCO_2e/kWh$. In several countries, thanks to an increasing share of renewable electricity supply, the average grid emission factor is already approaching such a value and would thus afford the electrochemical production of these products at full annual capacity. The levelized costs would reduce from our base case value of 3.7 €/kg for 4000 FLH to 2.2 €/kg for 8000 FLH. A totally different situation occurs for production routes 3 and 6 because the fossil reference emissions for ethylene production are relatively low and the electricity use of the electrochemical process is high. Only with a very low grid emission factor of around 50 $gCO_2e/kWh$, a product emission factor is obtained that is similar to the fossil reference. A >70% reduction target is within reach, but the grid emission factor should be close to zero.

The HT route 4 to produce CO is more efficient than the LT alternative and requires less electricity usage. The emission factor of the grid can be nearly 450 $gCO_2e/kWh$ for this route based on point source $CO_2$ to achieve a emission breakeven point with the fossil reference. To realize >70% GHG savings, the difference between route 1 and 4 becomes smaller in absolute terms and emissions from the grid may amount to 125 $gCO_2e/kWh$ or 25 $gCO_2e/kWh$ more than for route 1. Syngas contains less carbon per GJ of product compared to pure CO and its associated emission factor is analogously lower, also for the fossil reference. With grid emissions below 250 $gCO_2e/kWh$, the electrochemical pathway can compete in emissions with the fossil-based alternative. From around 70 $gCO_2e/kWh$ and lower, substantial GHG savings (>70%) can be reached, purely based on electricity use of the process. Background emissions throughout the entire supply chains and other environmental aspects are not (fully) analyzed and may have an impact on our preliminary conclusions on the competitivity of these routes with fossil refence pathways. Full life-cycle assessment can provide more detailed insights into these aspects but is not part of this study.

# 6 Identified knowledge gaps and proposed research directions

Here we discuss the challenges and knowledge gaps that we identified in our study. We also proffer recommendations for further research.
Below we list specific technical challenges to be addressed for each technology. Additionally, a general research question for both SOEC and LT technologies is how integration with existing chemical clusters can be arranged, e.g. are there specific use cases for different technologies for which system integration can be implemented more efficiently next to specific industries, at specific locations or in connection with sustainable electricity sources like wind parks or large scale solar plants.

## 6.1 Knowledge gaps and research directions in the low-temperature $CO_2$ electrolysis routes

Uncertainty whether the roadmap for the future process performance indicators for the 2020 – 2030 decade is to be achieved.
The routes to electrochemically produce CO and HCOOH show already high performance in terms of selectivity, cell voltage and current density, given their low electron exchange number. For more complex molecules with a higher number of electrons exchanged, such as $C_2H_4$, it is uncertain that the outlined projections of process parameters for CO and FA will hold true, especially for high faradaic efficiency and current density. Important challenges in LT $CO_2$ electrolysis technology development need to be overcome to realise the stipulated roadmap. The most important one is to ensure long-term stable operation (> 10,000 h) at high current densities and efficiencies, and low cell voltage (solving the problems of carbonates precipitation at the cathode, as stated by Küngas, 2020 and Stephens *et al.*, 2022). As well, the novel LT CO electroconversion from the tandem route (route 6) is gaining increasing attention amongst researchers, and the efficiency and selectivity is expected to improve with catalyst, electrode and material development. However, it is uncertain whether LT CO electroconversion will reach the same performance as the projected LT $CO_2$ electrolysis goals for the next decade postulated in the roadmap by Nørskov *et al.*, 2019.

Costly purification unit for the HCOOH case.
From Figure 26, it is clear that the chosen purification strategy to produce a concentrated HCOOH aqueous stream (85%wt.) has a decisive contribution in the total investment costs. This is especially relevant in the future scenarios for electrolysis stacks with higher productivity, entailing a required higher production capacity in the downstream purification train. It is of paramount importance to highlight the necessity of selecting an energy and cost-efficient purification strategy for any LT $CO_2$ electrolysis products, and more importantly, for liquid products. Alternatives to the selected hybrid-extraction distillation system can already be found in the literature, as for instance a pervaporation-driven process with potential low capital and operational expenses, as described by Kaczur *et al.* (2020).

LT $CO_2$ electrolyzer lifetime.
The presumed lifetime for LT $CO_2$ electrolyzers for the economic analysis has been taken from the current process indicators for water PEM electrolysis (see Table 7). This figure can also be understood as a performance target to be achieved for LT $CO_2$ electrolysis, as it is for the future scenario projected for 2030 by Nørskov *et al.*, 2019 (see Figure 8). Lifetime is one of the most influential aspects for the economics of an electrolyzer stack. It is the maximal operational time for a stack before it needs to be replaced by another one due to excessive performance loss (lower current, higher energy consumption) . Ample research efforts have been dedicated to study and understand the phenomena that dictate the durability and long-term stability of LT $CO_2$ electrolysis processes, such as the membrane degradation, water management in the GDE, and the electrocatalyst stability, as pointed out by Stephens *et al.*, 2022.

Best State-of-the-Art lifetime data for LT $CO_2$ electrolysis (for CO production) lifetime are ca. 5,000 h at low current densities (500 $A \cdot m^{-2}$) and small scale (10 $cm^2$) (Küngas, 2020). It is therefore important to understand that the LT $CO_2$ electrolysis process is a technology under development, and a special R&D emphasis on ensuring the long-term stability (Kibria *et al.* (2019) states that the necessary lifetime to have a feasible business case for LT $CO_2$ electrolysis must be higher than 80,000 h are necessary) at high current densities (5,000 – 10,000 $A \cdot m^{-2}$) is critical to make this concept industrially feasible.

Required $CO_2$ purity and role of impurities for $CO_2$ electroreduction.
The $CO_2$ stream supply to the electrochemical unit has been left out of the scope of the present work. The role of impurities and unwanted contaminants in the inlet $CO_2$ gas stream in the electrolysis operation has not yet received enough attention amongst the researchers, even though these trace components can have significant consequences in the stability and lifetime of the electrochemical unit. The presence of impurities such as nitrogen oxides, or sulphur-derived compounds can lead to severe catalyst deactivation, as reported by Martín *et al.* (2015). While the $NO_x$ compounds can lead to temporary catalyst deactivation, having the possibility of *in situ* regenerating the active metal catalyst with pure $CO_2$ streams (as reported by Ko *et al.* (2020)), other contaminants, such as $SO_2$, can irreversibly change the catalyst morphology and render the metal catalyst ineffective for $CO_2$ conversion, like copper-based systems, as pointed out by Overa *et al.* (2022).
These impurities are commonly found in $CO_2$ streams coming for post-combustion plants for cement and natural gas power plants, so it is then essential to think about possible processing steps to remove these trace components prior to considering the recovered $CO_2$ for CCU options.

$CO_2$ crossover towards the anode and associated costs for $CO_2$ recovery.
The LT $CO_2$ electrolysis technology is characterised by the net loss of part of the $CO_2$ feedstock in the form of bicarbonates, migrated towards the anode side of the cell, as explained in section 3.2 (Reinisch *et al.*, 2020). The crossed over $CO_2$ has then to be reclaimed from the $O_2$ containing stream from the anode, with high associated capital (see Figure 26) and operational costs (see Table 6). The chosen $CO_2$ reclaiming process is based on an energy-intensive DAC technology that can work with $O_2$-rich inlets, and potential new solutions can be proposed for the $CO_2$ separation from this stream. In the literature, several approaches have been proposed to specifically tackle the $CO_2$ crossover challenge for LT electrolysis. Kim *et al.* (2022) suggest a similar solution as for the LT $CO_2$ to HCOOH route (see section 3.3), with an acidic middle compartment that will strip the $CO_2$ from the bicarbonate anions, avoiding the mixing with $O_2$ in the anodic side. Xie *et al.* (2022) propose an alternative anodic reaction with a liquid product that will permit to strip a pure $CO_2$ stream in the anode side (Samipour *et al.*, 2020). From the plasma-based processes for CO2 conversion to CO, Pérez-Carbajo *et al.* (2018) report a promising CO2-CO-O2 separation technology using zeolites in a PSA process that can be applicable for the crossed over CO2 towards the anode.

Need for a $CO_2/H_2$ separation process in the LT route for HCOOH.
Assuming that $H_2$ is only by-product in the LT HCOOH process (route 2, see section 3.3), it will accumulate in the cathode gas loop if not bled (with the concomitant $CO_2$ emissions). A $H_2/CO_2$ separation process needs to be implemented in case the efficiency for the $CO_2$ to HCOOH reaction is not 100% (to be achieved by 2030, according to Nørskov *et al.*, 2019). Industrially available technology using Palladium-based membranes (Samipour *et al.*, 2020) can be adopted for this application, normally used for $H_2$ purification for $CO_2$-containning streams.

Role of the anodic reaction in the economic feasibility for $CO_2$ electroreduction. The chosen anodic reaction for all proposed route has been the Oxygen Evolution Reaction (OER), producing $O_2$. For the LT area, this reaction is chosen because it's non-limiting for the cathodic $CO_2$RR, despite being an energy-intensive reaction (high anodic overpotential), and being $O_2$ a difficult to valorise economically (barely \$ 24 – 40/t $O_2$, according to Vass *et al.*, 2022). Several authors have already pointed out the potential of the anodic oxidation reaction for alternative products or applications, like product upgrade or wastewater treatment

(Jack *et al.*, 2021). Pérez-Gallent *et al.* (2019) demonstrated that the coupling of 1,2-propanediol oxidation to lactic acid with $CO_2$ reduction to CO effectively doubles the product value per unit of electrical energy that is used by the electrolyzer (compared to the $O_2$ co-production system).
By selecting a sensible anodic product that can easily be assimilated by the CCU value chain, the economic feasibility drastically improves (Vass *et al.*, 2021; Vass *et al.*, 2022). An example of this strategy is the electrochemical co-production of CO and $Cl_2$ in equimolar amounts, the combination of which make the precursor mixture for phosgene, a key intermediate for plastic and rubber manufacturing (Lister *et al.,* 2013). Also other chemicals, such as glycerol, can be oxidized at the anode to reduce energy consumption and increase product value (Verma *et al.*, 2019). Despite its potential economic advantages, the implementation of alternative anodic reactions to OER is haled due to the: 1) low cost of water as reactant for OER; 2) simplicity of disposing $O_2$ to the atmosphere instead of implementing costly purification strategies for the alternative anodic product; and 3) compatibility of OER with the intended CO2RR systems (Shin *et al.*, 2021).

## 6.2 Knowledge gaps and research directions in the high-temperature $CO_2$ electrolysis routes

Required purity of CO.
In today's conventional process, CO is produced as 'captive' CO and used on-site with a bespoke composition for the subsequent process. It is not straightforward to compare the electrochemical products with a reference in terms of levelized production cost, purity, and associated $CO_2$ emission. Higher purity can be achieved with further down-stream processing at higher cost and vice versa. CO costs and emissions also strongly depend on the reference technology: coal gasification or SMR with WGS.

Required purity and composition of syngas.
Syngas is typically produced as captive syngas and used on-site for different applications such as methanol production or Fischer-Tropsch synthesis (H2:CO = 2:1). The application in which the syngas is applied determines the required composition of produced syngas from the SOEC system outlet. Hence, the ratio of steam and $CO_2$ feedstock must be changed to obtain a syngas with a specified CO/$H_2$ ratio. Moreover, in the case of syngas, separation technology costs for CO/$CO_2$/$H_2$ depend strongly on the intended end-use of the product.

Separation of CO from $CO_2$/CO stream.
Currently, there is not enough data regarding separation technologies for a CO/$CO_2$ stream. As discussed earlier, Halder-Topsøe mentions use of a PSA unit to obtain a high purity CO stream (Topsøe (2022)) . However, data regarding yield, purity, and costs of such PSA unit is not publicly available.

Required purity of the $CO_2$ feed.
Purity requirements of the $CO_2$ feed are usually considered out-of-scope in research projects and not reported in the published research. Different sources of $CO_2$ may contain different levels of impurities and require different degree of purification, as sulphur and other compounds can negatively impact the lifetime of the reactor. This will affect both the Capex for the purification unit and the associated energy consumption. More details can be found in section 3.5.

From uninstalled cost to total plant cost.
As most of the discussed technologies are at low and medium TRL, reported costs usually focus on stack costs. Real life total plant costs are unknown yet. Hence, total plant costs are estimated based on assumptions for balance-of-plant costs and using installation factors based on comparable technologies. These assumptions introduce uncertainties in the assessment of the total CAPEX.

Need for system level pilots. A general issue with all investigated pathways is that the research is usually limited to cell-level and stack-level research. Pilot projects in which the entire product chain from industrial $CO_2$ stream to final product is demonstrated are needed to accurately determine CAPEX and O&M costs in an industrial environment.

Stack and system level research directions. On the solid oxide stack, several research directions are aimed at lowering cost. The FCH program aims at lowering stack cost to below 150 EUR / kW (FCH, 2022). Other research aims at reducing the dependence on raw materials on cell level (Cobalt, Nickel, Yttrium). Upscaling beyond MW level requires optimal system design for better heat management (Min *et al.*, 2020). Lowering stack replacement costs by improving stack lifetime via reduction of degradation at the cell level may further reduce production cost (Küngas, 2020).

# 7 Concluding remarks

Our analysis has shown that several electrochemical technologies are available to convert $CO_2$ into different products. All routes are currently significantly more expensive in comparison with fossil-based approaches, but stringent climate targets in combination with technology development may in the future favour the renewable alternative approaches. The chlor-alkali process, as an example of a mature electrochemical process, can function as a starting point for reference and potential technology developments, especially for LT technology. The LT routes seem to be mainly based on membrane-type electrolyzer systems and can benefit from developments in water electrolysis and fuel cell applications, e.g. PEM technology. HT systems are less comparable to membrane technology and are better compared with solid state fuel cell technology, such as SOFC and MCFC. Solid oxide technology seems most advanced in technology readiness and applied in larger scale $CO_2$ electroconversion demonstrators . These HT systems operate at relatively high power density , which is comparable to water electrolysis. The investment costs per unit output are for HT systems significantly lower to those of their LT counterparts.

Besides this current advantage in investment costs, the projected costs also reduce faster for our HT $CO_2$ conversion routes. This is mainly because in our learning curve analysis the assumed learning rate, which is based on solid oxide fuel cell technology, is slightly higher compared to LT technology for which the LR is based on water electrolysis, and the initial cumulative installed capacity of HT technology is relatively low, which makes relative capacity additions more likely to occur faster. The economic performance of all routes is mainly determined by the CAPEX component and thanks to steep learning of the HT pathways, these routes are likely first to reach break-even levelized production cost in comparison to the fossil reference. Low-temperature electrolysis processes still need a substantial reduction in investment costs to achieve break-even.

All electrochemical production routes to produce CO, formic acid, and syngas avoid or can soon avoid $CO_2$ emissions when compared to the fossil reference processes. $CO_2$ taxation can therefore play a substantial role in the competitivity of electrochemical $CO_2$ conversion routes. In our base case projections, we find that for CO, formic acid, and syngas production, $CO_2$ taxation should range between at least 60 and 636 €/t $CO_2$ to break-even with the fossil reference price. Most promising to reach break-even costs are LT formic acid production ($CO_2$ tax of 72 €/t $CO_2$) and HT CO production ($CO_2$ tax of 60 €/t $CO_2$). A higher $CO_2$ penalty would be required if the electricity that is used in the electroconversion routes is accompanied by an emission factor greater than zero. For ethylene production, saving GHG emissions by the electrochemical routes (3 and 6) becomes difficult if the efficiency and power density cannot be substantially improved without raising the investment costs. Our projections indicate that only with a $CO_2$ taxation of more than 2000 €/t $CO_2$ these routes may become competitive with the current fossil-based benchmark, which is not realistically feasible.

The early development stage of the investigated technologies also proffers opportunity for improvements and innovation that can drastically increase the technological performance. Research gaps are identified on various levels: materials, catalysts, electrodes, lifetime and associated maintenance costs of the active materials. Purification of both the feedstock and product, and down-stream processing costs depend on the feedstock and product requirements. The early-stage research often does not focus on these up- and downstream processes and further study is necessary. Pilot projects demonstrating the entire product chain, from industrial or atmospheric $CO_2$ source to final product, can aid in the accurate assessment of the performance, total investment costs, and operating and maintenance costs in an industrial environment. More development and investments are deemed necessary to ensure technological learning effects and cost reductions of electrochemical $CO_2$ conversion routes. An advantage for these specific processes is that they can benefit from experience obtained in comparable technologies, such as water electrolyzers and fuel cells.

# 8 References

Agora Verkehrswende, Agora Energiewende and Frontier Economics (2018): The Future Cost of Electricity-Based Synthetic Fuels. Retrieved from: https://www.agora-energiewende.de/en/publications/the-future-cost-of-electricity-based-synthetic-fuels-1/

Air Products, 2022. Retrieved from: https://www.airproducts.com/-/media/airproducts/files/en/900/900-13-100-us-carbon-monoxide-safetygram-19.pdf?la=en&hash=096C21CCC240E1CAADBA72A6CF2CD995

Albo, J., Sáez, A., Solla-Gullón, J., Montiel, V., & Irabien, A. (2015). Production of methanol from CO2 electroreduction at Cu2O and Cu2O/ZnO-based electrodes in aqueous solution. Applied Catalysis B: Environmental, 176–177, 709–717. https://doi.org/10.1016/j.apcatb.2015.04.055

Barecka, M. H., Ager, J. W., & Lapkin, A. A. (2021). Techno-economic assessment of emerging $CO_2$ electrolysis technologies. STAR Protocols, 2(4), 100889. https://doi.org/10.1016/j.xpro.2021.100889

Berkel, F.P.F. van, Ferchaud, C.J., Partenie, O., Linders, M.J.G., Delft, Y.C. van (2021). Solid Oxide Cell Technology Development at TNO, ECS Transactions, 103 (1) 591-602.

Blok, K., Nieuwlaar, E. (2016). Introduction to Energy Analysis 2nd, Routledge, 2nd edn., 2016.

Böhm, H., Goers, S., & Zauner, A. (2019). Estimating future costs of power-to-gas – a component-based approach for technological learning. International Journal of Hydrogen Energy, 44(59), 30789–30805. https://doi.org/10.1016/j.ijhydene.2019.09.230

Bove, R., Moreno, A., McPhail, S. (2008). International Status of Molten Carbonate Fuel Cell (MCFC) Technology. EUR 23363 EN. Luxembourg (Luxembourg): European Commission JRC44203

Brinkmann, T., Giner Santonja, G., Schorcht, F., Roudier, S., & Delgado Sancho, L. (2014). Best Available Techniques Reference Document for the Production of Chlor-alkali. https://doi.org/10.2791/13138

ChemAnalist (2022a). Retrieved from: Formic Acid Prices, Price, Pricing, News | ChemAnalyst

ChemAnalist (2022b). Retrieved from: Ethylene Prices, News, Market Analysis | ChemAnalyst

Clean Hydrogen Joint Undertaking (CHJU) (2021). Strategic Research and Innovation Agenda 2021 – 2027, table 4, p. 153.

Crook, J., Mousavi, A. (2016). The chlor-alkali process: A review of history and pollution. Environ. Forensics, 17 (3), 211–217. http://dx.doi.org/10.1080/15275922.2016.1177755

Detz, R.J.; Reek, J.N.H.; van der Zwaan, B.C.C. (2018). The future of solar fuels: when could they become competitive? Energy & Environmental Science, 11(7), 1653 - 1669.

Detz, R., Weeda, M. (2022). Projections of electrolyzer investment cost reduction through learning curve analysis, TNO 2022 P10111

Detz, R.J., Zwaan, B. van der (2019). Transitioning towards negative $CO_2$ emissions, Energy Policy 2019, 133, 110938. (doi.org/10.1016/j.enpol.2019.110938)

Dinh, C. T., Burdyny, T., Kibria, G., Seifitokaldani, A., Gabardo, C. M., Arquer, F. P. G. de, Kiani, A., Edwards, J. P., Luna, P. De, Bushuyev, O. S., Zou, C., Quintero-Bermudez, R., Pang, Y., Sinton, D., & Sargent, E. H. (2018). Sustained high-selectivity CO 2 electroreduction to ethylene via hydroxide-mediated catalysis at an abrupt reaction interface. Science, 787(May), 783–787. https://pubs.acs.org/sharingguidelines

Duhn, J. D. (2017). Development of highly efficient solid oxide electrolyzer cell systems. Technical University of Denmark.

E2c (2022). Retrieved from: Electrons to high value Chemical products | 2 Mers Seas Zeeën (interreg2seas.eu)

Eco (2019). Retrieved from: eco-soec-project.eu

Energiforskning (2022), Retrieved from: Electrochemical CO2 reduction to Ethylene for industrial applications | Energiforskning

Eurochlor (2018), The Electrolysis process and the real costs of production. https://www.eurochlor.org/wp-content/uploads/2019/04/12-electrolysis_production_costs.pdf

Eurochlor, 2022, personal communication (Ton Manders on 29-04-2022)

European Commission, 2020. COMMUNICATION FROM THE COMMISSION TO THE EUROPEAN PARLIAMENT, THE COUNCIL, THE EUROPEAN ECONOMIC AND SOCIAL COMMITTEE AND THE COMMITTEE OF THE REGIONS (2020) IMMC.COM%282020%29474%20final.ENG.xhtml.1_EN_ACT_part1_v4.docx (europa.eu)

Fasihi, M., Efimova, O., Breyer, C. (2019). Techno-economic assessment of $CO_2$ direct air capture plants, Journal of Cleaner Production, 224, 957e980. https://doi.org/10.1016/j.jclepro.2019.03.086

Ferioli, F., Schoots, K., van der Zwaan, B.C.C. (2009). Energy Policy, 2009, 37, 2525–2535.

Foit, S., Dittrich, L., Duyster, T., Vinke, I., Eichel, R. and de Haart, L. (2020). Direct Solid Oxide Electrolysis of Carbon Dioxide: Analysis of Performance and Processes. Processes, 8(11), p.1390.

Frøhlke, U. (2021). Retrieved from: Topsoe to build large-scale SOEC electrolyzer manufacturing facility to meet customer needs for green hydrogen production and SOEC efficiency | Large scale electrolysis

Fuel Cell Energy (2022). MCFC system product data sheet, retreived from: https://www.fuelcellenergy.com/

FCH (2022). More information can be find at: www.fch.europa.eu

Gabardo, C. M., O'Brien, C. P., Edwards, J. P., McCallum, C., Xu, Y., Dinh, C. T., Li, J., Sargent, E. H., & Sinton, D. (2019). Continuous Carbon Dioxide Electroreduction to Concentrated Multi-carbon Products Using a Membrane Electrode Assembly. Joule, 3(11), 2777–2791. https://doi.org/10.1016/j.joule.2019.07.021

Glenk, G., & Reichelstein, S. (2019). Economics of converting renewable power to hydrogen. Nature Energy, 1.

Global Carbon Budget, 2021

Haldor Topsøe (2022). Retreived from: Haldor Topsoe to build large-scale SOEC electrolyzer manufacturing facility to meet customer needs for green hydrogen - Green Car Congress

A. Hauch, M.L. Traulsen, R. Küngas, T.L. Skafte (2020). $CO_2$ electrolysis – Gas impurities and electrode overpotential causing detrimental carbon deposition, Journal of Power Sources, Volume 506.

Hu L. (2016). Molten Carbonate Fuel Cells for Electrolysis, Doctoral Thesis of KTH Royal Institute of Technology, ISSN 1654-1081, ISBN 978-91-7595-928-3

Hu L., Rexed I., Lindbergh G., Lagergren C. (2014). Electrochemical performance of reversible molten carbonate fuel cells, International Journal of Hydrogen Energy, vol. 39, Issue 23, pp. 12323-12329

Hydrogen Europe (2020). Strategic Research and Innovation Agenda

Hydrohub Innovation Program (2022). A One-GigaWatt Green-Hydrogen Plant. Advanced Design and Total Installed-Capital Costs.

International Energy Agency (IEA) (2016). 20 Years of Carbon Capture and Storage, Accelerating
Future Deployment. Retrieved from: https://www.iea.org/publications.

International Energy Agency (IEA) (2019). Putting $CO_2$ to use. Creating value from emissions.

International Energy Agency (IEA) (2020). Energy Technology Perspectives 2020. Special Report on Carbon Capture, Utilisation and Storage.

International Energy Agency (IEA) (2021). Net Zero by 2050 - A Roadmap for the Global Energy Sector.

IEAGHG (2021a). $CO_2$ as a Feedstock: Comparison of CCU Pathways. IEAGHG Technical Report, 2021-02

IEAGHG (2021b). $CO_2$ Utilisation: Hydrogenation Pathways. IEAGHG Technical Report, 2021-03

International Renewable Energy Agency (IRENA), (2020). Green Hydrogen Cost Reduction: Scaling up Electrolysers to Meet the $1.5^0C$ Climate Goal, International Renewable Energy Agency, Abu Dhabi.

International Technology Roadmap for Photovoltaic (ITRPV) (2022). Retrieved from: https://www.vdma.org/international-technology-roadmap-photovoltaic

Irlam, L., Global CCS Institute, Global costs of carbon capture and storage, 2017 update. Retrieved from: https://www.globalccsinstitute.com/

Jack, J., Zhu, W., Avalos, J. L., Gong, J., & Ren, Z. J. (2021). Anode co-valorization for scalable and sustainable electrolysis. Green Chemistry, 23(20), 7917–7936. https://doi.org/10.1039/d1gc02094c

Jiang Y., Su M., Zhang Y., Zhan G., Tao Y., Li D. Bioelectrochemical systems for simultaneously production of methane and acetate from carbon dioxide at relatively high rate Int. J. Hydrog. Energy, 38 (2013), pp. 3497-3502

Jouny, M., Luc, W., & Jiao, F. (2018a). General Techno-Economic Analysis of $CO_2$ Electrolysis Systems. Industrial and Engineering Chemistry Research, 57(6), 2165–2177. https://doi.org/10.1021/acs.iecr.7b03514

Jouny, M., Luc, W., & Jiao, F. (2018b). High-rate electroreduction of carbon monoxide to multi-carbon products. Nature Catalysis, 1(10), 748–755. https://doi.org/10.1038/s41929-018-0133-2

Jouny, M., Hutchings, G. S., & Jiao, F. (2019). Carbon monoxide electroreduction as an emerging platform for carbon utilization. Nature Catalysis, 2(12), 1062–1070. https://doi.org/10.1038/s41929-019-0388-2

Jung, J., Postels, S., & Bardow, A. (2014). Cleaner chlorine production using oxygen depolarized cathodes? A life cycle assessment. Journal of Cleaner Production, 80, 46–56. https://doi.org/10.1016/j.jclepro.2014.05.086

Kaczur, J. J., McGlaughlin, L. J., & Lakkaraju, P. S. (2020). Investigating Pervaporation as a Process Method for Concentrating Formic Acid Produced from Carbon Dioxide. C — Journal of Carbon Research, 6(2), 42. https://doi.org/10.3390/c6020042

Kaplan V., Wachtel E., Gartsman K., Feldman Y., Lubomirsky I. (2010). Conversion of $CO_2$ to CO by Electrolysis of Molten Lithium Carbonate, J. Electrochem. Soc. 157 B552

Kaplan V., Ellen Wachtel E., Lubomirsky I. (2014). $CO_2$ to CO Electrochemical Conversion in Molten $Li_2CO_3$ is Stable with Respect to Sulfur Contamination, J. Electrochem. Soc. 161 F54

Karapinar, D., Creissen, C.E., Guillermo Rivera de la Cruz, J., Schreiber, M.W., Fontecave, M. (2021). Electrochemical $CO_2$ Reduction to Ethanol with Copper-Based Catalysts. ACS Energy Lett. 6, 2, 694–706

Kasuya, F., Tsuji, T. (1991). High purity CO gas separation by pressure swing adsorption, Gas Separation & Purification, Volume 5, Issue 4, 1991, Pages 242-246.

Keith, D. W., Holmes, G., St. Angelo, D., & Heidel, K. (2018). A Process for Capturing $CO_2$ from the Atmosphere. Joule, 2(8), 1573–1594. https://doi.org/10.1016/j.joule.2018.05.006

Kibria, M. G., Edwards, J. P., Gabardo, C. M., Dinh, C. T., Seifitokaldani, A., Sinton, D., & Sargent, E. H. (2019). Electrochemical CO2 Reduction into Chemical Feedstocks: From Mechanistic Electrocatalysis Models to System Design. *Advanced Materials*, 31(31), 1–24. https://doi.org/10.1002/adma.201807166

Kim, J. Y. 'Timothy,' Zhu, P., Chen, F.-Y., Wu, Z.-Y., Cullen, D. A., & Wang, H. (2022). Recovering carbon losses in $CO_2$ electrolysis using a solid electrolyte reactor. Nature Catalysis, 5 (April). https://doi.org/10.1038/s41929-022-00763-w

Ko, B. H., Hasa, B., Shin, H., Jeng, E., Overa, S., Chen, W., & Jiao, F. (2020). The impact of nitrogen oxides on electrochemical carbon dioxide reduction. *Nature Communications*, 11(1), 1–9. https://doi.org/10.1038/s41467-020-19731-8

König, M., Lin, S.-H., Vaes, J., Pant, D., Klemm, E. (2021). Integration of the aprotic $CO_2$ reduction to oxalate at a Pb catalyst into a GDE flow cell configuration, Faraday Discuss. https://doi.org/10.1039/D0FD00141D.

Kopernikus (2019). Retreived from: Kopernikus-Projekte: Kopernikus-Project: P2X

Krishnan S., Fairlie, M., Andres, P., de Groot, T., Kramer, G.J. (2020). Chapter 10: Power to gas ($H_2$): alkaline electrolysis. Technological Learning in the Transition to a Low-Carbon Energy System, Conceptual Issues, Empirical Findings, and Use in Energy Modeling, Pages 165-187

Küngas, R., Blennow, P., Heiredal-Clausen, T., Holt Nørby, T., Rass-Hansen, J., Hansen, J. B., Moses, P. G. (2019). Progress in SOEC development activities at Haldor Topsøe. ECS Trans. 91 215.

Küngas, R. (2020). Review—Electrochemical $CO_2$ Reduction for CO Production: Comparison of Low- and High-Temperature Electrolysis Technologies. Journal of The Electrochemical Society, 167(4), 044508. https://doi.org/10.1149/1945-7111/ab7099

Lang, H.J. (1948). Chem. Eng. 55 112.

Li, K., Fan, Q., Chuai, H., Liu, H., Zhang, S., & Ma, X. (2021). Revisiting Chlor-Alkali Electrolyzers: from Materials to Devices. *Transactions of Tianjin University*, 27(3), 202–216. https://doi.org/10.1007/s12209-021-00285-9

Li, C., Wang, T., Liu, B., Chen, M., Li, A., Zhang, G., Du, M., Wang, H., Liub, S.F., Gong, J. (2019). Photoelectrochemical $CO_2$ Reduction to Adjustable Syngas on Grain-boundary-mediated a-Si/TiO2/Au Photocathodes with Low Onset Potentials, Energy Environ. Sci., 12, 923-928. https://doi.org/10.1039/C8EE02768D

Lister, T. E., & Dufek, E. J. (2013). Chlor-syngas: Coupling of electrochemical technologies for production of commodity chemicals. Energy and Fuels, 27(8), 4244–4249. https://doi.org/10.1021/ef302033j

Liu, Z., Yang, H., Kutz, R., & Masel, R. I. (2018). $CO_2$ Electrolysis to CO and $O_2$ at High Selectivity, Stability and Efficiency Using Sustainion Membranes. Journal of The Electrochemical Society, 165(15), J3371–J3377. https://doi.org/10.1149/2.0501815jes

Lu, S., Shi, Y., Meng, N., Lu, S., Yu, Y., Zhang, B. (2020). Electrosynthesis of Syngas via the Co-Reduction of $CO_2$ and $H_2O$. Cell Rep. Phys. Sci., 1 (11), Article 100237

Martín, A. J., Larrazábal, G. O., & Pérez-Ramírez, J. (2015). Towards sustainable fuels and chemicals through the electrochemical reduction of CO2: Lessons from water electrolysis. Green Chemistry, 17(12), 5114–5130. https://doi.org/10.1039/c5gc01893e

Masini, A., Strohbach, T., Siska, F., Chlup, Z., Slouhy, I. (2019). Electrolyte-Supported Fuel Cell: Co-Sintering Effects of Layer Deposition on Biaxial Strength, Materials 12, 306

Mayyas, A., Ruth, M., Pivovar, B., Bender, G., & Wipke, K. (2019). Manufacturing Cost Analysis for Proton Exchange Membrane Water Electrolyzers. https://doi.org/NREL/TP-6A20-72740

McDonald, A., and Schrattenholzer, L., 2001, Learning rates for energy technologies. Energy Policy 2001, 29, 255–261.

MegaSyn (2022). Retreived from: Megawatt scale co-electrolysis as syngas generation for e-fuels synthesis | www.fch.europa.eu

Meskine H., Gurbuz E., Albin V., Melendez-Ceballos A., Cassir M., Ringuede, Lair A.V. (2021). $CO_2$ electrolysis in a reversible molten carbonate fuel cell: Online chromatographic detection of CO, International Journal of Hydrogen Energy, 14913-14921

Methanex (2022). Retreived from: Pricing | Methanex Corporation

Min, G., Park, Y. and Hong, J. (2020). Thermodynamic analysis of a solid oxide co-electrolysis cell system for its optimal thermal integration with external heat supply. Energy Conversion and Management, 225, p.113381.

Monforti Ferrario A., Santoni F., Della Pietra M., Rossi M, Piacente N., Comodi G., Simonetti L. (2021). A System Integration Analysis of a Molten Carbonate Electrolysis Cell as an Off-Gas Recovery System in a Steam-Reforming Process of an Oil Refinery, Front. Energy Res. 9:655915., doi: 10.3389/fenrg.2021.655915

Nakata, K., Ozaki, T., Terashima, C., Fujishima, A., & Einaga, Y. (2014). High-yield electrochemical production of formaldehyde from CO2 and seawater. Angewandte Chemie - International Edition, 53(3), 871–874. https://doi.org/10.1002/anie.201308657

Nationale Organisation Wasserstoff- und Brennstoffzellentechnologie – NOW GmbH, (2018). Smolinka, T., Wiebe, N., Sterchele, P., Palzer, A., Lehner, F., Jansen, M., Kiemel, S., Miehe, R., Wahren, S., Zimmermann, F., Studie IndWEDe, Industrialisierung der Wasserelektrolyse in Deutschland: Chancen und Herausforderungen für nachhaltigen Wasserstoff für Verkehr, Strom und Wärme.

NewSoc (2022). Next Generation of Solid Oxide Fuel Cell and Electrolysis Technology. Retrieved from: Home - NewSoc English

Ng, S.-F., Jie Foo, J., Ong, W.-J. (2022). Solar-powered chemistry: Engineering low-dimensional carbon nitride-based nanostructures for selective $CO_2$ conversion to C1 C2 products, InfoMat, 4, 1, e12279.

NIH (2022). Retrieved from: Ethylene - Some Industrial Chemicals - NCBI Bookshelf (nih.gov)

Norsk e-fuel (2022). Retrieved from: Norsk e-Fuel - Sustainable aviaton (norsk-e-fuel.com)

Nørskov, J. K., Latimer, A., & Dickens, C. F. (2019). Research needs towards sustainable production of fuels and chemicals. https://www.energy-x.eu/research-needs-report/

Nyári, J., Magdeldin, M., Larmi, M., Järvinen, M., Santasalo-Aarnio, A. (2020). Techno-economic barriers of an industrial-scale methanol CCU-plant, Journal of $CO_2$ Utilization, 39, 101166. https://doi.org/10.1016/j.jcou.2020.101166

O'Brien, T.F., and Bommaraju, T.V. Hine, F. (2005). Handbook of Chlor-alkali Technology. Volume 1: Fundamentals, New York: Springer.

OCEAN, 2022. Retrieved from: Oxalic acid from $CO_2$ using Electrochemistry At demonstratioN scale | SPIRE (aspire2050.eu)

Overa, S., Feric, T. G., Park, A. H. A., & Jiao, F. (2021). Tandem and Hybrid Processes for Carbon Dioxide Utilization. *Joule*, 5(1), 8–13. https://doi.org/10.1016/j.joule.2020.12.004

Overa, S., Ko, B. H., Zhao, Y., & Jiao, F. (2022). Electrochemical Approaches for CO2 Conversion to Chemicals: A Journey toward Practical Applications. *Accounts of Chemical Research*, 55(5), 638–648. https://doi.org/10.1021/acs.accounts.1c00674

Patonia, A., & Poudineh, R. (2022). Cost-competitive green hydrogen: how to lower the cost of electrolysers?

Paturska, A., Repele, M., & Bazbauers, G. (2015). Economic Assessment of Biomethane Supply System based on Natural Gas Infrastructure. Energy Procedia, 72, 71–78. https://doi.org/10.1016/j.egypro.2015.06.011

Pérez-Carbajo, J., Matito-Martos, I., Balestra, S. R. G., Tsampas, M. N., Van De Sanden, M. C. M., Delgado, J. A., Águeda, V. I., Merkling, P. J., & Calero, S. (2018). Zeolites for CO2-CO-O2 Separation to Obtain CO2-Neutral Fuels. *ACS Applied Materials and Interfaces*, 10(24), 20512–20520. https://doi.org/10.1021/acsami.8b04507

Pérez-Gallent, E., Turk, S., Latsuzbaia, R., Bhardwaj, R., Anastasopol, A., Sastre-Calabuig, F., Garcia, A. C., Giling, E., & Goetheer, E. L. V. (2019). Electroreduction of $CO_2$ to CO Paired with 1,2-Propanediol Oxidation to Lactic Acid. Toward an Economically Feasible System. Industrial & Engineering Chemistry Research, 58(16), 6195–6202.

Perez-Trujillo JP, Elizalde-Blancas F, Della Pietra M, McPhail SJ. (2018). A numerical and experimental comparison of a single reversible molten carbonate cell operating in fuel cell mode and electrolysis mode. Appl Energy 226, p.1037-1055.

Perez-Trujillo JP, Elizalde-Blancas F, McPhail SJ, Della Pietra M, Bosio B. (2020). Preliminary theoretical and experimental analysis of a Molten Carbonate Fuel Cell operating in reversible mode. Appl Energy 263:114630.

Petrochemicals Europe (2022). Cracker capacity published on website, retrieved from: https://www.petrochemistry.eu/about-petrochemistry/petrochemicals-facts-and-figures/cracker-capacity/

POSCO (2022). POSCO Energy website – Fuel cell development, retreived from: posco energy : Products

Posdziech O. (2021). Production of renewable Hydrogen and Syngas via High-Temperature Electrolysis, Presentation Sunfire on Heat-to-Fuel interfaces to advanced Power-to-Gas and Power-to-Liquids Technologies (e-fuels).

Ramdin, M., Morrison, A. R. T., De Groen, M., Van Haperen, R., De Kler, R., Irtem, E., Laitinen, A. T., Van Den Broeke, L. J. P., Breugelmans, T., Trusler, J. P. M., Jong, W. De, & Vlugt, T. J. H. (2019). High-Pressure Electrochemical Reduction of $CO_2$ to Formic Acid/Formate: Effect of pH on the Downstream Separation Process and Economics. Industrial and Engineering Chemistry Research, 58(51), 22718–22740. https://doi.org/10.1021/acs.iecr.9b03970

Reinisch, D., Schmid, B., Martić, N., Krause, R., Landes, H., Hanebuth, M., Mayrhofer, K. J. J., & Schmid, G. (2020). Various CO2-to-CO Electrolyzer Cell and Operation Mode Designs to avoid CO2-Crossover from Cathode to Anode. Zeitschrift Fur Physikalische Chemie, 234(6), 1115–1131. https://doi.org/10.1515/zpch-2019-1480

Renewable Energy Directive II (2018), Official Journal of the European Union, Directive (EU) 2018/2001 of the European Parliament and of the Council of 11 December 2018 on the promotion of the use of energy from renewable sources.

Riegraf, M., Amaya-Duenas, D.-M., Surrey, A., Costa, R. (2016). Evaluation of the stability of Ni/CGO-based electrolyte supported cells in co-electrolysis, 12th European SOFC & SOE Forum, B0504

Ripatti, D. S., Veltman, T. R., & Kanan, M. W. (2019). Carbon Monoxide Gas Diffusion Electrolysis that Produces Concentrated C2 Products with High Single-Pass Conversion. Joule, 3(1), 240–256. https://doi.org/10.1016/j.joule.2018.10.007

Rivera-Tinoco, R., Schoots, K., van der Zwaan, B.C.C. (2012). Energy Convers. Manag. 57, 86–96.

van Rooij, G.J., Akse, H.N., Bongers, W.A., van de Sanden, M.C.M. (2018). Plasma Phys. Control. Fusion, 60, 014-019.

Rubin, E.S., Azevedo, I.M.L., Jaramillo, P., Yeh, S. (2015). A review of learning rates for electricity supply technologies, Energy Policy 86, 198–218

Samipour, S., Manshadi, M. D., & Setoodeh, P. (2020). $CO_2$ removal from biogas and syngas. Advances in Carbon Capture, 1, 455–477. https://doi.org/10.1016/b978-0-12-819657-1.00020-7

Shin, H., Hansen, K. U., & Jiao, F. (2021). Techno-economic assessment of low-temperature carbon dioxide electrolysis. *Nature Sustainability*, 1–10. https://doi.org/10.1038/s41893-021-00739-x

Schoots, K., Ferioli, F., Kramer, G.J., van der Zwaan, B.C.C. (2008)., Int. J. Hydrogen Energy, 33, 2630–2645.

Schoots, K., Kramer, G.J., van der Zwaan, B.C.C. (2010). Energy Policy, 38, 2887–2897.

Schmidt, O., Hawkes, A., Gambhir, A., Staffell, I. (2017). The future cost of electrical energy storage based on experience rates. Nat. Energy, 2, 17110.

Schreiber, A., Peschel, A., Hentschel, B., & Zapp, P. (2020). Life Cycle Assessment of Power-to-Syngas: Comparing High Temperature Co-Electrolysis and Steam Methane Reforming. *Frontiers in Energy Research*, *8* (November), 1–17. https://doi.org/10.3389/fenrg.2020.533850

Schuler, E., Demetriou, M., Shiju, N. R., & Gruter, G. J. M. (2021). Towards Sustainable Oxalic Acid from $CO_2$ and Biomass. ChemSusChem, 14(18), 3636–3664. https://doi.org/10.1002/cssc.202101272

Sedighian Rasouli, A., Wang, X., Wicks, J., Lee, G., Peng, T., Li, F., McCallum, C., Dinh, C.-T., Ip, A.H., Sinton, D., Sargent, E.H. (2020). $CO_2$ Electroreduction to Methane at Production Rates Exceeding 100 mA/cm$^2$, ACS Sustainable Chem. Eng. 8, 39, 14668–14673

SELECT $CO_2$ (2022). Retrieved from: Home (selectco2.eu)

Siemens, 2020. Rheticus: World's-first-automated-$CO_2$-electrolyzer, Siemens Energy Global (siemens-energy.com)

Sisler, J., Khan, S., Ip, A. H., Schreiber, M. W., Jaffer, S. A., Bobicki, E. R., Dinh, C. T., & Sargent, E. H. (2021). Ethylene Electrosynthesis: A Comparative Techno-economic Analysis of Alkaline vs Membrane Electrode Assembly vs CO2–CO–C2H4 Tandems. ACS Energy Letters, 6(3), 997–1002. https://doi.org/10.1021/acsenergylett.0c02633

Singhal, S.C. (2014). Solid oxide fuel cells for power generation, WIREs Energy and Environment, Volume 3, Issue 2 p. 179-194. https://doi.org/10.1002/wene.96

Stephens, I. E. L., Chan, K., Bagger, A., Boettcher, S. W., Bonin, J., Boutin, E., Buckley, A., Buonsanti, R., Cave, E., Chang, X., Chee, S. W., Silva, A. H. M. da, Luna, P. De, Einsle, O., Endrődi, B., Escudero-Escribano, M., Araujo, J. V. F. de, Figueiredo,

M. C., Hahn, C., … Zhou, Y. (2019). 2022 Roadmap on Low Temperature Electrochemical CO2 Reduction. *Materials Today: Proceedings*, 27(xxxx), 0–31. https://doi.org/10.1088/2515-7655/ac7823

Sunfire (2021). Retrieved from: https://www.sunfire.de/files/sunfire/images/content/Produkte_Technologie/factsheets/Sunfire-SynLink_FactSheet.pdf (Sunfire-Factsheet-SynLink-SOEC-20210303)

Sunfire (2022a). Retrieved from: 60173949ebf7aa1f60af6f66_sunfire-imagefolder-eng-498521.pdf (webflow.com)

Sunfire (2022b). Retrieved from: Renewable Syngas (SynLink) - Sunfire

Thyssenkrupp (2015). Chlor-Alkali electrolysis plants. Superior membrane process. http://www.thyssenkrupp-industrial-solutions-rus.com/assets/pdf/TKIS_Chlor-Alkali_Electrolysis.pdf

Thyssenkrupp (2020). Chlor-Alkali Electrolysis.

Topsøe (2022). Retrieved from: http://www.topsoe.com/products/ecos- containerized-co-generation-plants

Tichler, R., Böhm, H., Zauner, A., Goers, S., Kroon, P., & Schirrmeister, S. (2018). Innovative large-scale energy storage technologies and Power-to-Gas concepts after optimization. Report on experience curves and economies of scale. https://www.storeandgo.info/fileadmin/downloads/deliverables_2019/20190801-STOREandGO-D7.5-EIL-Report_on_experience_curves_and_economies_of_scale.pdf

Vass, Á., Endrődi, B., & Janáky, C. (2021). Coupling electrochemical carbon dioxide conversion with value-added anode processes: An emerging paradigm. Current Opinion in Electrochemistry, 25, 1–9. https://doi.org/10.1016/j.coelec.2020.08.003

Vass, Á., Kormányos, A., Kószó, Z., Endrődi, B., & Janáky, C. (2022). Anode Catalysts in $CO_2$ Electrolysis: Challenges and Untapped Opportunities. ACS Catalysis, 1037–1051. https://doi.org/10.1021/acscatal.1c04978

Verma, S., Lu, S., & Kenis, P. J. A. (2019). Co-electrolysis of $CO_2$ and glycerol as a pathway to carbon chemicals with improved technoeconomics due to low electricity consumption. Nature Energy, 4, 466–474. https://doi.org/10.1038/s41560-019-0374-6

Wain, Y.A. (2014). PM World Journal, 3, 10.

Wang, X., Ou, P., Ozden, A. *et al.* (2022). Efficient electrosynthesis of n-propanol from carbon monoxide using a Ag–Ru–Cu catalyst. Nat Energy 7, 170–176 (2022). https://doi.org/10.1038/s41560-021-00967-7

Wei, M., Smith, S.J., Sohn, M.D. (2017). Experience curve development and cost reduction disaggregation for fuel cell markets in Japan and the US. Applied Energy 191, 346–357

Yang, H., Kaczur, J. J., Sajjad, S. D., & Masel, R. I. (2017). Electrochemical conversion of $CO_2$ to formic acid utilizing SustainionTM membranes. Journal of $CO_2$ Utilization, 20 (April), 208–217. https://doi.org/10.1016/j.jcou.2017.04.011

Yang, H., Kaczur, J. J., Sajjad, S. D., & Masel, R. I. (2020). Performance and long-term stability of $CO_2$ conversion to formic acid using a three-compartment electrolyzer design. Journal of $CO_2$ Utilization, 42(October), 101349. https://doi.org/10.1016/j.jcou.2020.101349

Yang, K., Li, M., Subramanian, S., Blommaert, M. A., Smith, W. A., & Burdyny, T. (2021). Cation-driven increases of $CO_2$ utilization in a bipolar membrane electrode assembly for $CO_2$ electrolysis. ACS Energy Letters, 6(12), 4291–4298. https://doi.org/10.1021/acsenergylett.1c02058

Xie, K., Ozden, A., Miao, R. K., & Sargent, E. H. (2022). Eliminating the need for anodic gas separation in anodic upgrading. Nature Communications, 13 (3070), 1–9. https://doi.org/10.1038/s41467-022-30677-x

Zhu, Q. (2019). Developments on CO2-utilization technologies. *Clean Energy*, *3*(2), 85–100. https://doi.org/10.1093/ce/zkz008

# 9 Appendix

Sensitivity analysis results:

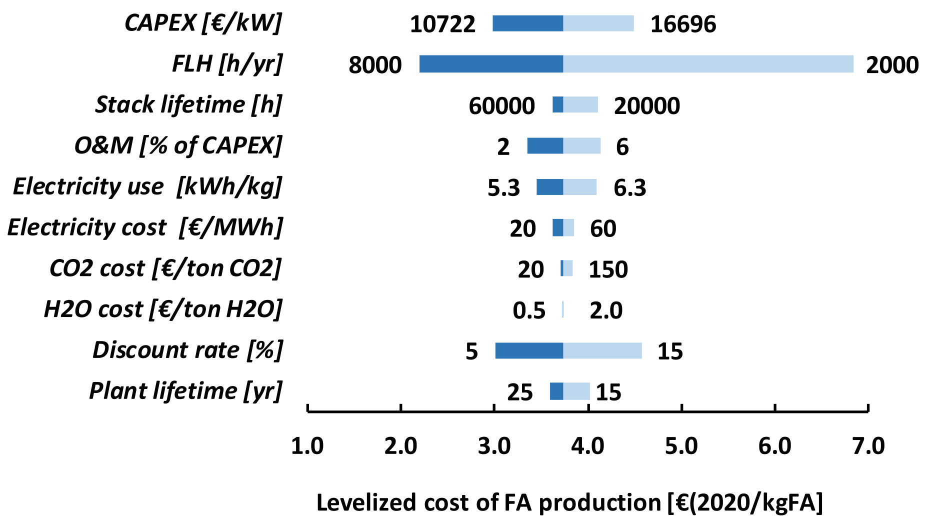

Figure A37. Sensitivity analysis for route 2 – LT electrochemical conversion of $CO_2$ to FA. Ten parameters are varied to explore their effect on the current levelized cost of formic acid production. The fossil reference formic acid price amounts to 0.70-0.80 €/kgFA.

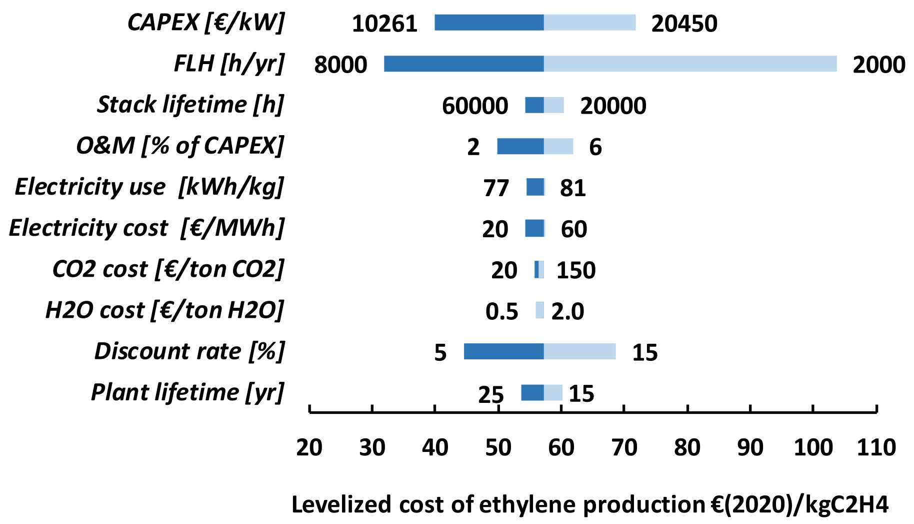

Figure A38. Sensitivity analysis for route 3 – LT electrochemical conversion of $CO_2$ to $C_2H_4$. Ten parameters are varied to explore their effect on the current levelized cost of ethylene production. The fossil reference ethylene price amounts to 0.70-1.30 €/kg$C_2H_4$

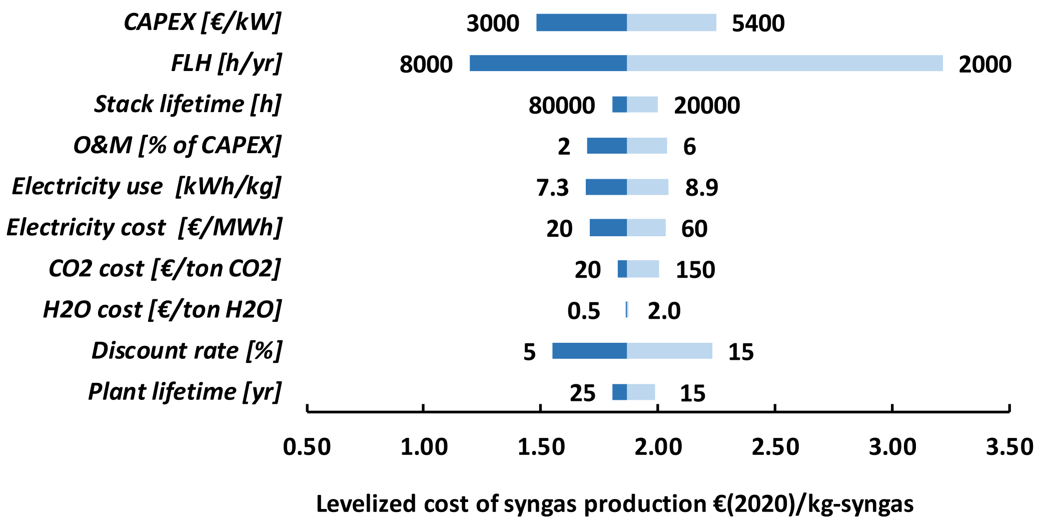

Figure A39. Sensitivity analysis for route 5 – HT electrochemical conversion of $CO_2$ to syngas. Ten parameters are varied to explore their effect on the current levelized cost of syngas production. The fossil reference syngas price amounts to 0.17-0.43 €/kg syngas.

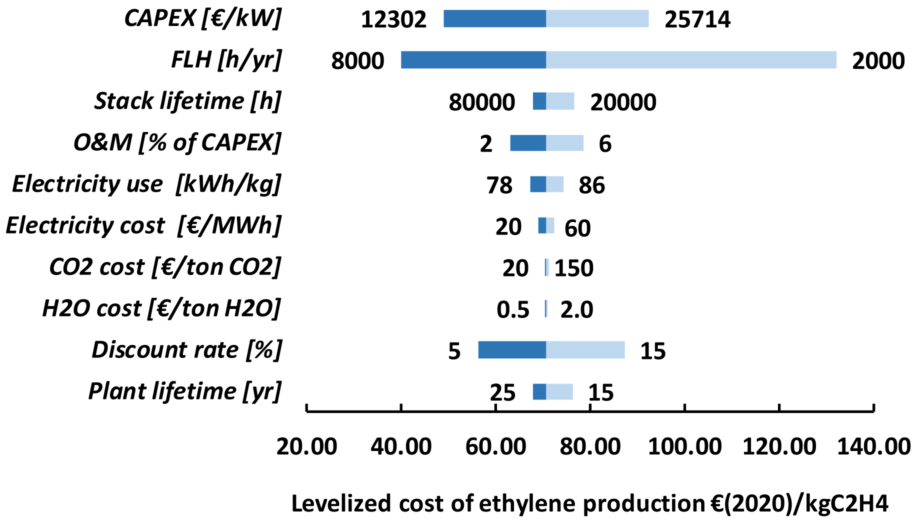

Figure A40. Sensitivity analysis for route 6 – Tandem HT/LT electrochemical conversion of $CO_2$ to $C_2H_4$. Ten parameters are varied to explore their effect on the current levelized cost of ethylene production. The fossil reference ethylene price amounts to 0.70-1.30 €/kg$C_2H_4$

IEA Greenhouse Gas R&D Programme

Pure Offices, Cheltenham Office Park, Hatherley Lane,
Cheltenham, Glos. GL51 6SH, UK

Tel: +44 1242 802911
mail@ieaghg.org
www.ieaghg.org